ΕΘΝΙΚΟ ΜΕΤΣΟΒΙΟ ΠΟΛΥΤΕΧΝΕΙΟ

ΣΧΟΛΗ ΗΛΕΚΤΡΟΛΟΓΩΝ ΜΗΧΑΝΙΚΩΝ ΚΑΙ ΜΗΧΑΝΙΚΩΝ ΥΠΟΛΟΓΙΣΤΩΝ

ΤΟΜΕΑΣ ΗΛΕΚΤΡΙΚΗΣ ΙΣΧΥΟΣ

Μοντελοποίηση του Τριφασικού Μετασχηματιστή Τύπου Πυρήνα – Θεωρία και Εφαρμογή

ΔΙΠΛΩΜΑΤΙΚΗ ΕΡΓΑΣΙΑ

Αθανάσιος Η. Κροντήρης

Επιβλέπων: Αντώνιος Κλαδάς
Αν. Καθηγητής Ε.Μ.Π

Αθήνα, Σεπτέμβριος 2005

ΕΘΝΙΚΟ ΜΕΤΣΟΒΙΟ ΠΟΛΥΤΕΧΝΕΙΟ

ΣΧΟΛΗ ΗΛΕΚΤΡΟΛΟΓΩΝ ΜΗΧΑΝΙΚΩΝ ΚΑΙ ΜΗΧΑΝΙΚΩΝ ΥΠΟΛΟΓΙΣΤΩΝ

ΤΟΜΕΑΣ ΗΛΕΚΤΡΙΚΗΣ ΙΣΧΥΟΣ

Μοντελοποίηση του Τριφασικού Μετασχηματιστή Τύπου Πυρήνα – Θεωρία και Εφαρμογή

ΔΙΠΛΩΜΑΤΙΚΗ ΕΡΓΑΣΙΑ

Αθανάσιος Η. Κροντήρης

Επιβλέπων: Αντώνιος Κλαδάς
Αν. Καθηγητής Ε.Μ.Π

Εγκρίθηκε από την τριμελή εξεταστική επιτροπή την 17η Οκτωβρίου 2003.

…….	…….	…….
Α. Κλαδάς Αν. Καθηγητής Ε.Μ.Π.	Ν. Χατζηαργυρίου Καθηγητής Ε.Μ.Π.	Σ. Παπαθανασίου Λέκτορας Ε.Μ.Π.

Αθήνα, Σεπτέμβριος 2005

.....

Αθανάσιος Η. Κροντήρης

Διπλωματούχος Ηλεκτρολόγος Μηχανικός και Μηχανικός Υπολογιστών Ε.Μ.Π.

ΠΡΟΛΟΓΟΣ

Η διπλωματική αυτή εργασία αναπτύχθηκε στα πλαίσια του ευρωπαϊκού προγράμματος Erasmus σε συνεργασία με το Τεχνικό Πανεπιστήμιο του Βερολίνου (Technische Universität Berlin), υπό την εποπτεία του κ. Rolf Hanitsch, καθηγητή στο Ινστιτούτο Ηλεκτρικών Μηχανών. Η γλώσσα πρωτοτύπου είναι, για το λόγο αυτό, η αγγλική. Στη σύντομη ελληνική μετάφραση που ακολουθεί θα γίνονται κάποιες αναφορές σε μαθηματικές σχέσεις και διαγράμματα του πρωτότυπου κειμένου, που παρατίθεται στη συνέχεια.

Η δομή της παρούσας εργασίας είναι η ακόλουθη:

Στο πρώτο κεφάλαιο γίνεται μια σύντομη εισαγωγή στη θεωρία μοντελοποίησης και στις κατηγορίες μοντέλων μετασχηματιστών.

Στο δεύτερο κεφάλαιο παρουσιάζεται η απαραίτητη θεωρία για τη μοντελοποίηση του μετασχηματιστή. Σχολιάζονται τα κύρια χαρακτηριστικά του μετασχηματιστή και αναλύονται τα μη γραμμικά φαινόμενα που εμφανίζονται κατά τη λειτουργία του. Καθώς ενδιαφέρει η προσομοίωση αργών μεταβατικών φαινομένων (χαμηλές συχνότητες), η ανάλυση αυτή εστιάζει στο μαγνητικό κύκλωμα του μετασχηματιστή και όχι στα τυλίγματα.

Το τρίτο κεφάλαιο ασχολείται με τη θεωρία της δυαδικότητας. Μετά από μια σύντομη τεκμηρίωση της θεωρίας, αναπτύσσεται ένα δυαδικό μοντέλο για τον τριφασικό μετασχηματιστή τύπου πυρήνα.

Στο τέταρτο κεφάλαιο παρουσιάζεται η προσέγγιση των αποσυζευγμένων ηλεκτρικών-μαγνητικών κυκλωμάτων. Θεμελιώνεται ένα μοντέλο μετασχηματιστή σύμφωνα με αυτήν την προσέγγιση και αναπτύσσεται εν μέρει ένα υπολογιστικό μοντέλο σε γλώσσα προγραμματισμού C.

Το πέμπτο και τελευταίο κεφάλαιο είναι αφιερωμένο σε κάποια γενικά συμπεράσματα, καθώς και σε προτάσεις για παραπέρα ανάπτυξη των μοντέλων μετασχηματιστών.

Αφορμή για την παρούσα εργασία αποτέλεσε η διάγνωση υψηλού περιεχομένου αρμονικών στην έξοδο ενός μετασχηματιστή ανύψωσης σε ένα αιολικό πάρκο. Οι αρμονικές αυτές εικάζεται ότι προέρχονταν από μία dc συνιστώσα στο ρεύμα εισόδου μίας φάσης. Για την αποδοχή ή την απόρριψη της εικασίας αυτής ήταν απαραίτητη η προσομοίωση της συγκεκριμένης λειτουργίας (με αυτή δηλαδή τη dc offset) του τριφασικού μετασχηματιστή τύπου πυρήνα.

ΕΛΛΗΝΙΚΗ ΜΕΤΑΦΡΑΣΗ

1. Εισαγωγή

Ο μετασχηματιστής – με την κλασσική του έννοια – είναι μια συσκευή σύζευξης ηλεκτρικών κυκλωμάτων μέσω ενός κοινού, μαγνητικού πυρήνα.

Η λειτουργία του μετασχηματιστή περιγράφεται από τις γνωστές εξισώσεις του Maxwell. Στην περίπτωση αργών μεταβατικών φαινομένων, ωστόσο, το μαγνητικό κύκλωμα μπορεί να αποσυμπλεχθεί του ηλεκτρικού, με αποτέλεσμα το σύστημα εξισώσεων (Ε.1), όπου, εκτός των απλοποιημένων εξισώσεων Maxwell, έχουμε προσθέσει και τις συντακτικές σχέσεις του υλικού.

$$\begin{cases} \oint_C \vec{E}d\vec{l} = -\dfrac{d}{dt}\int_S \vec{B}d\vec{S} \\ \oint_C \vec{H}d\vec{l} = \int_S \vec{J}d\vec{S} \\ \oint_S \vec{B}d\vec{S} = 0 \\ \oint_S \vec{J}d\vec{S} = 0 \\ \vec{B} = \mu\vec{H} \\ \vec{J} = \sigma\vec{E} \end{cases} \qquad \text{(Ε.1)}$$

2. Βασική θεωρία

Το σημαντικότερο ρόλο κατά τη μοντελοποίηση του μετασχηματιστή έχει ο μαγνητικός πυρήνας. Η περιγραφή του πυρήνα πρέπει να συμπεριλαμβάνει τόσο την τοπολογία του όσο και τα μη γραμμικά φαινόμενα που εμφανίζει αυτός.

Ο μαγνητικός πυρήνας των μετασχηματιστών αποτελείται από σιδηρομαγνητικά υλικά, υλικά δηλαδή των οποίων η σχετική μαγνητική διαπερατότητα είναι κατά πολύ μεγαλύτερη της μονάδας. Τα σιδηρομαγνητικά υλικά λειτουργούν ως «ενισχυτές» του μαγνητικού πεδίου, εμφανίζουν όμως ορισμένα μη γραμμικά φαινόμενα που καθιστούν τη μοντελοποίησή τους ιδιαίτερα πολύπλοκη. Τα φαινόμενα αυτά είναι:

Μαγνητικός κορεσμός. Η σχετική μαγνητική διαπερατότητα των σιδηρομαγνητικών υλικών δεν παραμένει σταθερή, αλλά μεταβάλλεται καθώς μεταβάλλεται το εξωτερικά επιβαλλόμενο μαγνητικό πεδίο. Αυτή η μη γραμμική σχέση φαίνεται σχηματικά στο γράφημα Ε.1 για ένα τυπικό σιδηρομαγνητικό υλικό. Το φαινόμενο του μαγνητικού κορεσμού μπορεί να εξηγηθεί βάσει της θεωρίας μαγνήτισης, σύμφωνα με την οποία η μαγνήτιση ενός υλικού, εν γένει, οφείλεται στην ευθυγράμμιση μικρών, μαγνητικών τομέων (magnetic domains) με το επιβαλλόμενο πεδίο.

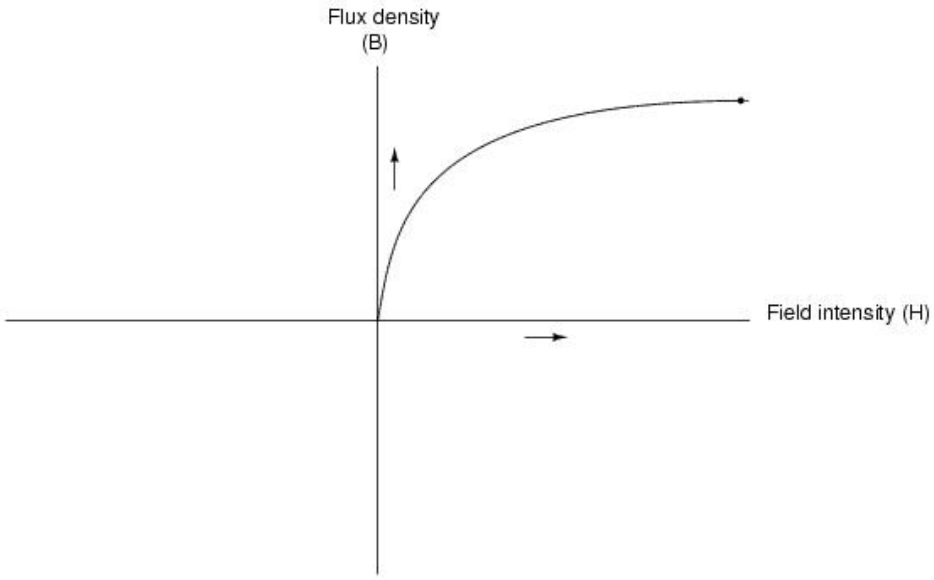

Γράφημα Ε.1
Καμπύλη κορεσμού τυπικού σιδηρομαγνητικού υλικού

Μαγνητική υστέρηση. Ως μαγνητική υστέρηση ορίζεται η ιδιότητα των σιδηρομαγνητικών υλικών να «καταγράφουν» την ιστορία μαγνήτισής τους. Με άλλα λόγια, η μαγνήτιση ενός σιδηρομαγνητικού υλικού δεν εξαρτάται μόνο από το εξωτερικά επιβαλλόμενο μαγνητικό πεδίο, αλλά και από την προηγούμενη κατάσταση μαγνήτισής του. Η υστέρηση οφείλεται σε τρία φαινόμενα: στην αλληλεπίδραση μεταξύ μαγνητικών τομέων, στην ανομοιομορφία του υλικού, καθώς και σε δυνάμεις τριβής προκαλούμενες από κρυσταλλικές ατέλειες. Το γράφημα Ε.2 παρουσιάζει τους τύπους βρόχων υστέρησης ενός τυπικού σιδηρομαγνητικού υλικού.

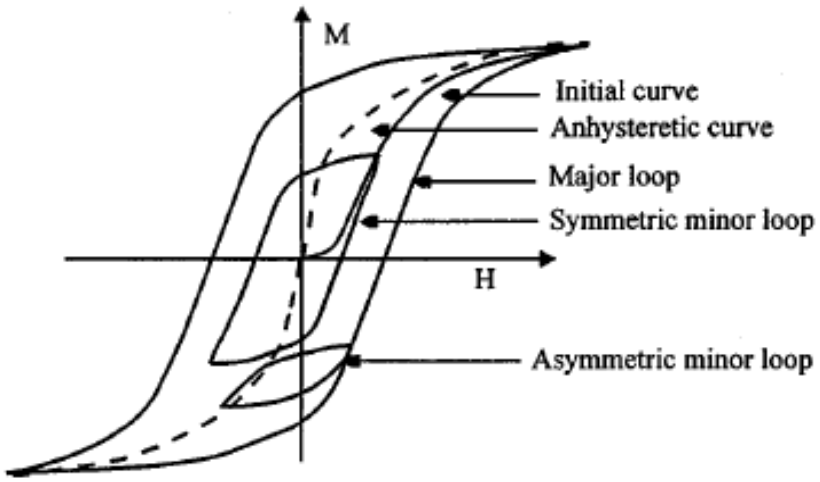

Γράφημα Ε.2
Τύποι βρόχων υστέρησης

Δινορρεύματα. Όταν ένα ηλεκτρικά αγώγιμα υλικό βρίσκεται εντός ενός μεταβαλλόμενου μαγνητικού πεδίου, επάγονται σε αυτό ηλεκτρικά ρεύματα. Τούτο συμβαίνει και στους μαγνητικούς πυρήνες των μετασχηματιστών. Τα ρεύματα αυτά ονομάζονται δινορρεύματα, λόγω της διεύθυνσής τους (σε μορφή δίνης). Η μοντελοποίηση των δινορρευμάτων είναι σχετικά πολύπλοκη, εξαιτίας της εξάρτησής τους από τη συχνότητα (η συχνότητα ορίζει το βάθος διείσδυσης του ηλεκτρομαγνητικού πεδίου εντός της μαγνητικής λαμαρίνας του πυρήνα, και συνεπώς την επαγόμενη ηλεκτρεγερτική δύναμη).

Στη συνέχεια θα εξετάσουμε τις κυριότερες μοντελοποιήσεις των μη γραμμικών φαινομένων του μαγνητικού πυρήνα των μετασχηματιστών.

Μαγνητικός κορεσμός. Υπάρχουν πολλές μαθηματικές περιγραφές της καμπύλης κορεσμού ενός σιδηρομαγνητικού υλικού, διάγραμμα Ε.1. Οι πιο διαδεδομένες είναι οι ακόλουθες:

- *Πολυωνυμική*, εξίσωση (Ε.2):

  $$i = A'\phi + B'\phi^n \qquad \text{(Ε.2)}$$

  Η τάξη του πολυωνύμου n μπορεί να υπολογισθεί από την ονομαστική ισχύ του μετασχηματιστή.

- *Υπερβολική*, της μορφής (Ε.3):

  $$H = \alpha \cdot \sinh(\beta \cdot B) \qquad \text{(Ε.3)}$$

  Με τις παραμέτρους α, β να προσδιορίζονται από πειραματικές μετρήσεις.

- *Εκθετική*, και
- *Τοξ εφαπτομενική*.

Μαγνητική υστέρηση. Μια πιο ακριβής μοντελοποίηση του μαγνητικού πυρήνα οφείλει να συμπεριλαμβάνει και το φαινόμενο της υστέρησης. Τα μοντέλα αυτά, στα οποία η υστέρηση και ο κορεσμός μοντελοποιούνται παράλληλα, μπορούν να ταξινομηθούν σε δύο κατηγορίες:

- *Μικροσκοπικής προσέγγισης*, στα οποία το φαινόμενο της υστέρησης περιγράφεται από τους φυσικούς νόμους που το διέπουν. Τα μοντέλα αυτά ενδείκνυνται για την κατανόηση του φαινομένου, ωστόσο, χαρακτηρίζονται από μεγάλη πολυπλοκότητα, ενώ συχνά είναι αδύνατος ο προσδιορισμός των παραμέτρων τους. Το πιο διαδεδομένο μικροσκοπικό μοντέλο είναι αυτό του Preisach.
- *Μακροσκοπικής προσέγγισης*, όπου επιδιώκεται η ταύτιση της μακροσκοπικής συμπεριφοράς του υλικού με τα αποτελέσματα της προσομοίωσης. Τα μοντέλα αυτά συχνά αδιαφορούν για τη φυσική που διέπει το φαινόμενο, ορισμένα δε είναι απλά μαθηματικές προσεγγίσεις των μετρήσεων.

Το μοντέλο του Preisach περιγράφεται από την εξίσωση (Ε.4) – ισοδύναμα από την εξίσωση (Ε.5). Πρόκειται ουσιαστικά για μία προσέγγιση στην οποία το μαγνητικό υλικό αποτελείται από άπειρο πλήθος μοναδιαίων στοιχείων, καθένα από τα οποία μπορεί να βρίσκεται σε μία από δύο ορισμένες μαγνητικές καταστάσεις (στοιχεία relay). Η γεωμετρική περιγραφή του μοντέλου, βάσει της εξίσωσης (Ε.5), φαίνεται στο γράφημα Ε.3, όπου το ισοσκελές τρίγωνο απεικονίζει τον κύριο βρόχο υστέρησης του μαγνητικού υλικού.

$$f(t) = \iint_{\alpha \geq \beta} \mu(\alpha, \beta) \hat{\gamma}_{\alpha\beta} u(t) d\alpha d\beta \tag{Ε.4}$$

$$f(t) = \iint_{S^+(t)} \mu(\alpha, \beta) d\alpha d\beta - \iint_{S^-(t)} \mu(\alpha, \beta) d\alpha d\beta \tag{Ε.5}$$

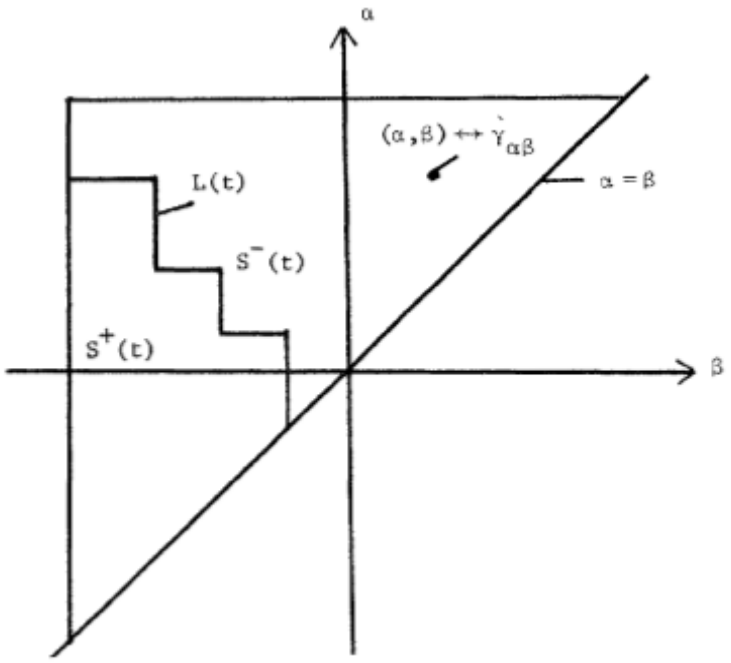

Γράφημα Ε.3
Γεωμετρική ερμηνεία του μοντέλου Preisach

Οι τροποποιήσεις του κλασσικού μοντέλου στοχεύουν αφενός στην απλοποίηση της μαθηματικής περιγραφής, αφετέρου στην ακριβέστερη μοντελοποίηση.

Το μοντέλο Stoner-Wolhfarth, είναι ακόμη ένα μικροσκοπικό μοντέλο, στο οποίο η μαγνήτιση του υλικού περιγράφεται μέσω της περιστροφής μοναδιαίων στοιχείων (magnetic particles) στη φορά διεύθυνσης του εξωτερικού μαγνητικού πεδίου. Το μοντέλο αυτό, ωστόσο, δεν εμφανίζει ιδιαίτερο πρακτικό ενδιαφέρον.

Το μοντέλο Globus, περιγράφει τη μαγνήτιση του υλικού μέσω της κίνησης των ορίων (wall – τοίχος) του μαγνητικού τομέα εντός της μέσης κρυσταλλικής κυψελίδας. Πρόκειται για ακόμη ένα μικροσκοπικό μοντέλο, που όμως δεν μπορεί να εφαρμοστεί – ακόμη – για πρακτικούς σκοπούς.

Ένα πολύ διαδεδομένο μακροσκοπικό μοντέλο είναι αυτό των Jiles καιAtherton. Η μαθηματική περιγραφή του μοντέλου γίνεται με το σύστημα εξισώσεων (Ε.6). Το γράφημα Ε.4 παρουσιάζει τον κύριο βρόχο υστέρησης για διάφορες τιμές των παραμέτρων του μοντέλου.

$$\begin{cases} \dfrac{dM_{irr}}{dH} = \dfrac{M_{an}(H) - M_{irr}(H)}{\delta k - \alpha\left(M_{an}(H) - M_{irr}(H)\right)} \\ \dfrac{dM_{rev}}{dH} = c\left(\dfrac{dM_{an}}{dH} - \dfrac{dM_{rev}}{dH}\right) \\ \dfrac{dM}{dH} = \dfrac{dM_{rev}}{dH} + \dfrac{dM_{irr}}{dH} \end{cases} \tag{E.6}$$

Όπου η μεταβλητή δ καθορίζεται από τη διεύθυνση μεταβολής του επιβαλλόμενου μαγνητικού πεδίου:

$$\delta = sign(dH) \tag{E.7}$$

Το μοντέλο Hodgdon είναι ένα ακόμη μοντέλο μακροσκοπικής προσέγγισης που ορίζεται από την εξίσωση (Ε.8) – ισοδύναμα από την εξίσωση (Ε.9). Στη δυαδική του μορφή περιγράφεται από τις εξισώσεις (Ε.10) και (Ε.11) αντίστοιχα. Η δυαδική μορφή του μοντέλου προσφέρεται για την περιγραφή φαινομένων υστέρησης που εξαρτώνται από το ρυθμό μεταβολής του μαγνητικού πεδίου.

$$\dot{B} = \alpha\left|\dot{H}\right|\left|f(H) - B\right| + \dot{H}g(H) \tag{E.8}$$

$$\frac{dB}{dH} = \begin{cases} \alpha\left|f(H) - B\right| + g(H) & for \quad \dot{H} > 0 \\ -\alpha\left|f(H) - B\right| + g(H) & for \quad \dot{H} < 0 \end{cases} \tag{E.9}$$

$$\dot{H} = \alpha\left|\dot{B}\right|\left|\tilde{f}(B) - H\right| + \dot{B}\tilde{g}(B) \tag{E.10}$$

$$\frac{dB}{dH} = \begin{cases} \left(\alpha\left|\tilde{f}(B) - H\right| + \tilde{g}(B)\right)^{-1} & for \quad \dot{H} > 0 \\ \left(-\alpha\left|\tilde{f}(B) - H\right| + \tilde{g}(B)\right)^{-1} & for \quad \dot{H} < 0 \end{cases} \tag{E.11}$$

Οι συναρτήσεις του μοντέλου πρέπει να ικανοποιούν ορισμένους περιορισμούς, οι οποίοι μπορούν να βρεθούν στο πρωτότυπο αγγλικό κείμενο (παράγραφος 2.4.2.7).

Ο πίνακας Ε.1 αποτελεί μία περιεκτική σύγκριση μεταξύ των τεσσάρων πιο διαδεδομένων μοντέλων υστέρησης (Preisach, Stoner-Wolhfarth, Globus, Jiles-Atherton). Δεν πρέπει να ληφθεί ως κανόνας, παρά μάλλον ως αναφορά για το ποιο μοντέλο ενδείκνυται για ποιο υλικό και ποια προσομοίωση.

	Stoner-Wolhfarth	***Jiles-Atherton***	***Globus***	***Preisach***
Mechanism	Rotation	Not specified	Wall motion	Not specified
Anisotropy	uniaxial	multi-axis	multi-axis	Not specified
Interaction	yes	yes	no	Moving model
Pinning	yes	yes	yes	Not specified
Texture	Anisotropic or isotropic	isotropic	uniaxial	Not specified
Wall energy	no	no	yes	No
Reversibility	yes	Additional model	yes	Additional model
Minor loops	yes	Approximation	-	Yes
Demagnetization	-	yes	-	Yes
Anhysteretic	yes	yes	yes	Yes
Parameters ***Measurable parameters ****	$M_s^*, K_u^*,$ $\overline{\eta}^*, \sigma, \alpha, p$	$M_s^*, c^*,$ a^*, α^*, k^*	$M_s^*, \gamma^*,$ R^*, f^*	$\mu(\alpha, \beta)$
Grains	Single domain	Multi-domain	Bi-domain	Not specified
Computational time	+++	++	+	++++
Materials	Hard magnetic materials	Bulk materials Medium ferrites	Soft ferrites	Magn. recording Thin films

Πίνακας Ε.1
Σύγκριση μοντέλων υστέρησης

Δινορρεύματα. Τα δινορρεύματα αποτελούν παράγοντα απόσβεσης κατά τη μεταβατική συμπεριφορά του μετασχηματιστή. Η ακριβής μοντελοποίησή τους είναι, λοιπόν, μεγάλης σημασίας.

Η πιο απλή και διαδεδομένη μοντελοποίηση των δινορρευμάτων είναι μέσω μίας ωμικής αντίστασης σταθερής τιμής, συνδεδεμένης παράλληλα με την εμπέδηση του τυλίγματος. Ωστόσο, αυτή η περιγραφή δε λαμβάνει υπόψη την εξάρτηση από την τάση και τη συχνότητα, που παρουσιάζουν οι απώλειες δινορρευμάτων. Δεν μπορεί επίσης να βρει εφαρμογή όταν η λειτουργία του μετασχηματιστή εμφανίζει ασυμμετρίες. Η εξίσωση (Ε.12) χρησιμοποιείται για τον υπολογισμό της παράλληλης αντίστασης που περιγράφει τα δινορρεύματα. Ορισμένες τροποποιήσεις αυτής της προσέγγισης χρησιμοποιούν αντίσταση μεταβλητής τιμής για να περιγράψουν την εξάρτηση από την τάση, εξίσωση (Ε.13). Η εξάρτηση από τη συχνότητα συνεχίζει όμως να αποτελεί ένα πρόβλημα για αυτή την αναπαράσταση.

$$R_k = \frac{V_{n,pri}^2}{3P_{loss}} \tag{Ε.12}$$

$$R_k(V) = \frac{V_{pri}(t)}{I_{pri}(t)} \tag{Ε.13}$$

Εκτός από την αναπαράσταση μέσω παράλληλα συνδεδεμένης ωμικής αντίστασης, η μοντελοποίηση των δινορρευμάτων μπορεί να γίνει και με ορισμένα ισοδύναμα κυκλώματα (αναπτύγματα σειράς και παράλληλα). Το μοντέλο συνεχών κλασμάτων (continued fraction) είναι το καταλληλότερο για τον αριθμητικό υπολογισμό των απωλειών λόγω δινορρευμάτων. Ωστόσο, όλα τα ισοδύναμα κυκλώματα που χρησιμοποιούνται για την περιγραφή των δινορρευμάτων πρέπει να συνδυαστούν κατάλληλα με αντίστοιχα μοντέλα για την περιγραφή των φαινομένων της μαγνητικής υστέρησης και του μαγνητικού κορεσμού.

Μία πολύ ενδιαφέρουσα προσέγγιση για το συνδυασμό όλων των μη γραμμικών φαινομένων που εμφανίζονται στο μαγνητικό πυρήνα του μετασχηματιστή παρουσιάζεται στην παράγραφο παρουσιάζεται στη συνέχεια. Σε αυτήν την προσέγγιση, η οποία βασίζεται στο μοντέλο Jiles-Atherton, η τιμή της έντασης του μαγνητικού πεδίου τροποποιείται κατάλληλα πριν οδηγηθεί ως είσοδος στο σύστημα εξισώσεων (Ε.6), ώστε να συμπεριλαμβάνει τις απώλειες λόγω δινορρευμάτων. Οι απώλειες αυτές διαχωρίζονται αρχικά στις «κλασσικές» απώλειες δινορρευμάτων και στις υπερβάλλουσες απώλειες. Ο διαχωρισμός αυτός είναι απαραίτητος, καθώς οι απώλειες που υπολογίζονται με την κλασσική αναπαράσταση των δινορρευμάτων είναι σημαντικά διάφορες των πειραματικά μετρούμενων, η διαφορά τους αυτή είναι οι προαναφερθείσες υπερβάλλουσες απώλειες. Η εξίσωση (Ε.14), με κατάλληλο υπολογισμό των παραμέτρων και σε συνδυασμό με το μοντέλο Jiles-Atherton, ίσως είναι σε θέση να περιγράψει συνολικά το μαγνητικό υλικό με απλότητα και ακρίβεια.

$$H_{tot} = H_{hyst} + H_{cls} + H_{exc} = H_{hyst} + k_1 \frac{dB}{dt} + k_2 \left(\frac{dB}{dt} \right)^{\frac{1}{2}} \qquad \text{(Ε.14)}$$

3. Δυαδικότητα

Η θεωρία της δυαδικότητας μεταξύ μαγνητικών και ηλεκτρικών κυκλωμάτων μπορεί να βρει εφαρμογή στη μοντελοποίηση του τριφασικού μετασχηματιστή τύπου πυρήνα. Οι βασικές ισοδυναμίες μεταξύ ηλεκτρικών και μαγνητικών ποσοτήτων περιγράφονται από την ακόλουθη ισοδυναμία:

$$\begin{cases} e \leftrightarrow d\Phi / dt \\ i \leftrightarrow MMF \\ \vec{S} \leftrightarrow 1 / \vec{Z} \end{cases}$$

Τα δυαδικά μοντέλα είναι σε θέση να ενσωματώσουν τις απώλειες πυρήνα με τη χρησιμοποίηση μιγαδικής μαγνητικής διαπερατότητας. Το πραγματικό μέρος της μαγνητικής αντίστασης θα μετασχηματιστεί σε ηλεκτρική επαγωγή, ενώ το φανταστικό θα μετασχηματιστεί σε ωμική αντίσταση.

Τα μοντέλα μετασχηματιστών που βασίζονται στην αρχή της δυαδικότητας ηλεκτρικού-μαγνητικού κυκλώματος χαρακτηρίζονται από απλότητα, ενώ μπορούν εύκολα να ενσωματωθούν σε υπάρχοντα προγράμματα για την προσομοίωση ηλεκτρικών δικτύων. Οι κυριότεροι περιορισμοί αυτών των μοντέλων είναι, ωστόσο, οι εξής:

- Όταν το μαγνητικό κύκλωμα του μετασχηματιστή δεν αποτελεί επίπεδο γράφο, δεν είναι γενικά άμεση η ανάπτυξη ενός δυαδικού ηλεκτρικού κυκλώματος. Είναι, βέβαια, δυνατή με την προσθήκη ορισμένων στοιχείων με αρνητικές τιμές, κατά τρόπο ώστε να ικανοποιούνται οι βασικές εξισώσεις του περιγράφουν την τοπολογία του μετασχηματιστή. Τα αρνητικά αυτά στοιχεία, όμως, δεν είναι εύκολο να προσδιορισθούν.
- Τα δυαδικά μοντέλα αναπτύσσονται υπό την προϋπόθεση σταθερής συχνότητας λειτουργίας. Για αυτό το λόγο δεν πρέπει να χρησιμοποιούνται για την προσομοίωση μεταβατικών καταστάσεων.

Στη συνέχεια εφαρμόζεται η αρχή της δυαδικότητας μαγνητικού-ηλεκτρικού κυκλώματος για την ανάπτυξη ενός ηλεκτρικού μοντέλου του τριφασικού μετασχηματιστή τύπου πυρήνα. Η πορεία ανάπτυξης του ηλεκτρικού ισοδύναμου κυκλώματος από την πραγματική γεωμετρία του μετασχηματιστή φαίνεται στο γράφημα Ε.4. Το τελικό ισοδύναμο ηλεκτρικό κύκλωμα δίνεται στο σχήμα Ε.4(c), όπου δεν έχουν σχεδιασθεί οι απαραίτητοι μετασχηματιστές απομόνωσης (με λόγο μετασχηματισμού 1:1), για λόγους απλότητας.

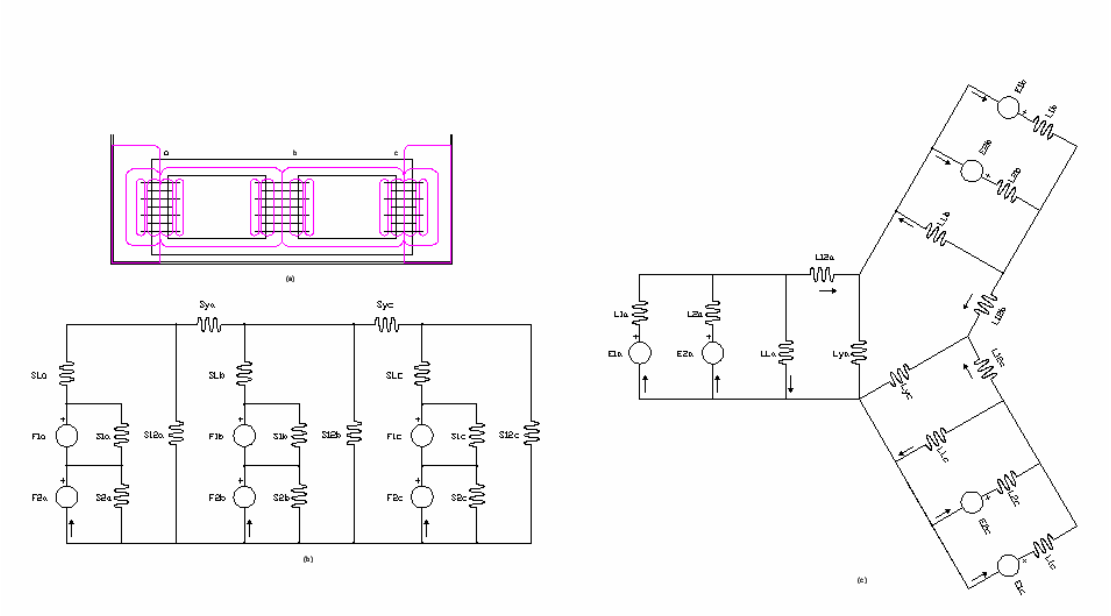

Γράφημα Ε.4
Ισοδύναμο κύκλωμα του τριφασικού μετασχηματιστή τύπου πυρήνα.
(a) Μέσες μαγνητικές διαδρομές
(b) Απλοποιημένο μαγνητικό κύκλωμα
(c) Ισοδύναμο ηλεκτρικό κύκλωμα

4. Αποσυζευγμένα κυκλώματα

Η προσέγγιση των αποσυζευγμένων ηλεκτρικών-μαγνητικών κυκλωμάτων είναι ουσιαστικά ο πιο προφανής τρόπος επίλυσης του συστήματος εξισώσεων (Ε.1) για το μετασχηματιστή. Στην παρούσα εργασία αναπτύσσεται ένα υπολογιστικό μοντέλο ενός τριφασικού μετασχηματιστή τύπου πυρήνα (δύο τυλιγμάτων), οι λεπτομέρειες του οποίου βρίσκονται στα παραρτήματα Α ως C. Το απλοποιημένο μαγνητικό κύκλωμα του μοντέλου φαίνεται στο γράφημα Ε.5.

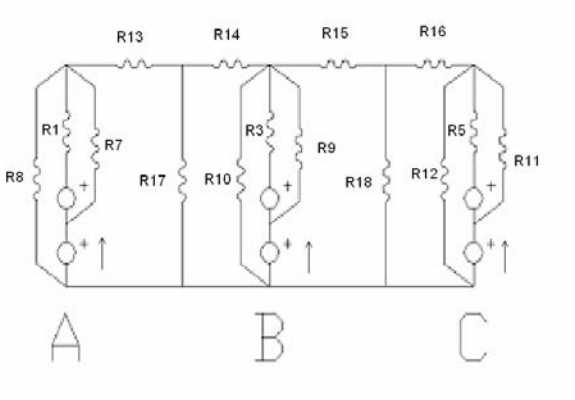

Γράφημα Ε.5
Μαγνητικό ισοδύναμο κύκλωμα

Το μοντέλο περιγράφεται μαθηματικά από τις εξισώσεις κατάστασης, εξισώσεις (Ε.15) και (Ε.16).

$$\dot{\underline{\phi}}_s = f\left(t, \underline{\phi}_s\right) = A\left(\underline{\phi}_s\right) \cdot \underline{\phi}_s + B \cdot \underline{u}_{pri}(t) \tag{Ε.15}$$

$$\underline{i}_s = C\left(\underline{\phi}_s\right) \cdot \underline{\phi}_s \tag{Ε.16}$$

Ως μεταβλητές κατάστασης λαμβάνονται οι πυκνότητες μαγνητικής ροής μέσω των έξι τυλιγμάτων. Για την επίλυση της εξίσωσης (Ε.15) είναι απαραίτητη η εφαρμογή προηγμένων αριθμητικών μεθόδων, συγκεκριμένα χρησιμοποιείται ο αλγόριθμος Runge-Kutta $4^{ης}$ τάξης. Το γράφημα 4.2 του πρωτοτύπου αποτελεί το διάγραμμα ροής του υπολογιστικού προγράμματος. Το πρόγραμμα αναπτύχθηκε σε γλώσσα C.

Ορισμένα αποτελέσματα προσομοίωσης για το μετασχηματιστή με τα χαρακτηριστικά του πίνακα 4.1 μπορούν να βρεθούν στην παράγραφο 4.3 του πρωτοτύπου. Μπορούμε να παρατηρήσουμε την ασυμμετρία που παρουσιάζει ο τριφασικός μετασχηματιστής τύπου πυρήνα λόγω της τοπολογίας του (π.χ. στο γράφημα 4.4). Με αντιπαράθεση των γραφημάτων (4.18) ως (4.21) μπορούμε επίσης να διαπιστώσουμε την επίδραση της παραμέτρου που περιγράφει τις απώλειες λόγω δινορρευμάτων (k_1).

5. Συμπεράσματα

Η μοντελοποίηση του τριφασικού μετασχηματιστή τύπου πυρήνα οφείλει να συμπεριλαμβάνει όλα τα μη γραμμικά φαινόμενα που εμφανίζονται στο μαγνητικό πυρήνα. Ο συνδυασμός των ξεχωριστών μοντέλων, όμως, σε ένα ενιαίο υπολογιστικό πλαίσιο δεν είναι εύκολος.

Ένα ιδιαίτερο πρόβλημα που παρουσιάζεται κατά τη μοντελοποίηση είναι η έλλειψη των απαραίτητων δεδομένων. Τα φύλλα δοκιμών των μετασχηματιστών δεν περιέχουν ουσιαστικά καμία πληροφορία για το υλικό του μαγνητικού πυρήνα, με αποτέλεσμα ο διαχειριστής του δικτύου να μην είναι σε θέση να μοντελοποιήσει τους μετασχηματιστές του.

Όπως μπορούμε να παρατηρήσουμε από τα ενδεικτικά αποτελέσματα της προσομοίωσης, υπάρχει ασυμμετρία στις διαφορετικές φάσεις του μετασχηματιστή. Αυτή η ασυμμετρία είναι άμεση συνέπεια της τοπολογίας του μαγνητικού κυκλώματος του τριφασικού μετασχηματιστή τύπου πυρήνα.

Ως προς το αναπτυχθέν μοντέλο, μπορούμε να παρατηρήσουμε τα εξής:

- Η προσομοίωση της συμπεριφοράς του τριφασικού μετασχηματιστή τύπου πυρήνα περιορίστηκε στην εν κενώ λειτουργία. Αυτό οφείλεται στην αριθμητική αστάθεια του μοντέλου όταν συνδεόταν το φορτίο στο δευτερεύον.
- Όπως ήδη αναφέρθηκε, ήταν αδύνατος ο προσδιορισμός των παραμέτρων του μοντέλου (λόγω αφενός των ελλιπών δεδομένων, αφετέρου της μη ύπαρξης πειραματικής μετρητικής διάταξης), έτσι ώστε τελικά τα αποτελέσματα της προσομοίωσης να μην μπορούν να γίνουν αποδεκτά χωρίς τη δέουσα αμφισβήτηση.

Οι κυριότερες προτάσεις για μελλοντική έρευνα θα μπορούσαν να είναι:

- Συνδυασμός των μοντέλων που περιγράφουν τη μαγνητική υστέρηση με τα μοντέλα που περιγράφουν τα δινορρεύματα σε ένα ενιαίο υπολογιστικό μοντέλο.
- Συστηματική προσπάθεια προσδιορισμού των παραμέτρων των διάφορων μοντέλων για διαφορετικούς τύπους μαγνητικών υλικών. Επιπλέον προτείνεται ο προσδιορισμός κάποιων τυπικών τιμών των παραμέτρων αυτών για διαφορετικές κλάσεις ισχύος των μετασχηματιστών.
- Μελέτη της επίδρασης του φορτίου στη μεταβατική συμπεριφορά του τριφασικού μετασχηματιστή τύπου πυρήνα.
- Ενσωμάτωση της χωρητικής σύζευξης των τυλιγμάτων, ώστε να είναι δυνατή η προσομοίωση υψίσυχνων μεταβατικών καταστάσεων (π.χ. κεραυνικά πλήγματα).

ΠΕΡΙΛΗΨΗ

Τα μοντέλα μετασχηματιστών είναι απαραίτητα για την προσομοίωση των σύγχρονων δικτύων ηλεκτρικής ενέργειας, τόσο κατά τη μόνιμη όσο και για τη μεταβατική κατάσταση λειτουργίας τους. Υπάρχουν πολλές δυνατότητες μοντελοποίησης που μπορούν να βελτιώσουν την προσομοίωση, περιλαμβάνοντας τα φαινόμενα του μαγνητικού κορεσμού του πυρήνα, της εξάρτησης από τη συχνότητα λειτουργίας, της χωρητικής σύζευξης των τυλιγμάτων, και της τοπολογίας του πυρήνα και των τυλιγμάτων. Η μοντελοποίηση του τριφασικού μετασχηματιστή τύπου πυρήνα έχει ιδιαίτερη σημασία, καθώς ο τελευταίος είναι ο πιο διαδεδομένος τύπος μετασχηματιστή στα δίκτυα ηλεκτρικής ενέργειας.

Η παρούσα εργασία είναι μια ανασκόπηση των μοντέλων μετασχηματιστών για προσομοιώσεις μεταβατικών καταστάσεων λειτουργίας (για χαμηλές συχνότητες). Σημαντικές σχετικές εργασίες παρουσιάζονται και σχολιάζονται, ενώ παράλληλα εξετάζονται αναλυτικά τα μη γραμμικά φαινόμενα των μετασχηματιστών, με σκοπό την παραπέρα ανάπτυξη και βελτίωση της μοντελοποίησής τους. Τέλος, αναπτύσσεται εν μέρει ένα υπολογιστικό μοντέλο του τριφασικού μετασχηματιστή τύπου πυρήνα για προσομοιώσεις με ηλεκτρονικό υπολογιστή.

Λέξεις Κλειδιά: Μοντέλα μετασχηματιστών, προσομοίωση, μαγνητικός πυρήνας, υστέρηση, κορεσμός, δινορρεύματα

ABSTRACT

Transformer models are essential for the steady-state as well as the transient simulation of modern power networks. Many opportunities exist to improve the simulation of its complicated behavior, which include magnetic saturation of the core, frequency-dependency, capacitive coupling, and topologically correctness of core and coil structure. The three-phase core-type transformer is of special interest, as it is the most common transformer used in power networks.

This work presents a review of transformer models for simulation of low-frequency transients. Salient points of key references are presented and discussed in order to give an accessible overview of development, implementation and limitations of the most useful models proposed to date. Techniques for representation of the most important phenomena are examined, with the intent of providing the needed foundation for continued development and improvement of transformer models. A computer model is being partly developed for the simulation of the three-phase core-type transformer.

Index Terms: Transformer modeling, simulation, magnetic core, hysteresis, saturation, eddy currents

ACKNOWLEDGEMENTS

This work was done at the Technical University of Berlin under an Erasmus Exchange with the Technical University of Athens. The author would like to thank the European Union for giving him the ability to participate for six months in the life of another university. It was not only my working with new people in another language, but also the vivid life – educational, personal and cultural – in such an interesting metropolis as Berlin that made my exchange time a unique experience. I hope a part of this experience will also be reflected in the present work.

I would also like to personally thank some people, whose assistance was very important for this work:

First of all, my professor at the Technical University of Berlin Prof. Dr.-Ing. Rolf Hanitsch for his advice and support. Even in the middle of his various occupations he would always give me one useful piece of advice.

Yiury Plotkin, currently working on his PhD thesis at TU Berlin, was the one I turned to almost every time I faced a problem. I would like to thank him for the interest he gave to my questions and I hope my work will be of some use to him.

Finally, there are some people whose contribution to this work cannot be seen at first glance, but whom I would also like to thank:

Prof. Friedrich Veuhoff of the Technische Fachhochschule Berlin gave me plenty of information on the software Electro Magnetic Transient Program, which was, however, not used in this work.

Prof. Ewart Fuchs of the University of Colorado at Boulder has granted me some of his precious holiday time as well as his permission to build on a previous work of him [81].

Modeling an electrical transformer is not a trivial work. Many researchers have dedicated their whole lives in modeling not even the transformer as a whole, but just one single part of it. I would like to apologize for the rather superficial way the subject will be presented here. The reader is kindly asked to realize that six months (the time specified for a diploma thesis) is an extremely short period, in which I had to first get to know what is happening inside a transformer, in order to then model it.

CONTENTS

APPENDICES

ILLUSTRATIONS

TABLES

1. Introduction

Transformers are perhaps the most important elements in electrical power networks; not only do they allow for cheap and efficient transportation of electrical power, but they also posses some control features that contribute to the stability of the electric systems – phase shifting, tap changing. It is this great importance that has made the need for accurate and simple transformer models so intense, even from the very early years of the electricity era.

1.1 About Modeling

Modeling is one of the most important tasks an engineer has to fulfill. A model has to incorporate the Physics which describes the operation of the modeled apparatus in a well-defined relationship between input and output, thus substituting it with a "black box" in the eyes of an external observer. In other words, modeling is a procedure of simplifying a set of physical equations to a sole input-output function $output = f(input)$. Representing the various elements of a network with their corresponding models allows the connection between these elements in a way that the output of one model is driven as input to the other. This is very useful because one can combine very different areas of Physics and solve them all together as a simple system.

However, care should be taken when defining a model. Following questions must first be answered before continuing with the development of a model:

- **What do I need the model for?**

  One must know from before which purpose is the model going to serve. It is this purpose which will define what the inputs and the outputs of the model should be.

- **What are the Physics involved?**

  Every device in the real world is described by a set of physical equations. These equations must be carefully investigated before proceeding with modeling.

- **What are the restrictions of the specific model?**

  In order to build a model, which is accurate, but in the same time easy to solve, one should simplify the set of physical equations stated above. It is during this simplification that the restrictions of the model are introduced. A well-defined model should always be accompanied by these restrictions of use.

1.2 Transformer Models

There are numerous models of transformers. They can be categorized with various criteria, among others:

1. With respect to the scope of view:
    a. Electrical models
    b. Mechanical models
    c. Thermal models
2. With respect to the time domain:
    a. Steady-state models
    b. Transients' models
3. With respect to the necessary accuracy:
    a. Models for system studies – low accuracy
    b. Atomic models (interest only for the specific item) – high accuracy
4. With respect to the modeled transformer itself:
    a. One-phase transformer models
    b. Three-phase transformer models (core-type)
    c. Three-phase transformer models (shell-type)
5. With respect to the analysis' approach:
    a. Duality-based models
    b. Decoupled electric-magnetic models
    c. Matrix representation

1.3 Objective of the present work and modus operandi

The present work is confined in modeling the **three-phase core-type transformer**, with respect to its electrical behavior during normal, but mostly during abnormal operation. The transformer is modeled with high accuracy for low-frequency transient phenomena and various operating conditions are simulated. The response of the transformer is studied and conclusions regarding power quality and emission of harmonics are reached.

More analytically, the structure of this work is as following:

In the second chapter we will present the necessary theory for transformer modeling. The main characteristics of a transformer will be briefly discussed and models for the various effects (saturation, hysteresis, eddy currents) that are observed during transformer operation will be presented. This approach will mainly focus on the magnetic core, as this is the most important part for low-frequency phenomena.

In the third chapter the principle of duality will be introduced. After presenting the basic theory, we will apply it to a three-phase core-type transformer, in order to finally get a duality-based model for such a transformer.

In the fourth chapter we will present the decoupled electric-magnetic approach. Again, a model for a three-phase core-type transformer will be formed. The model will also be written in C programming language for computer simulations.

Finally, the fifth and last part of this work is dedicated to some general comments, conclusions and proposals for further development.

2. Basic Theory

2.1 Transformer

Definition 1

An electrical transformer is every apparatus used for the transformation of electrical power.

The main characteristics of electrical power – also called electricity – that can be transformed are the following:

- Voltage level
- Frequency

The only characteristic which is not allowed to change significantly during a "transformation" of electrical power is the power itself, this means that a generator or a load are no electrical transformers.

The previous, general definition includes not only the "traditional" electromagnetic transformers, but also the newer static transformers like rectifiers and inverters, which are based on power electronics technology. It even includes the combination of two electrical machines with different number of poles coupled on the same shaft which was used in the past for the transformation of frequency, the so-called cyclotransformer.

In this work we will deal with the "traditional" transformers, so we are obliged to give here a definition for this kind of transformers.

Definition 2

A transformer is an apparatus which couples a set of electrical circuits through a common magnetic core.

Let us now analyze the main terms of this definition:

- ***Transformer***: the electrical power is transformed first to magnetic power and then back to electrical once again. The physical laws governing this transformation are described by Maxwell's Equations.
- ***Set of electrical circuits***: a transformer may have various inputs and outputs. However, the terms input and output are only a matter of convention: they just refer to power flow through the transformer. Which electrical circuit is input and which output plays absolutely no role to the operation of a transformer.
- ***Common magnetic core***: The coupling of the inputs and outputs of the transformer is done through a magnetic core. This core is usually from silicon steel, in order to achieve high efficiency. It is this magnetic core which introduces all the nonlinearities that make the analysis and modeling of the transformer a difficult task for the electrical engineer.

If one reads this definition, one would see that there is nothing said about voltage or frequency transformation (of course frequency transformation is not possible in a "traditional" transformer). This was intended, since there are transformers which do not change the voltage level, but only offer galvanic isolation (these transformers have a turn ratio 1:1).

2.2 Electromagnetism

The relationship between the electric field intensity $\vec{E}$ and the magnetic field intensity $\vec{H}$ is provided by the well known Maxwell's equations and can be found in every textbook of electromagnetism. One of the main characteristics of Maxwell's equations is the coupling between electric and magnetic field trough the time variation of the magnetic flux $\vec{B}$ and the displacement current $\vec{D}$. By omitting the source term of the displacement currents, the magnetic field can be determined independently from the electric field through the Ampere's circuital law [8]. This quasi-static approach is efficient for slowly time varying, low-frequency currents, which give rise to slowly varying fields. However, it must be emphasized that it is not suitable for studying high-frequency phenomena, such as the impact of lightning surges. Hence, at the present work, transformer modeling will be restricted in low-frequency phenomena, which can be described with the set of equations:

$$\begin{cases} \oint_C \vec{E}d\vec{l} = -\dfrac{d}{dt}\int_S \vec{B}d\vec{S} \\ \oint_C \vec{H}d\vec{l} = \int_S \vec{J}d\vec{S} \\ \oint_S \vec{B}d\vec{S} = 0 \\ \oint_S \vec{J}d\vec{S} = 0 \\ \vec{B} = \mu\vec{H} \\ \vec{J} = \sigma\vec{E} \end{cases} \tag{2.1}$$

2.3 The magnetic core

The most common type of core is a steel composed mainly of iron with a few percent of other materials, notably silicon. Nevertheless, regardless of the core composition, the term "iron" is used by engineers in praxis to describe the core's magnetic material. In this chapter we will present some of the magnetic materials used in transformers' cores.

There are five main groups of magnetically soft alloys classified by the chief constituents of the metal [1]. These are:

- **Low-carbon steel**. Sometimes described simply as cold-rolled steel, this is the cheapest and least sophisticated of the alloys. Compared with other materials it has relatively high losses and low permeability.
- **Silicon steel**. This was one of the first alloys to be used for cores and still the most common. Silicon steel consists mainly of iron with a small but significant addition of silicon in percentages of from about 1.0 to about 4.0 percent. This addition increases the electrical resistance, thus reducing the eddy currents (see §2.3.4), and also improves the material's stability. Silicon steel has a high saturation point, good permeability at high flux density and moderate losses. An important member of this group is grain-oriented silicon steel, which takes advantage of the fact that the easiest direction of magnetization is along the cube-spaced crystals of which the material is composed. Silicon steel in all its forms is widely used in power transformers [4], [10].

- **Nickel-Iron (Permalloy)**. This important alloy, consisting primarily of nickel and iron (with nickel-iron content from about 45 percent to over 85 percent), is characterized by exceedingly high initial permeability. Saturation occurs, however, at a relatively low flux density.
- **Cobalt-Nickel-Iron (Perminvar)**. In this material cobalt has been added to nickel and iron to produce an alloy that exhibits a substantially constant permeability and low hysteresis loss at low flux density.
- **Cobalt-Iron (Permendur)**. The mating of cobalt and iron yields an alloy having high permeability at high flux density and a very high saturation point.

After giving the main definitions and presenting the basic theory, we are ready to cope with the main problem of transformer modeling: the magnetic core.

2.3.1 Basic theory for magnetic materials

The total magnetic field $\vec{B}$ in a material is given by:

$$\vec{B} = \overrightarrow{B_0} + \mu_0 \overrightarrow{M} \tag{2.2}$$

where $\overrightarrow{M}$ is the magnetization of the material. The magnetic susceptibility χ_m specifies how much the relative permeability μ_r differs from one:

$$\chi_m = \mu_r - 1 \tag{2.3}$$

The larger the magnetic susceptibility (and thus the relative permeability), the larger the magnetization of the material. All technical materials are categorized by the value of their relative permeability μ_r into three groups:

- Diamagnetic ($\mu_r < 1$)
- Paramagnetic ($\mu_r \approx 1$)
- Ferromagnetic ($\mu_r >> 1$)

In most technical applications of electromagnetism, ferromagnetic materials are preferred. For this reason we will study the physics of magnetization in ferromagnetic materials a little further.

Ferromagnetic materials have a large and positive susceptibility to an external magnetic field. They exhibit a strong attraction to magnetic fields and are able to retain their magnetic properties after the magnetic field has been removed. Ferromagnetic materials have some unpaired electrons so their atoms have a net magnetic moment. They get their strong magnetic properties due to the presence of magnetic domains. In these domains, large numbers of atoms moments (10^{12} to 10^{15}) are aligned parallel so that the magnetic force within the domain is strong. When a ferromagnetic material is in the unmagnetized state, the domains are nearly randomly organized and the net magnetic field for the part as a whole is zero. When a magnetizing force is applied, the domains become aligned to produce a strong magnetic field within the part.

The magnetization of a material can be described by two main magnetization mechanisms, namely domain wall movement and magnetic moment rotation, or by a combination of these mechanisms.

The main characteristics of ferromagnetic materials are presented in the following paragraphs.

2.3.2 Saturation

In ferromagnetic materials the relative permeability shown in equation (2.3), and thus the magnetization $\vec{M}$, has no constant value. Instead, the value of μ_r in these materials depends largely on the magnetic field strength $\vec{H}$ applied to it.

The reason for this dependence lies again in the magnetic domains of the material. As more and more from these magnetic domains are forced to align with the external magnetic field, the value of the relative permeability will appear to fall. When almost all magnetic domains are aligned with the external field the relative permeability will reach the value 1, which means that the material will have lost its ferromagnetic character. The material is then called to be **saturated**. Since the magnetic field $\vec{B}$ in a material is related to the magnetic field strength $\vec{H}$ through the relative permeability μ_r (which has been shown for ferromagnetic materials to have a non constant value), the relationship between $\vec{B}$ and $\vec{H}$ has to be nonlinear. The nonlinear function $\vec{B}\left(\vec{H}\right)$ is the expression for the saturation of the ferromagnetic material. Figure 2.1 shows a saturation curve for a typical ferromagnetic material.

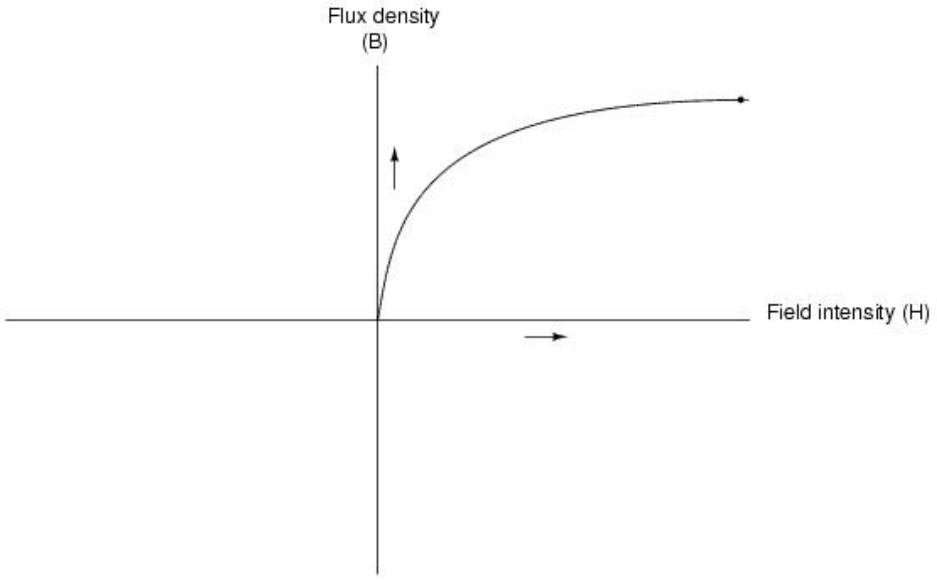

Figure 2.1
Saturation curve of a typical ferromagnetic material

2.3.3 Hysteresis

When a ferromagnetic material is magnetized in one direction, it reaches a state of minimum energy. This means that it will not relax back to zero magnetization when the imposed magnetizing field is removed. It must be driven back to zero by a field in the opposite direction. If an alternating magnetic field is applied to the material, its magnetization will trace out a loop called a hysteresis loop. The lack of retraceability of the magnetization curve is the property called hysteresis and it is related to the

existence of magnetic domains in the material. Once the material's domains are reoriented, it takes some energy to turn them back again.

Hysteresis can be caused by three types of phenomena: interaction between domains, anisotropy or internal frictional type pinning forces caused by crystallographic impurities, dislocations etc. The dominant cause varies with the material being studied.

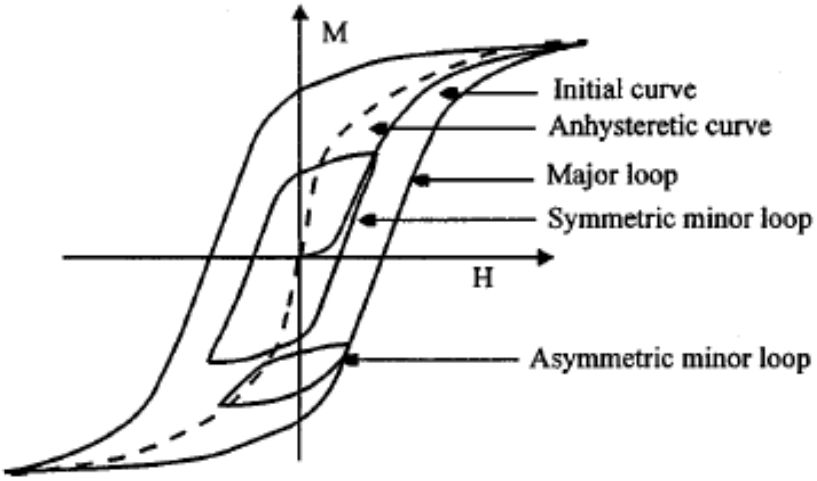

Figure 2.2
Hysteresis loops for a typical ferromagnetic material [1]

Figure 2.2 shows an $M(H)$ characteristic for a typical ferromagnetic material. With respect to this plot we can define some important terms concerning electromagnetic hysteresis:

Imagine a dc magnetic field applied on a formerly unmagnetized material. The $M(H)$ trace plotted is the **initial magnetization curve** (figure 2.2). Imagine now that, after reaching the saturation of the material, the applied magnetic field changes direction and is increased until the material reaches saturation again, but from the negative side. If this process is repeated, the **major hysteresis loop** illustrated in figure 2.2 is plotted. As already stated, the mechanism of hysteresis is general. This means that besides the major hysteresis loop at the ends of which the magnetic material is completely saturated, there is an infinite number of other, smaller hysteresis loops, which all lie inside the major hysteresis loop. These are the so-called **minor hysteresis loops**. The formation of a minor hysteresis loop is also illustrated in figure 2.2. Assume that we are ascending on the major hysteresis loop. Assume again that before reaching the positive saturation point, the applied magnetic field changes direction. Then the trace $M(H)$ will start to descend in a way similar to that of the major hysteresis loop, in fact it will asymptotically reach the major loop at the point of negative saturation. If the applied field changes direction again before reaching complete saturation, then the trace will start to ascend once again. The ascending branch will pass through the first reversal point and reach asymptotically the ascending branch of the major loop, unless the field changes direction again. As can be already seen, there is no limit of the order of minor loops, but they all have to lie within the boundaries of the major hysteresis loop. The minor loop described above is

[1] Source: [41], p. 418

an **asymmetric minor loop**. If the first reversal point lies on the initial curve, then it is also possible that **symmetric minor loops** are build.

In figure 2.2 there is also another curve, shown with the dotted line. This is the **anhysteretic magnetization curve**, which is of great importance for the modeling of magnetic materials. By definition, the anhysteretic curve is the $M(H)$ relationship that would be obtained if there was no hysteresis effect present in the material [41]. This means that each point of the anhysteretic curve corresponds to the domain configuration that gives the lowest possible energy or global energy minimum for a given external field, while points on a hysteresis curve correspond to domain configurations where the energy is only at a local minimum. Because of its special character, the anhysteretic curve cannot be measured directly. Instead, each point on the curve must be generated in a manner similar to the demagnetization process by superimposing a slowly decaying low-frequency ac magnetic field upon a constant dc bias field. Another proposed methodology is to apply normal ac excitation under different applied voltages. Connecting all tips of the major hysteresis loops plotted, the anhysteretic magnetization curve is formed (shown with the dotted line in figure 2.3). This curve is found to be located only in the first and third quadrants.

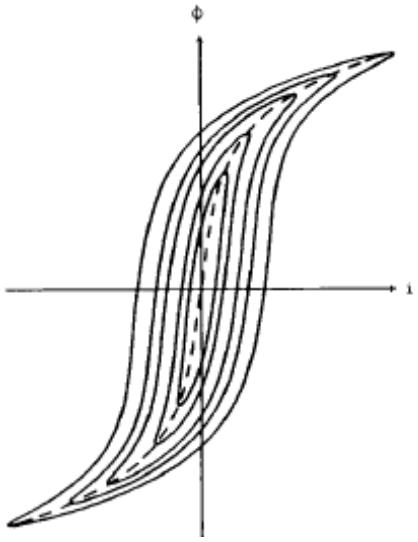

Figure 2.3
Anhysteretic magnetization loop[1]

The energy losses due to hysteresis are calculated by the area of the hysteresis loops. While the hysteresis of ferromagnetic materials is of use for some applications (like audio tape recording), it is not wanted in electrical power transformation, since it causes losses inside the magnetic core of the transformers in form of thermal energy. For this reason, transformer producers use ferromagnetic materials with narrow hysteresis loops. It must be stated that hysteresis losses depend on the operating voltage and frequency.

Saturation and hysteresis are not the only characteristics that introduce nonlinearities. There is also another important phenomenon when a conducting material (ferromagnetic materials are also conductors) lies in a time-varying magnetic field:

[1] source: [45], p. 2707

2.3.4 Eddy currents:

When a conducting material lies inside a time-varying magnetic field, voltages are induced to it according to Faraday's Law. The induced voltages produce currents which flow in eddies perpendicular to the direction of the magnetic field, the so-called eddy currents, which cause thermal losses inside the magnetic core of the transformers. For the elimination of these thermal losses the magnetic core of induction machines is constructed from very thin laminations of magnetic material, which are insulated to each other. Eddy currents losses are mostly frequency dependent.

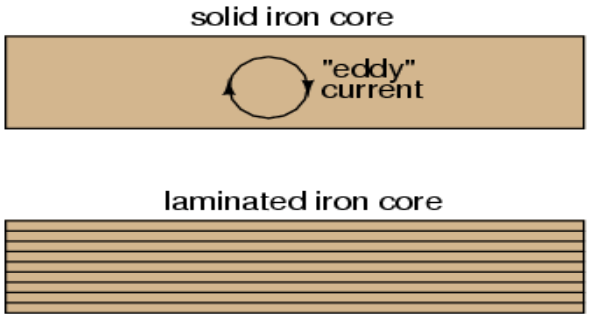

Figure 2.3
Eddy currents in a magnetic core section[1]

2.4 Modeling the magnetic core

In the previous chapter we presented the basic theory for the various nonlinearities introduced by the magnetic core. In this chapter we will present some modeling guidelines as well as some complete models for these nonlinearities.

2.4.1 Saturation

Saturation is included in the forms of the hysteresis loops, so it can be modeled together with hysteresis. However, in most existing models – especially in three-phase transformer models – hysteresis is not modeled because of its great complexity. For this reason we will present a simple model for core magnetization when hysteresis is excluded, which is based on the **anhysteretic magnetization curve**, also called normal magnetization curve. The definition of this curve, as well as the method to determine it, was given in §2.2.3.

As illustrated in figure 2.3 saturation is a nonlinear function $\vec{B}\left(\vec{H}\right)$. Many researchers have tried to represent the saturation curve with some function. The representations vary from empirical relationships to more sophisticated analytical expressions such as exponential, hyperbolae, polynomials, arctangent, and differential relay equations. We will now shortly present some of these representations:

[1] Source: http://www.ibiblio.org/obp/electricCircuits/AC/AC_9.html

2.4.1.1 Polynomial representation

The single-value saturation characteristic can be assumed by a general polynomial form as:

$$i = A'\phi + B'\phi^n \tag{2.4}$$

The value n of the nonlinear magnetizing curve can be found by referring to the capacity of the modeled transformer. For low capacities n takes values in the region 3-5, for higher capacities it lies in the region 7-9 [45].

Another representation proposed in [73] combines the use of a polynomial of the 13th order for the unsaturated region of the magnetizing curve with a parabola for the saturated region:

$$\begin{cases} H(B) = \sum_{i=0}^{13} c_i B^i \\ H - H(T_0) = k\left(B - B(T_0)\right)^2 \end{cases} \tag{2.5}$$

The fitting of the polynomial is done with minimization of the quadratic error. In the common point $\boldsymbol{T_0}$ the polynomial and the parabola must have the same functional and derivative values. The parabola that fulfils the requirements can be obtained from the system of equations:

$$\begin{cases} H(T_1) = k\left(B(T_1) - B(T_0)\right)^2 + H(T_0) \\ H(T_2) = k\left(B(T_{21}) - B(T_0)\right)^2 + H(T_0) \\ \frac{dH}{dB}(T_1) = 2k\left(B(T_1) - B(T_0)\right) \end{cases} \tag{2.6}$$

k, $B(T_0)$ and $H(T_0)$ are the parameters obtained as the solution of the system of equations (2.6).

2.4.1.2 Hyperbolic representation

Another representation for the magnetization curve is that with a hyperbola. In [77] following function is used:

$$H = \alpha \cdot \sinh(\beta \cdot B) \tag{2.7}$$

where the parameters α and β are determined from experimental results by an iterative procedure.

In [76] and [72] another, more complicated hyperbola approximation of the magnetization curve was used, described by equation (2.8):

$$F(i,\phi) = (m_1 i + b_1 - \phi)(m_2 i + b_2 - \phi) - b_1 b_2 = \varepsilon\phi \tag{2.8}$$

where $\varepsilon\phi$ is a correction term that provides the desired curvature to the knee region, m_1 and m_2 are the slopes of the unsaturated and saturated region respectively and b_1, b_2 are the ordinates to the origin of asymptote to m_1 and m_2 respectively.

2.4.1.3 Exponential representation

Pedra et al have approximated the magnetizing curve with an exponential function in [88]. The definition of their function is as follows:

$$H = \frac{\phi}{\frac{K_1}{\left(1+\left(\frac{|\phi|}{\phi_0}\right)^p\right)^{1/p}} + K_2} \tag{2.9}$$

where K_1 and K_2 are defined by the slope in the linear and the nonlinear zones of the magnetization curve, p is a parameter which influences the shape of the curve and ϕ_0 is the magnetic potential at the knee of the curve.

2.4.1.4 Arc tangential representation

Perhaps one of the most interesting representations of the magnetization curve is with an arctangent function. Such a representation may be found in [17], where one can also see how the modeled curve can be included into a more general hysteresis model. Here we will present only the anhysteretic curve:

$$\phi(i) = \phi_n \arctan(mi) + \Delta\phi \cdot i \tag{2.10}$$

The three parameters of equation (2.10) are calculated from the actual magnetization curve with equations (2.11):

$$\begin{cases} \phi_n = \phi_x \dfrac{2}{\pi} \\ m = \dfrac{\phi_2 - \phi_1}{i_2 - i_1} \dfrac{\pi}{2\phi_s} \\ \Delta\phi = \dfrac{\phi_s - \phi_n \arctan(mi_s)}{i_s} \end{cases} \tag{2.11}$$

where:

ϕ_x is the value of ϕ at the intersection of slopes,

ϕ_n is the value of ϕ_x normalized to the maximum of the arctangent function, π/2,

ϕ_s is the saturated value of ϕ in the actual magnetizing characteristic,

m is the curve's initial slope, normalized to the maximum arctangent value π/2 and to the saturation value ϕ_s,

i_s is the value of i corresponding to ϕ_s,

$\Delta\phi$ is the linear increment of ϕ,

ϕ is the magnetizing flux linkage, and

$\imath$ is the magnetizing current.

Evaluating the parameters of (2.11) uses a simple procedure directly from the actual characteristic of the magnetization curve.

2.4.2 Hysteresis & Saturation

Modeling the magnetic core's saturation without including the hysteresis may be accurate enough for some system studies, but it may be inaccurate for representing some nonlinear effects of transformers' transients. When there is need for higher accuracy, one should include also hysteresis in the representation. Numerous problems arise when trying to model magnetic hysteresis:

- The form of the hysteresis loops is similar to the anhysteretic magnetization curve. This means that it cannot be described easily by an analytical function.
- Modeling the minor hysteresis loops may prove to be a very tricky task, because of various restrictions. For example one restriction is the stability of minor loops: when applying the same field fluctuation, the $B(H)$ trace must remain on the same minor loop (this problem exists in some models of hysteresis).

Hysteresis models can be divided into two main categories:

- Micro magnetic models, which consider all known energies on a very small scale and find the magnetic configuration that gives the minimum energy. The well-known Preisach model and its improved versions are perhaps the most representative case of these models [18], [20], [21].
- Models of the nonlinear hysteresis phenomenon appearing in transformer magnetic circuits; in this case, hysteresis effect is represented by the transformer macroscopic behavior at several operating voltage levels, many of these representations being just curve fits which ignore the underlying physics. An example of this approach may be found in [44].

The first models are considered accurate but demanding data often unavailable, whereas the second have in most cases been proven to be not satisfactorily precise.

In the following paragraphs we will shortly present some important hysteresis models, which can be considered now as classical [41]. Some newer modifications of them, as well as few other models which can be found in literature, will also be briefly presented.

2.4.2.1 Preisach model

In 1935, the German physicist F. Preisach proposed a scalar model of magnetic hysteresis [18]. This model was primarily known in the area of magnetics where it was the focus of considerable research far many years, thus being further developed. Among the many improvements and valuable results of the development of the model the most significant was the better understanding of the stability problem associated with the Preisach model [20].

The main development of the model is due to the Russian mathematician Krasnoselskii, who came across Preisach's model and understood that it contained a new general mathematical idea. Krasnoselskii represented the model in a pure mathematical form which is similar to a spectral resolution of operators [19]. As a result, a new mathematical tool has evolved which can now be used for the mathematical description of hysteresis of any physical nature. Krasnoselskii's mathematical description has also made possible to determine the conditions under which actual hysteresis nonlinearities can be represented by Preisach's model.

According to Preisach's approach, the magnetic core is an interface system for which the excitation is the magnetizing force $\vec{H}$ and the response is the flux density $\vec{B}$. It is supposed that the magnetic material comprises of an infinite number of elemental dipoles, described by the elementary hysteresis operator of figure 2.5. Numbers α and β correspond to the "up" and "down" switching values of input $\vec{H}$. It is obvious that each of these elemental dipoles has a **local** memory, which means that the past exerts its influence upon the future trough instantaneous values of input.

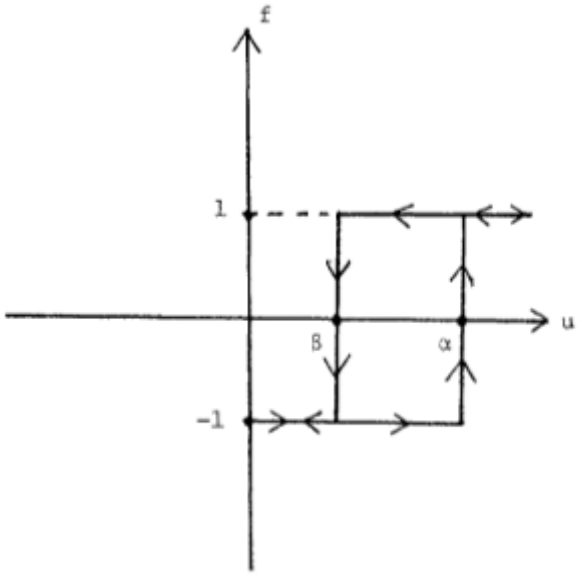

Figure 2.5
An elementary hysteresis operator $\hat{\gamma}_{\alpha\beta}$ [1]

Preisach-Krasnoselskii model is described by the following equation:

$$f(t) = \iint_{\alpha \geq \beta} \mu(\alpha, \beta) \hat{\gamma}_{\alpha\beta} u(t) d\alpha d\beta \tag{2.12}$$

where $\mu(\alpha, \beta)$ is an arbitrary weight function, being nonzero within the limits of the major hysteresis loop.

The investigation of model (2.12) is considerably facilitated by its geometric interpretation (figure 2.6). At its instant of time, the triangle T is subdivided into two sets:

- $S^+(t)$ consisting of points (α, β) for which $\hat{\gamma}_{\alpha\beta} = 1$ (positively saturated) and
- $S^-(t)$ consisting of points (α, β) for which $\hat{\gamma}_{\alpha\beta} = -1$ (negatively saturated).

[1] source: [20], p. 604

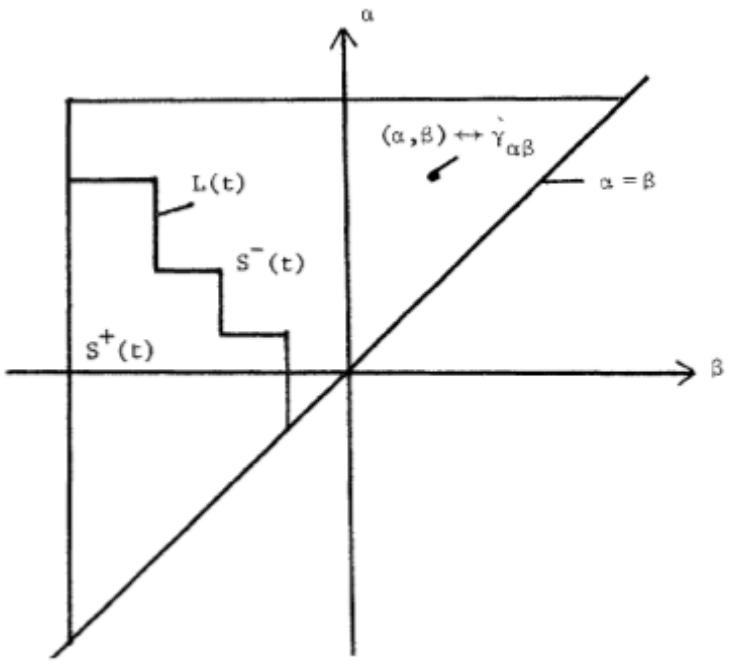

Figure 2.6
Geometrical interpretation of Preisach's model [1]

It can be shown that the interface $L(t)$ between $S^+(t)$ and $S^-(t)$ is a staircase line whose vertices have α and β coordinates coinciding with local maxima and minima at previous instants of time. The final link of $L(t)$ is attached to the line $\alpha = \beta$ and moves when the input changes. Using the above geometric interpretation, the model (2.12) can be written in the equivalent form [20]:

$$f(t) = \iint_{S^+(t)} \mu(\alpha,\beta) d\alpha d\beta - \iint_{S^-(t)} \mu(\alpha,\beta) d\alpha d\beta \tag{2.13}$$

From this equivalent form it may be seen that past extremum values of input form the interface $L(t)$, leaving in this way their mark upon future. In other words, model (2.12) or respectively (2.13) has a non-local memory, although it is only a superposition of elemental dipoles with local memories.

In order to define $\mu(\alpha,\beta)$ one has to experimentally find the set of first order transition (reversal) curves. If this set is found, then it is easy to determine $\mu(\alpha,\beta)$ with a simple numerical evaluation, which can be found in [20], equation (7).

[1] source: [20], p. 604

2.4.2.2 Modified Preisach model

When the classical Preisach model, described in the previous paragraph, is used for electromagnetic transient studies, three major problems arise [23]:

1. *Increased data requirements*. In most cases, a utility engineer is provided only with the fundamental data of the core's magnetic material, i.e. the initial magnetization curve and the major hysteresis loop.
2. *Increased memory requirements*. Accurate representation of hysteresis effect with the Preisach model requires a two-dimensional matrix $M_{\alpha\times\beta}$ where the weight function $\mu(\alpha,\beta)$ is stored. If this hysteresis model was implemented in a power system analysis package, there would be increased demand on computer memory.
3. *Input-output inverse relationship*. Usually, for system analysis, the voltages at a time instant are given and the currents are sought. This would mean that the $B(H)$ relationship has to be inversed, as the field density $\vec{B}$ is directly proportional to the voltage (applied) while the field intensity $\vec{H}$ is proportional to the current (output).

In [23] a modification of the classical Preisach approach is proposed. According to the proposed model, the weight function $\mu(\alpha,\beta)$ is decomposed in two single variable functions:

$$\mu(\alpha,\beta)=\mu_1(\alpha)\mu_2(\beta) \tag{2.14}$$

The determination of the two new functions $\mu_1(\alpha)$ and $\mu_2(\beta)$ is done in a similar way with the determination of the normal weight function $\mu(\alpha,\beta)$. Details about the numerical procedure may be found in paragraph §3 of [23].

The decomposition of the weight function offers a solution to the first two aforementioned problems, namely those of input data and computer memory requirements.

2.4.2.3 Nonlinear Preisach model (Mayergoyz model)

An extension of the classical Preisach model was proposed by Mayergoyz in [21]. The generalized model allows one to fit not only the first-, but also the second-order transition curves. This leads to higher accuracy, as well as to very good minor loops stability. The basic concept of the generalized model is the addition of another kind of elemental unit, which is described by the elementary operator $\hat{\lambda}_\alpha$ shown in figure 2.7.

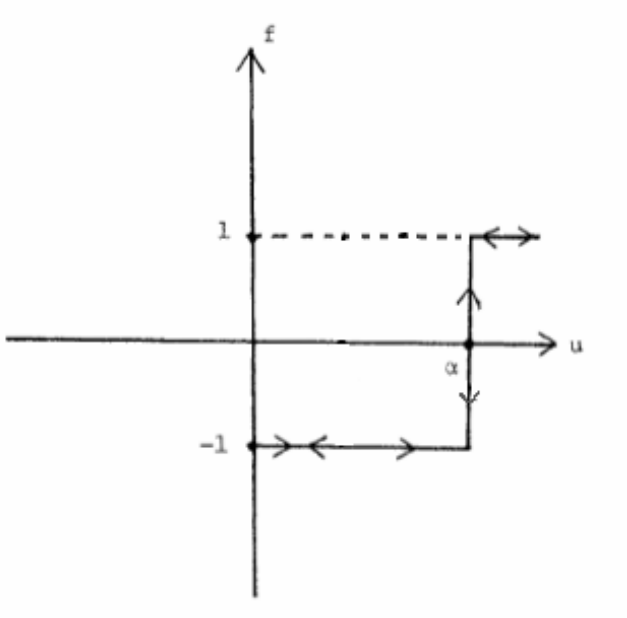

Figure 2.7
Elementary step operator $\hat{\lambda}_\alpha$

Along with the new operator, two new weight functions are introduced:

1. The distribution function $\mu(\alpha,\beta,u(t))$, which depends on the current value of input (this is the introduced nonlinearity of the model), and
2. The distribution function $v(\alpha)$ for the new elementary step operator.

The nonlinear Preisach model is described by the equation:

$$f(t)=\iint_{\alpha\geq\beta}\mu(\alpha,\beta,u(t))\hat{\gamma}_{\alpha\beta}u(t)d\alpha d\beta+\int_{-\infty}^{+\infty}v(\alpha)\hat{\lambda}_\alpha u(t)d\alpha \tag{2.15}$$

The new model admits a geometrical interpretation which is similar to that for that of the classical model. There is also another representation of model (2.15), similar to that of equation (2.13), namely:

$$f(t)=\iint_{S^+(t)}\mu(\alpha,\beta,u(t))d\alpha d\beta-\iint_{S^-(t)}\mu(\alpha,\beta,u(t))d\alpha d\beta+\int_{-\infty}^{u(t)}v(\alpha)d\alpha-\int_{u(t)}^{+\infty}v(\alpha)d\alpha \tag{2.16}$$

To determine $\mu(\alpha,\beta,u(t))$ and $v(\alpha)$, the sets of first- and second-order transition curves are required. The numerical implementation of the nonlinear Preisach model may be found in §IV of [21].

The nonlinear Preisach model is perhaps one of the most accurate existing models of hysteresis. However, the required input data as well as the very large mapping matrix (three-dimensional, for all possible input values), makes the model inappropriate for system analysis.

2.4.2.4 Stoner-Wolhfart model

The Stoner-Wolhfarth (S-W) model was first introduced in 1948 in [30]. In its original form, it describes the magnetization curves of a polycrystalline material consisting of an assembly of non-interacting single-domain particles with uniaxial anisotropy. Here we will present the main ideas of the model, as well as some improvements suggested in [41].

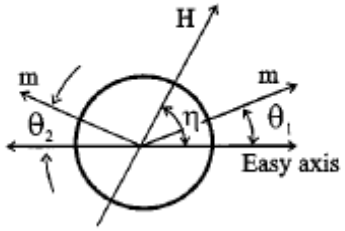

Figure 2.8
Diagram of an S-W particle with both stable energy configurations shown [1]

Consider the case of the single S-W particle of figure 2.8. The angles θ and η are the angles between the particle magnetization vector $\vec{m}$ and the easy axes and the applied field $\vec{H}$ and the easy axes, respectively. The magnetization of the particle is assumed to always have the same magnitude, but its direction can vary. The minimum energy of the particle is a sum of the magnetocrystalline energy and the magnetostatic energy:

$$E = K_u \sin^2(\theta) - \mu_0 \left|\vec{m}\right|\left|\vec{H}\right| \cos(\eta - \theta) \tag{2.17}$$

where K_u is the uniaxial anisotropy constant and μ_0 is the free space magnetic permeability. Both reversible and irreversible magnetization can be described by the equation (2.17).

In order to simulate the behaviour of the whole material, we sum the contribution of a collection of S-W particles. In the original model a crystal preferential orientation is expressed with a Gaussian particle easy axis orientation distribution function:

$$F(\eta) = \frac{1}{\sqrt{2\pi}\sigma} \exp\left(\frac{-(\eta - \bar{\eta})^2}{2\sigma^2}\right) \tag{2.18}$$

where σ is the effective distribution width associated with the mean angle $\bar{\eta}$ between the field direction and the bulk easy axis direction of the sample. Figure 2.9 shows two hysteresis loops which are obtained for different kinds of textures.

[1] source: [41], p. 419

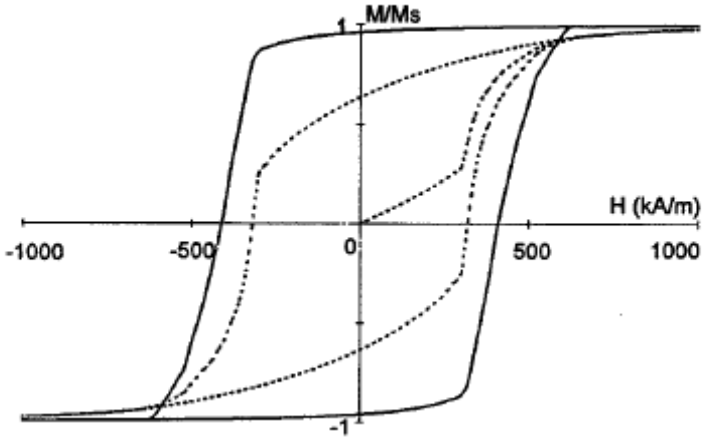

Figure 2.9
Hysteresis loops obtained for different kinds of texture ($\sigma = 15^o$) [1]
dotted line: isotropic distribution of S-W particle easy axes
full line: anisotropic distribution of S-W particle easy axes

As one may already have noticed, hysteresis in the S-W model is introduced only by means of anisotropy. Interactions between magnetic particles and pinning effects are ignored. In [41] some improvements for the S-W model are presented:

The first modification was proposed in [31] and considers the incorporation of inter-particle interaction. This is done by the addition of a mean field term similar to Weiss's molecular theory. The magnetic field experienced by the particle is now:

$$H_{eff} = H + \alpha M \tag{2.19}$$

Examples of hysteresis loops obtained for different values of the mean field interaction parameter α are shown in figure 2.10.

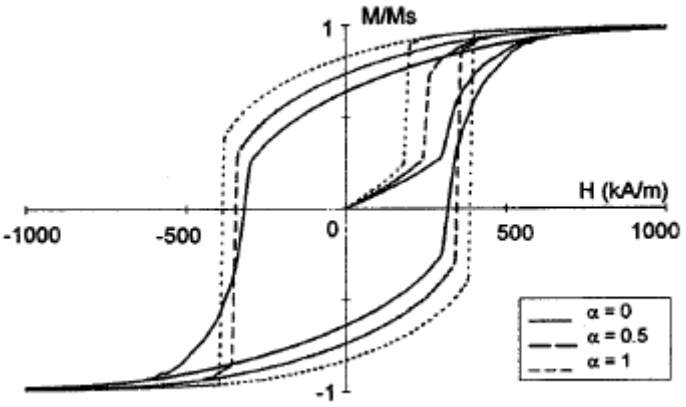

Figure 2.10
Major hysteresis loops calculated for different values of α [1]
(isotropic distribution of the particle easy axes, $K_u = 1.5 \cdot 10^5 \, J/m^3$)

[1] source: [41], p.420

The second modification is the introduction of pinning effects in the model. **Pinning** means that the rotation of the particle is impeded by lattice defects such as dislocations, residual stress etc. In [41] the pinning torque applied on the particle is supposed to be proportional to the bulk magnetization with a proportionality coefficient p. Figure 2.11 shows a comparison of hysteresis loops obtained with and without including the pinning effect.

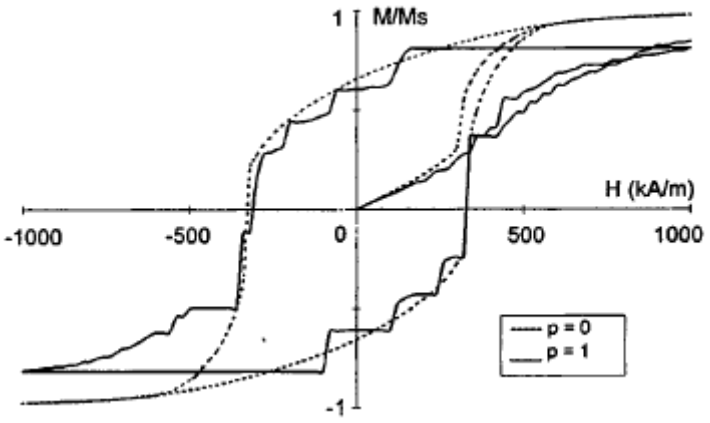

Figure 2.11
Effect of the pinning parameter on the major hysteresis loop [1]
doted line: no pinning
full line: with pinning effect

The complete Stoner-Wolhfarth model is determined by six parameters, from which three $\left(M_s, K_u, \overline{\eta}\right)$ are measurable while the other three (α, p, σ) are adjustable.

[1] source: [41], p.420

2.4.2.5 Jiles-Atherton model

The Jiles-Atherton (J-A) model was introduced in [25] to describe isotropic polycrystalline materials where the main magnetization progress is the domain wall motion. The model is built up on the anhysteretic magnetization curve, in a manner which will be described briefly here.

The energy per unit volume E of a typical domain with magnetic moments per unit volume $\vec{m}$ and an internal magnetic field $\vec{H}$ is given by equation (2.20)

$$E = -\mu_0 \vec{m} \cdot \vec{H} \tag{2.20}$$

If we consider also the interaction between magnetic domains, which is expressed in (2.19), we have:

$$E = -\mu_0 \vec{m} \cdot \left(\vec{H} + \alpha \vec{M} \right) \tag{2.21}$$

where the mean field parameter α is determined experimentally. The response of the anhysteretic magnetization to the effective field $\vec{H}_{eff}$ of equation (2.19) can be written as:

$$\vec{M}_{an} = M_S f\left(\vec{H}_{eff} \right) \tag{2.22}$$

$f\left(\vec{H}_{eff} \right)$ is an arbitrary function that takes the value zero when H_{eff} is zero and one when H_{eff} goes to infinity. Jiles and Atherton proposed a function that fulfills these criteria, namely the modified Langevin function:

$$M_{an} = M_S \left(\coth\left(\frac{H_{eff}}{a} \right) - \left(\frac{a}{H_{eff}} \right) \right) \tag{2.23}$$

with a being a constant with dimensions of magnetic field.

At this point the pinning effect can be included into the model. Pinning of domain walls is due to defect sites such as dislocations, impurities, grain boundaries etc. The energy lost by moving a magnetic domain due to pinning is proportional to the magnetic moment change of the domain, i.e.

$$dE_p = k \cdot dM \tag{2.24}$$

Where k is a microstructural parameter proportional to the pinning sites density and to pinning site energy. This parameter is taken to be constant at the original model, however, variations of this parameter have been discussed in [24].

The energy of the material is now equal to the energy supplied if it were anhysteretic, reduced by the energy lost in overcoming the pinning sites, the energy balance thus being:

$$\mu_0 \int M_{irr}(H) dH_{eff} = \mu_0 \int M_{an}(H) dH_{eff} - \mu_0 \int k \left(\frac{dM_{irr}}{dH_{eff}} \right) dH_{eff} \tag{2.25}$$

Equation (2.25) describes only the irreversible magnetization changes M_{irr}. In order to include also the reversible magnetization, Jiles and Atherton used the following form:

$$M_{rev} = c\left(M_{an} - M_{irr}\right) \tag{2.26}$$

The total magnetization being thus:

$$M = M_{rev} + M_{irr} \tag{2.27}$$

The J-A model is defined by the following set of equations:

$$\begin{cases} \dfrac{dM_{irr}}{dH} = \dfrac{M_{an}(H) - M_{irr}(H)}{\delta k - \alpha\left(M_{an}(H) - M_{irr}(H)\right)} \\ \dfrac{dM_{rev}}{dH} = c\left(\dfrac{dM_{an}}{dH} - \dfrac{dM_{rev}}{dH}\right) \\ \dfrac{dM}{dH} = \dfrac{dM_{rev}}{dH} + \dfrac{dM_{irr}}{dH} \end{cases} \tag{2.28}$$

Where δ is a directional parameter:

$$\delta = sign\left(dH\right) \tag{2.29}$$

Hence, the model is defined by five physical parameters which are:

M_s: the spontaneous magnetization,
k: parameter to describe the pinning effect,
α: mean field parameter for the interaction between magnetic domains,
a: parameter for the modified Langevin function (2.23),
c: parameter for the reversible magnetization component.

Figure 2.12 shows examples of hysteresis loops calculated for different values of these parameters.

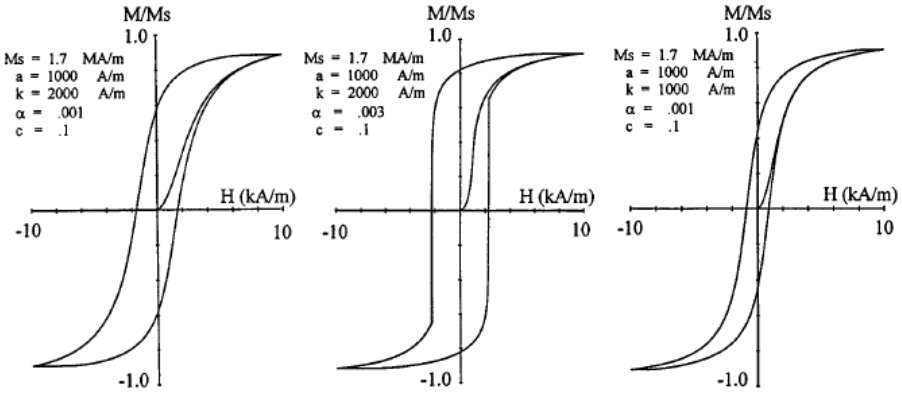

Figure 2.12
Calculated hysteresis loops for different values of the J-A parameters [1]

A fitting procedure is proposed in [27] to enable the user to determine the value of each parameter for a specific material.

[1] source: [27]

2.4.2.6 Globus model

The Globus model was first proposed in [32] and it is based on the fact that a polycrystalline soft ferrite of high microstructural quality shows a ring-like distribution of 180^o domain walls. In order to simplify the sample representation as an oriented assembly of grains, it is assumed that only one 180^o domain wall crosses each grain (figure 2.13).

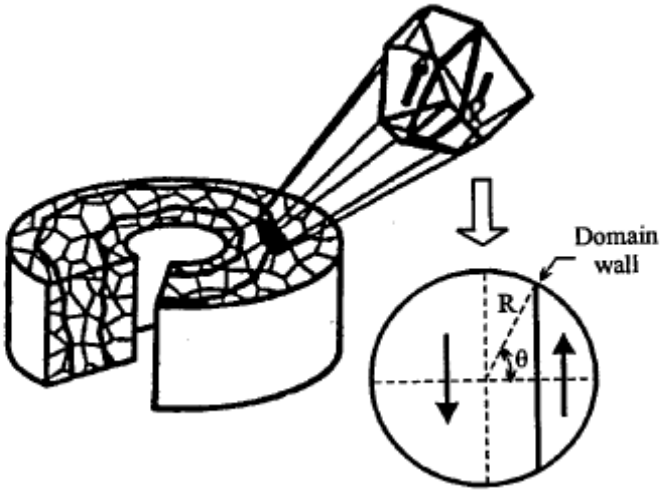

Figure 2.13
Reduction of polycrystalline sample to the mean Globus grain [1]

Under this assumption, the magnetization process is described by the motion of the wall inside the mean grain. Both reversible and irreversible magnetization processes are described by first examining wall bowing, a reversible process, and then, when the pinning force is overcome, parallel displacement of the wall, an irreversible process. To evaluate the magnetic field intensity H, Globus minimized the sum of the following three energies:

$dE_f = 2\pi f R^2 \sin(\theta) d\theta$ Friction of the domain wall at the grain boundary

$dE_\gamma = 2\pi\gamma R^2 \sin(\theta)\cos(\theta) d\theta$ Wall energy

$dE_H = -2\pi M_s H R^3 \sin^3(\theta) d\theta$ Magnetostatic energy

with θ, R as shown in figure 2.13, f, γ being parameters for the model. It should be noted here that the first energy term (friction of the domain wall) is another expression for the pinning effect already referred to in the previous models. By minimizing the sum of these three energies, we obtain the following expression for the magnetic field, as a function of the position of the wall inside the mean grain:

$$H = \frac{f + \gamma\cos(\theta)}{M_s R \sin^2(\theta)} \tag{2.30}$$

[1] source: [41], p.423

The magnetization change dM during a small displacement of the wall is proportional to the volume variation of the domain:

$$dM = 2M_s \frac{dV}{V_0} \tag{2.31}$$

where V_0 is the volume of the grain. By integrating equation (2.31) with respect to $R\cos(\theta)$, we obtain following expression for the magnetization, as a function of the position of the wall inside the mean grain:

$$M = \frac{1}{2} M_s \cos(\theta)\left(2 + \sin^2(\theta)\right) \tag{2.32}$$

Equations (2.30) and (2.32) describe the magnetization curve when only the displacement of a flat domain wall is taken into account, that is they describe only the irreversible magnetization process. However, there is also a reversible part of magnetization which is due to the ability of the domain wall to bend. In [33] following expression is proposed for the reversible magnetization:

$$M_{rev} = \frac{3}{8} M_s^2 \frac{D}{\gamma} H \tag{2.33}$$

Figure 2.14(a) shows the typical qualitative loop proposed by Globus in case of a weak magnetizing field. Figure 2.14(b) is another representation of the Globus hysteresis loop, proposed in [41], which also takes into account the anhysteretic magnetization curve.

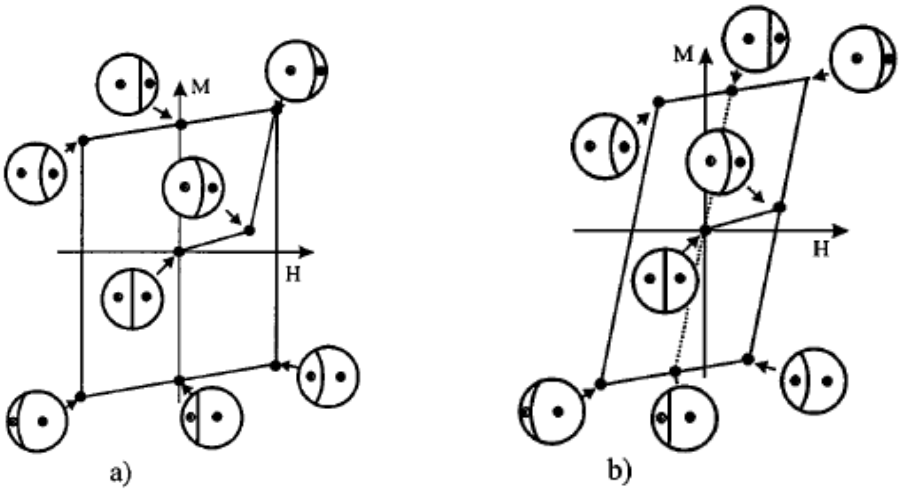

Figure 2.14
(a) Single Globus grain hysteresis loop [1]
(b) New shape of Globus hysteresis loop. The dotted line represents the anhysteretic curve [2]

[1] source: [34]
[2] source: [41], p. 424

The Globus model is now described by the set of equations (2.30), (2.32) and (2.33). The four physical parameters of the model are:

M_s: can be measured directly as already discussed in previous sections
R: can be evaluated by observation of the sample grain size
f, γ: experimentally evaluated parameters

An experimental procedure for the determination of the two latter parameters of the model is described in [35].

The Globus model is a relatively simple model of hysteresis, still rather unsuitable for engineering purposes. However, the concept of the domain wall model introduces an efficient physical representation of reversible and irreversible magnetization processes.

2.4.2.7 Hodgdon model

The Hodgdon model is a macroscopic approach to hysteresis; that is to say, it tries to just find an input-output relationship which corresponds to reality, without getting in the physics of the phenomenon.

Coleman and Hodgdon have shown in [37] and [38] that equation (2.34), along with a set of constraints on α and on the magnetic material functions f and g, yields a theory that is in agreement with the one-dimensional, rate independent ferromagnetic hysteresis, which can find application in isoperm ferromagnetic materials.

$$\dot{B} = \alpha \left| \dot{H} \right| \left| f(H) - B \right| + \dot{H} g(H) \tag{2.34}$$

The functions f and g must meet the following restrictions [39]:

1. f must be a piecewise smooth, monotonic increasing, odd function of H, with a derivative, f', that obtains a finite limit $f'(\infty)$ for large H;
2. g must be a piecewise continuous, even function of H, with a finite limit satisfying $g(\infty) = f'(\infty)$; and
3. for all finite H, the functions f' and g must satisfy the inequalities:

$$f'(H) \geq g(H) \geq \alpha \cdot e^{\alpha \cdot H} \int_{H}^{\infty} \left[f'(z) - g(z) \right] \cdot e^{\alpha \cdot z} dz \tag{2.35}$$

As shown in [37] and [38] equation (2.34) can be also written in the form:

$$\frac{dB}{dH} = \begin{cases} \alpha \left| f(H) - B \right| + g(H) & for \quad \dot{H} > 0 \\ -\alpha \left| f(H) - B \right| + g(H) & for \quad \dot{H} < 0 \end{cases} \tag{2.36}$$

Equations (2.36) are convenient forms of equation (2.34) for both analytical and numerical work.

A modification based on exchanging the positions of B and H in the equation (2.34) and on allowing for the dependence of the material functions on $\dot{H}$ extends the theory to rate dependent, nonisoperm materials [39]. Under these modifications, the differential equation (2.34) becomes:

$$\dot{H} = \alpha\left|\dot{B}\right|\left|\tilde{f}(B) - H\right| + \dot{B}\tilde{g}(B) \tag{2.37}$$

which can be also written as:

$$\frac{dB}{dH} = \begin{cases} \left(\alpha\left|\tilde{f}(B) - H\right| + \tilde{g}(B)\right)^{-1} & for \quad \dot{H} > 0 \\ \left(-\alpha\left|\tilde{f}(B) - H\right| + \tilde{g}(B)\right)^{-1} & for \quad \dot{H} < 0 \end{cases} \tag{2.38}$$

The restrictions on $\tilde{f}, \tilde{g}$ and α are now:

1. $\tilde{f}$ must be a piecewise smooth, odd function of B, with a derivative, $\tilde{f}'$, that obtains a finite limit $\tilde{f}'(\infty)$ for large B;
2. $\tilde{g}$ must be a piecewise continuous, even function of B, with a finite limit satisfying $\tilde{g}(\infty) = \tilde{f}'(\infty)$; and
3. for all finite B, the functions $\tilde{f}'$ and $\tilde{g}$ must satisfy the inequality:

$$\tilde{g}(B) \geq \max\left\{\tilde{f}'(B), \alpha \cdot e^{\alpha \cdot B}\left|\int_B^{\infty}\left[\tilde{f}'(z) - \tilde{g}(z)\right] \cdot e^{-\alpha \cdot z}\, dz\right|\right\} \tag{2.39}$$

In [39] equation (2.39) is applied on a variety of materials. For this purpose it is first rewritten in a form of finite differences:

$$B_{i+1} = B_i + \left[{}^{+}_{-}\alpha\left[\tilde{f}(B_i) - H_i\right] + \tilde{g}(B_i)\right]^{-1}(H_{i+1} - H_i) \tag{2.40}$$

which, along with a specification of an initial state (H_0, B_0), the initial sign of $\dot{H}$, and a stack of the turning points of H, appears sufficient for modelling.

Hodgdon has found following forms for $\tilde{f}$ and $\tilde{g}$ useful, in that they scale well for a variety of materials:

$$\tilde{f}(B) = \begin{cases} A_1 \tan(A_2 B) & for \quad |B| \leq B_{cl} \\ A_1 \tan(A_2 B_{cl}) + \dfrac{B - B_{cl}}{\mu_{cl}} & for \quad B > B_{cl} \\ -A_1 \tan(A_2 B_{cl}) + \dfrac{B + B_{cl}}{\mu_{cl}} & for \quad B < -B_{cl} \end{cases} \tag{2.41a}$$

and

$$\tilde{g}(B) = \begin{cases} \tilde{f}'(B)\left[1 - A_3 \exp\left(\dfrac{-A_4|B|}{B_{cl} - |B|}\right)\right] & for \quad |B| \leq B_{cl} \\ \tilde{f}'(B) & for \quad |B| \geq B_{cl} \end{cases} \tag{2.41b}$$

where B_{cl} is the absolute value of the flux density at the closure point of the major loop and μ_{cl} is the slope of the $B(H)$ characteristic beyond the closure point (see also figure 2.15).

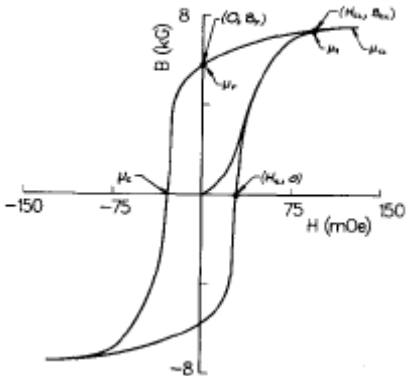

Figure 2.15
Initial magnetization curve from equations (2.38) and (2.39) [1]
Flux densities, fields and slopes at the labeled points are used to calculate the model parameters

The Hodgdon model can be extended in order to describe hysteresis effects in fast-varying magnetizing fields, however, equations (2.34)-(2.41) are sufficient to model the magnetic core of transformers in low-frequency studies.

2.4.2.8 Some other models

There exist numerous other models of hysteresis in the literature. However, they are either to simple, unable to represent the whole magnetization process, or to specific, developed only for a pre-defined application. Here we will briefly quote two of these models:

1. In [43] an interesting approach to hysteresis is proposed, based on fractal theory. This theory uses simple processes and iterations to model dynamic phenomena of complex systems. The similarity of the major hysteresis loop to the minor loops reveals that fractal features are present in ferromagnetic hysteresis. The proposed method uses linear-varied factors to compress the major loop and obtain the minor hysteresis loops.
2. In [44] hysteresis is modeled as a superposition of a linear difference term $K_{hyst}(B - B_{rev})$ on a steep basis magnetization curve. This basis curve is described by a polynomial approximation:

   $$H_{basis} = K_{basis} B + K_{n_1} B^{n_1} + K_{n_2} B^{n_2} \tag{2.42}$$

   Then, the hysteresis equation becomes:

   $$H = H_{basis} + K_{hyst}(B - B_{rev}) \tag{2.43}$$

   with B_{rev} being the last reversal point.

[1] source: [39], p. 219

2.4.2.9 Comparison of hysteresis models

There is no answer to the question "*Which is the best model for hysteresis effects*". Every model has its own advantages and disadvantages, the final choice must thus be made in accordance to the purpose of the model. It seems, however, obvious that, the more accurate the model, the more input data and computational time it requires. A comparison of the different models will be very helpful to the user who is searching for the appropriate model for his application.

In [41] the four classical models (Preisach, Stoner-Wolhfarth, Jiles-Atherton and Globus) are compared. The conclusions are summarized in the following table:

	Stoner-Wolhfarth	***Jiles-Atherton***	***Globus***	***Preisach***
Mechanism	Rotation	Not specified	Wall motion	Not specified
Anisotropy	uniaxial	multi-axis	multi-axis	Not specified
Interaction	yes	yes	no	Moving model
Pinning	yes	yes	yes	Not specified
Texture	Anisotropic or isotropic	isotropic	uniaxial	Not specified
Wall energy	no	no	yes	no
Reversibility	yes	Additional model	yes	Additional model
Minor loops	yes	Approximation	-	yes
Demagnetization	-	yes	-	yes
Anhysteretic	yes	yes	yes	yes
Parameters ***Measurable parameters ****	$M_s{*}, K_u{*}, \overline{\eta}{*}, \sigma, \alpha, p$	$M_s{*}, c{*}, a{*}, \alpha{*}, k{*}$	$M_s{*}, \gamma{*}, R{*}, f{*}$	$\mu(\alpha, \beta)$
Grains	Single domain	Multi-domain	Bi-domain	Not specified
Computational time	+++	++	+	++++
Materials	Hard magnetic materials	Bulk materials Medium ferrites	Soft ferrites	Magn. recording Thin films

Table 2.2
Comparison of classical hysteresis models [1]

In [40] four hysteresis models are compared with experimental results: two versions of a simple polynomial model proposed in [48], the Hodgdon model and the Mayergoyz model. The comparison shows that the Mayergoyz (nonlinear Preisach) model is the most accurate and stable of these four models.

[1] source: [41], p.426

2.4.3 Eddy Currents

The nonlinear phenomena of saturation and hysteresis, the modeling of which has been discussed in the previous paragraphs, are mainly governed by the low-frequency operating currents. On the other hand, as already stated in §2.3.3, eddy currents losses are largely dependent on frequency. Calculation of the instantaneous eddy currents inside a magnetic core can be done with a finite-elements-approach easily and with great accuracy [55]. There are also some analytical approaches to the calculation of eddy currents [56], [54]. However, in transformer models for system studies it is enough to just describe the effect of eddy currents on the transformer's behavior with as low complexity as possible.

In most transformer models for system studies eddy currents losses are represented by a constant resistance in parallel with the magnetization inductance. The determination of the eddy currents resistance is done by measurements at nominal frequency [50]. The frequency-independency of this representation restricts the usage of such transformer models in a narrow frequency band. In this section we will present the traditional constant-resistance representation of eddy currents losses, as well as some more sophisticated, frequency-dependent models.

2.4.3.1 Constant-resistance representation

In the vast majority of transformer models (especially in the duality-based models, see §3), a magnetic core section is modeled as a nonlinear inductance, representing the saturation effect, in parallel with a constant resistance, representing both hysteresis and eddy currents losses.

The main constraints of such a representation are the following:

- In order to determine the values of the constant shunt resistances, a symmetric sinusoidal steady state is assumed to govern the core's behavior; this assumption leads to severe constraints in the use of such models, i.e. they are not suitable for non-symmetrical operation of the transformer. However, for some applications the assumption of symmetry may be well justified (for example in five-limbed three-phase transformers).
- Core's losses are both voltage- and frequency-dependent. The simple representation with constant shunt resistances does not accommodate any of these dependencies.

The determination of these shunt resistances is usually done by the open-circuit tests in nominal operating frequency. For a three phase transformer with one shunt resistance for each phase on the primary side, the evaluation of the model's parameter is done with equation (2.44):

$$R_k = \frac{V_{n,pri}^2}{3P_{loss}} \tag{2.44}$$

where P_{loss} are the no-load losses (accounting for both hysteresis and eddy currents) and $V_{n,pri}$ is the nominal primary-side voltage.

In order to draw the constraints of this classical representation, several modification have been proposed:

- If the transformer's model already accommodates a representation for the hysteresis effect, the losses due to hysteresis can be calculated from the hysteresis model. They are then subtracted from the no-load losses and the shunt resistance which is determined with equation (2.44) stands only for the eddy currents losses.
- Another modification is the usage of a voltage-varying resistance, the characteristic of which is obtained by online monitoring the source voltage and currents during open-circuit tests [81]. This approach is described by equation (2.45):

$$R_k(V) = \frac{V_{pri}(t)}{I_{pri}(t)} \tag{2.45}$$

  However, with such a representation it is difficult to separate the hysteresis losses, if one wants to represent hysteresis with a different model.
- Finally, if the model of the transformer is based on the decoupled electric-magnetic approach, eddy currents losses can be represented by a constant resistance which is connected to a one-turn winding wound around the magnetic core's section to be modeled. This way of modeling eddy currents is actually the physically right one, as it is the change of magnetic flux inside the core that causes the eddy currents losses:

$$P_{eddy-currents} \propto \left(d\phi / dt \right)^2 \tag{2.46}$$

The above modifications may add to the accuracy of the simple eddy currents shunt-resistor model, but they still do not solve the major problem of it: the frequency-independency. In the next paragraphs we will present some more sophisticated models of eddy currents losses, which do take frequency-dependency into account.

2.4.3.2 Series expansion model

In [51], the following expression for the equivalent impedance of a coil wound around a laminated iron core limb was derived by solving Maxwell's Equations with the assumption that the magnetic field is identical in all laminations:

$$Z(j\omega) = \frac{4N^2 Ax}{ld^2\gamma} \tanh(x) \tag{2.47}$$

where

$$x = d\sqrt{j\omega\mu}\frac{\gamma}{2}$$

μ: magnetic permeability of the steel lamination
γ: electric conductivity of the steel lamination
A: total cross-sectional area of all laminations
d: thickness of lamination
l: length of core limb
N: number of coil turns

The term $\tanh(x)$ in equation (2.47) can be expanded in partial fraction series [50]:

$$\tanh(x) = 2x\sum_{k=1}^{\infty}\frac{1}{x^2+\left(\pi\frac{2k-1}{2}\right)^2} \tag{2.48}$$

By substituting this expression in equation (2.47) we get an expansion for the impedance $Z(j\omega)$ which can be synthesized using the series connection of parallel RL branches illustrated in figure 2.16(a), or its dual circuit shown in figure 2.16(b). These circuits are widely known as the series and parallel Foster equivalents.

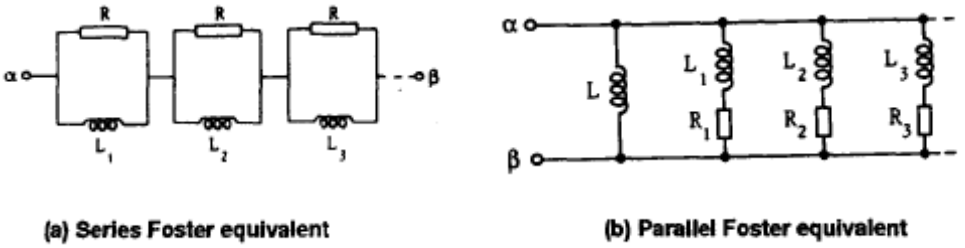

(a) Series Foster equivalent (b) Parallel Foster equivalent

Figure 2.16
Foster equivalent circuits

For the determination of the parameters of the series and parallel Foster equivalents equations (2.49a) and (2.49b), respectively, are used:

$$\begin{cases} R = \dfrac{8N^2A}{d^2l\gamma} \\ L_k = \dfrac{L}{(2k-1)^2} \quad L = \dfrac{8N^2A\mu}{\pi^2 l} \end{cases} \tag{2.49a}$$

$$\begin{cases} R_k = Rk^2 \quad R = \dfrac{2N^2\pi^2A}{ld^2\gamma} \\ L = \dfrac{N^2A\mu}{l} \\ L_k = \dfrac{L}{2} \end{cases} \tag{2.49b}$$

In order to incorporate saturation and hysteresis the inductive components of the Foster equivalents representing the magnetizing reactances have to be made nonlinear. The accuracy of the model depends on the number of terms retained in the partial fraction expansion. It should be stated that the computational requirements of the series expansion model make it unsuitable for higher frequency applications.

2.4.3.3 Uniformly discretized model

In [52] each lamination is first subdivided into a number of sublaminations and then Maxwell's Equations are solved under the assumption of uniform flux distribution inside each sublamination. The corresponding equivalent circuit is then formed by connected all sublaminations in a cascade (figure 2.17).

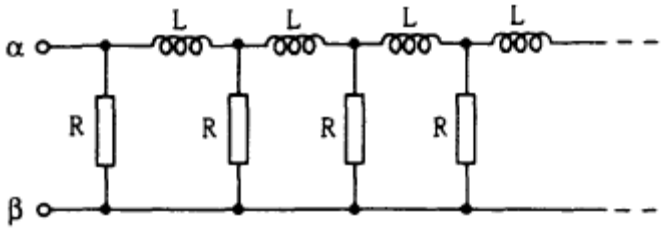

Figure 2.17
Uniformly discretized model [1]

The parameters of the model are defined according to equation (2.50):

$$\begin{cases} R = \dfrac{4N^2 An}{d^2 l\gamma} \\ L = \dfrac{N^2 A\mu}{nl} \end{cases} \tag{2.50}$$

where n is the number of sublaminations and the other parameters are as defined in §2.4.3.2. The accuracy of the uniformly discretized model depends on the thickness of the sublaminations, that is on the number n.

Both models presented in the previous paragraphs (the series expansion and the uniformly discretized model) are unsuitable for higher frequency applications because of computational requirements. In the next two paragraphs we shall present modifications of these models which show greater accuracy at high frequency.

2.4.3.4 Continued fraction model

$\tanh(x)$ is now represented by a continued fraction expansion (equation 2.51), rather than with the series expansion of equation (2.48).

$$\tanh(x) = \cfrac{x}{1+\cfrac{x^2}{3+\cfrac{x^2}{5+\cfrac{x^2}{7+\ldots}}}} \tag{2.51}$$

[1] source: [50], p. 590

If we substitute (2.51) in (2.47) we get an expression which can be realized with the ladder network of figure 2.18 (for 4 sections).

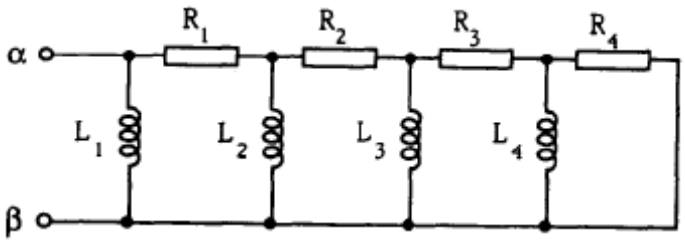

Figure 2.18
Four section continued fraction model [1]

where:

$$\begin{cases} L_k = \dfrac{L_0}{4k-3} & L_0 = \dfrac{N^2 A\mu}{l} \\ R_k = \dfrac{R_0}{4k-1} & R_0 = \dfrac{4N^2 A}{d^2 l\gamma} \end{cases} \tag{2.52}$$

The first section of the equivalent circuit governs its characteristics at the lower frequencies, so, in order to introduce saturation, only the first inductance must be made nonlinear. This dramatically saves computational time. However, to determine the nonlinear characteristic of L_1 a curve-fitting procedure must be followed.

2.4.3.5 Non-uniformly discretized model

This model is a modification of the previously described uniformly discretized model. The large number of the ladder sections of the latter can be reduced recognizing that, for increasing frequency, the flux becomes confined to an increasing thinner layer near the lamination surface (the so-called skin effect). Therefore, we can progressively double the thickness of the sublaminations while moving from the surface to the center of the lamination. The resulting equivalent for 6 sublaminations is illustrated in figure 2.19.

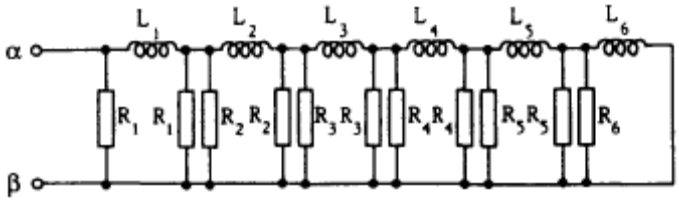

Figure 2.19
Six section non-uniformly discretized model [2]

[1] source: [50], p.590
[2] source: [50], p.591

The determination of the parameters of the equivalent of figure 2.19 is done according to equation (2.53):

$$\begin{cases} L_k = \dfrac{N^2 A\mu}{l} \dfrac{2^{k-1}}{\sum_{i-1}^{M} 2^{i-1}} \\ R_k = \dfrac{8N^2 A}{d^2 l\gamma} \dfrac{\sum_{i-1}^{M} 2^{i-1}}{2^{k-1}} \end{cases} \tag{2.53}$$

where

M : number of sections

k : sublamination number starting from the lamination surface

In contrary to the continued fraction model, every inductance of the non-uniformly discretized model has to be nonlinear to represent saturation and hysteresis, which introduces considerable computational burden.

2.4.3.6 Combined hysteresis & eddy currents model

In this last section about eddy currents modeling we shall present an interesting approach, introduced in [57], which tries to combine all core nonlinearities (saturation, hysteresis, eddy currents). According to this approach, the core losses can be separated into three parts:

$$P_{total} = P_{hyst} + P_{cls} + P_{exc} \tag{2.54}$$

where

P_{hyst} : hysteresis losses

P_{cls} : classical eddy currents losses

P_{exc} : excess losses

The "classical" eddy currents losses are calculated under the assumption of uniform magnetization. However, and because of this assumption, there exists a difference between the total measured core losses and the hysteresis and eddy currents losses, denoted as excess losses.

The proposed approach incorporates the classical eddy currents and the excess losses into the Jiles-Atherton model of hysteresis [25].

The instantaneous power loss per unit volume due to classical eddy currents is proportional to the rate of magnetization [57]:

$$P_{cls} = \frac{d^2}{2\rho\beta}\left(\frac{dB}{dt}\right)^2 \tag{2.55}$$

where d is the lamination thickness, ρ is the lamination resistance and β is a constant ($\beta = 6$ for laminations).

Equation (2.55) can be also written in the following form:

$$P_{cls}dt = \oint \underbrace{\frac{d^2}{\rho\beta}\frac{dB}{dt}}_{H_{cls}\propto\frac{dB}{dt}} dB \tag{2.56}$$

In [59], [60] an expression is derived for the instantaneous excess loss:

$$P_{exc} = \left(\frac{GSH_0}{\rho}\right)^{\frac{1}{2}}\left(\frac{dB}{dt}\right)^{\frac{3}{2}} \tag{2.57}$$

where G is a constant, S is the cross sectional area and H_0 is a parameter representing the internal potential experienced by domain walls. Equation (2.57) can also be rewritten in a form similar to (2.56):

$$P_{exc}dt = \oint \underbrace{\left(\frac{GSH_0}{\rho}\right)^{\frac{1}{2}}\left(\frac{dB}{dt}\right)^{\frac{1}{2}}}_{H_{exc}\propto\left(\frac{dB}{dt}\right)^{\frac{1}{2}}} dB \tag{2.58}$$

The final equation of the model is:

$$H_{tot} = H_{hyst} + H_{cls} + H_{exc} = H_{hyst} + k_1\frac{dB}{dt} + k_2\left(\frac{dB}{dt}\right)^{\frac{1}{2}} \tag{2.59}$$

where H_{hyst} is the magnetic field intensity due to hysteresis. The modified H_{tot} is calculated by equation (2.59) and then fed into the Jiles-Atherton model, equation (2.28).

3. Duality-based models

3.1 Basic theory

There exists a simple geometrical relation between inverse - also called dual- circuits, of electric impedances, which is based on the interchange of junction-points and meshes. This relation has been shown by Cauer (1934) to be based on the topological principle of duality. An identical relation of pattern exists also between an electric and its "equivalent" magnetic circuit and vice versa, i.e. between electric and magnetic dual circuits. Details about the duality between electric and magnetic circuits can be found in [68]. Here we will point out some important features for the relation between the magnetic circuit of a transformer and its equivalent electric circuit.

To form the dual circuit we have to replace mesh connections in one circuit by star-point connections in the other circuit and vice versa. The elements must also be replaced by their inverse elements. Let us consider the magnetic circuit of an ideal four-limb transformer having windings with an arbitrary equal number of turns N, illustrated in figure 3.1(a). Figure 3.1(b) shows the dual electric circuit of such a transformer.

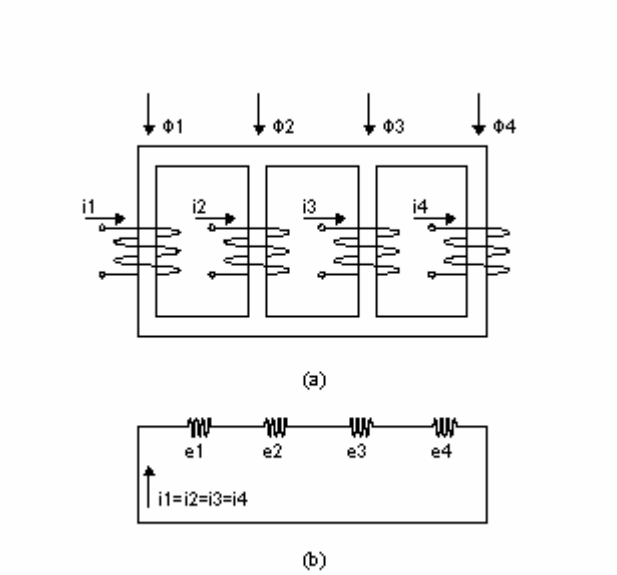

Figure 3.1
Ideal transformer (a) and the apparent condition of their windings into the equivalent circuit (b)

Such an arrangement is not a true equivalent circuit in that the impedances of the various coils are unknown since the original transformer was ideal. It should be regarded merely as a possible pattern in which the various voltages and currents of the transformer may be arranged in order to fulfill the basic equations deriving from the true geometry, namely of the system:

$$\begin{cases} \Phi_1 + \Phi_2 + \Phi_3 + \Phi_4 = 0 \\ MMF_1 = MMF_2 = MMF_3 = MMF_4 \end{cases} \tag{3.1}$$

which can be also written as:

$$\begin{cases} e_1 + e_2 + e_3 + e_4 = 0 \\ i_1 = i_2 = i_3 = i_4 \end{cases} \tag{3.2}$$

It may be seen that the circuit 3.1(b) can be formed by applying the rules for dual figures stated before, so that the meshes of the first circuit are replaced by junction points in the second. The physical dual quantities used to form the electric dual of a magnetic circuit are:

$$e \leftrightarrow {d\Phi}/{dt}, \quad i \leftrightarrow MMF \tag{3.3}$$

that is one has to replace the rate of change of the magnetic flux ${d\Phi}/{dt}$ by the induced voltage, and the Magneto Motive Force (MMF) by the current.

Every possible magnetic circuit can be transformed to its dual electric circuit by the described routine method, provided that:

- All coils have equal number of turns, N
- The transformer's magnetic circuit is a planar figure.

Regarding the second constraint, we should state that there exists generally no dual circuit, if the magnetic circuit of a transformer is not a planar figure. However, equivalent circuits of multi-winding transformers having non-planar magnetic circuits have been developed using negative elements.

Let us now consider a loaded (ideal) transformer. The external circuit, i.e. the load, exercises certain constraints on the currents and voltages. When the transformer is replaced by an equivalent circuit, this must be arranged so as to exercise the same constraints. In order to form the electric equivalent circuit of a transformer one has to first disconnect the external circuit and then apply the rules of duality described above. After the equivalent circuit is formed one can reconnect the external circuit to the corresponding points so as to support the same currents and voltages as originally.

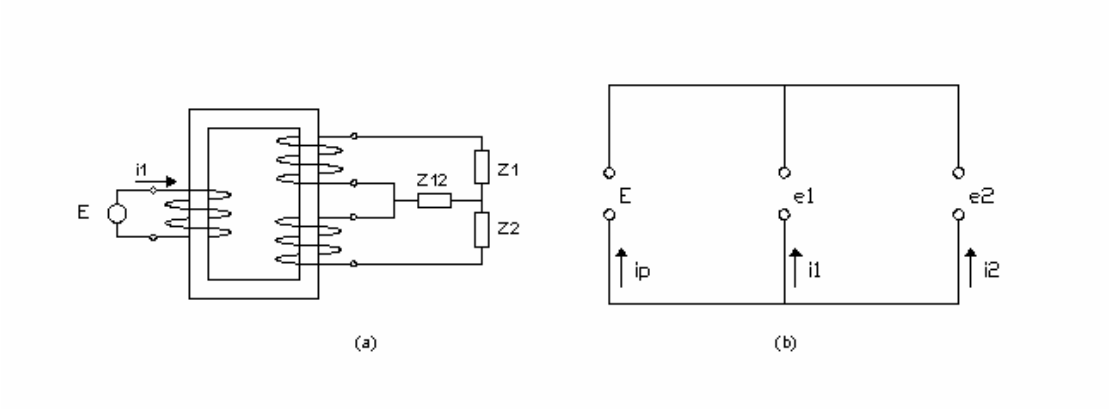

Figure 3.2
A transformer with interconnected windings (a) and the failure of the equivalent circuit (b)

It may sometimes be found that it is not possible to carry out this process. For example, let us consider the case of an external impedance common to two windings, illustrated in figure 3.2(a). The equivalent circuit of the transformer is shown in figure 3.2(b). It can be easily seen that there is no way in which the external circuit may be connected so as to support the same currents and voltages as in the actual system. Generally speaking it is only when each winding is connected to a separate load that connection of such loads in an equivalent circuit is guaranteed. Of course one can transform the external circuit, in order to bring it to a form which can be connected to the equivalent circuit of the transformer (in our example a star-delta transformation would do the job).

Finally, let us consider the general case of a practical transformer where loss phenomena such as core hysteresis and eddy currents are also present. Figure 3.3(a) shows a simple two-winding transformer with primary and secondary leakage fluxes, Φ'_p and Φ'_s respectively, and a finite core reluctance S. S_p and S_s are the reluctances of the air paths of the primary and secondary leakage fluxes. In this example we assume zero core losses and same number of turns for the two windings.

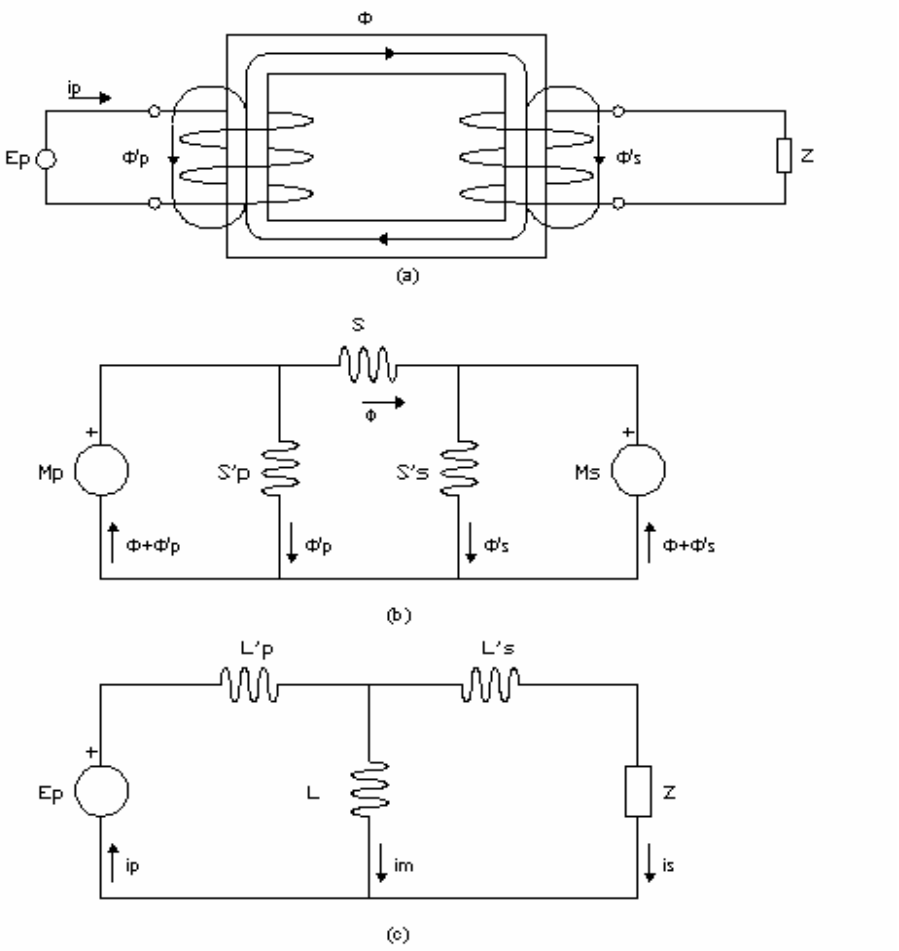

Figure 3.3
The practical transformer.
(a) transformer with leakage fluxes
(b) magnetic circuit
(c) equivalent circuit

The dual figure of the magnetic circuit may now be formed according to the rules, but the question arises: what electric element is dual to reluctances? Reluctances causes a loss of MMF proportional to the flux passing through it $MMF = \Phi \cdot S$. In the dual circuit MMF is replaced by current, and this must flow through an electric admittance to give a drop in voltage, dual to $d\Phi/dt$. This admittance is then the dual of reluctance, and furthermore it must be inductive. The duality relationship between magnetic reluctances and their equivalent electrical admittances can be shown to be independent of frequency:

$$S_1 : S_2 : S_3 : ... = 1/L_1 : 1/L_2 : 1/L_3 : ... \tag{3.4}$$

The previous statement can be easily proved:

In the steady state the ratio between the induced voltages is equal to the corresponding ratio of the rates of change of magnetic fluxes, that is:

$$j\omega\Phi_1 : j\omega\Phi_2 : j\omega\Phi_3 : ... = e_1 : e_2 : e_3 : ... \tag{3.5}$$

A similar relation between the MMFs and the currents may be found:

$$MMF_1 : MMF_2 : MMF_3 : ... = i_1 : i_2 : i_3 : ... \tag{3.6}$$

By dividing corresponding sides of equations (3.5) and (3.6) we have:

$$\frac{MMF_1}{j\omega\Phi_1} : \frac{MMF_2}{j\omega\Phi_2} : \frac{MMF_3}{j\omega\Phi_3} : ... = \frac{i_1}{e_1} : \frac{i_2}{e_2} : \frac{i_3}{e_3} : ... \tag{3.7}$$

which is the same as equation (3.4) if we define an electrical admittance as the dual of a magnetic reluctance.

In the previous example we have excluded the loss phenomena (hysteresis, eddy currents). The presence of the hysteresis in a magnetic sample is indicated by the finite area of the hysteresis loop; the average loop is of such a shape as to necessitate a nonlinear relationship between $\vec{B}$ and $\vec{H}$. However, if the production of harmonics is ignored, then the hysteresis loop may be regarded as a thin ellipse. In such a case we can use the idea of complex permeability, and extend it so as to regard the magnetic circuit elements, reluctance and "magnetic loss", as a complex magnetic impedance $\vec{S}$. The complex magnetic impedance may be calculated in a similar way to the normal magnetic reluctance, that is:

$$\vec{S} = \frac{l}{A}\frac{1}{\vec{\mu}} = \frac{l}{A}(\tau + j\psi) \tag{3.8}$$

where l is the mean magnetic path length, A is the cross-section and $\vec{\mu}$ is the complex permeability of the core section.

With the use of such a magnetic impedance we can find an equivalent electric circuit for the coil, namely an admittance:

$$\frac{1}{\vec{Z}} = (G - jB) \tag{3.9}$$

which is illustrated in almost every equivalent circuit as a resistance R parallel with an inductance L.

Comparison of the real and imaginary parts shows that:

- the real part of the reluctance $\vec{S}$ gives rise to a susceptance B in the equivalent circuit
- the imaginary part of the reluctance $\vec{S}$ gives rise to a conductance G, which stands for the core losses.

It should be emphasized here that the equivalent circuit depends on angular frequency ω and thus may be applied only to transformers working at a constant frequency.

Until now we have seen the duality relationship between magnetic and electric circuit of transformers with windings having equal number of turns, N. In order to form equivalent circuits for transformers with windings of unequal number of turns, one has to include ideal transformers. Thus if such a practical transformer has windings possessing unequal numbers of turns $N_1, N_2, N_3 \ldots$ these may be reduced to an equal number n by associating an ideal two-winding transformer with each separate winding, each of these ideal transformers having turn ratios of $N_1/n, N_2/n, N_3/n \ldots$ Care must be taken to include these ideal transformers as part of the external loads and not to apply the duality rules to them.

3.2 Advantages and disadvantages of duality-based models

The development of an electric equivalent circuit with application of the principle of duality offers some major advantages:

- The transformation of the magnetic circuit to its dual electric equivalent is described by a small set of well-defined rules, namely:

$$\begin{cases} e \leftrightarrow d\Phi/dt \\ i \leftrightarrow MMF \\ \vec{S} \leftrightarrow 1/\vec{Z} \end{cases}$$

- It is possible to include loss phenomena, such as hysteresis and eddy currents with application of the idea of complex magnetic permeability and complex reluctance.
- When the elements of the equivalent electric circuit have been defined, the solution can be found with normal network analyzers.
- With the use of ideal isolating transformers it is possible to connect any load to the transformer without any need to re-develop the equivalent circuit. Moreover, if one chooses to express the equivalent circuit in p.u. system, then the need for the ideal transformers is removed.

However, there are also some main restrictions for the duality-based models:

- When the magnetic circuit of the transformer is not a planar figure, it is generally not possible to build the equivalent circuit with the previous mentioned simple transformations. In such a case one can still develop an equivalent circuit, but some negative elements are then necessary in order to fulfill the original equations. These negative elements make the development of the equivalent circuit complicated, and the calculation of their values is not easy.
- Duality-based models are developed with the presumption of steady-state constant-frequency operation. It is for this reason that one cannot use such models for transient analysis.
- Winding resistance and capacitive coupling effects are not obtained directly from the transformation, they can, however, be added to the equivalent electrical circuit.

3.3 Development of a duality-based model for a three-phase core-type transformer

The development of the duality-based model for a three-phase two-winding core-type transformer presented here is based on the approach of Slemon [69]. A transformer as well as every electro-magnetic machine consists basically of a three-dimensional magnetic field linked with a number of coils. The first and most difficult step in developing an equivalent circuit is the reduction of this magnetic field into a magnetic circuit of lumped magnetic reluctances. When defining this lumped-parameters magnetic network one must carefully divide the magnetic core to sections which have a substantially uniform flux density. The proper division of the core to core-sections is of great importance, since the permeability of iron varies largely with the flux density. For the three-phase core-type transformer illustrated in figure 3.4(a) we assume the lumped-parameters magnetic circuit of figure 3.4(b).

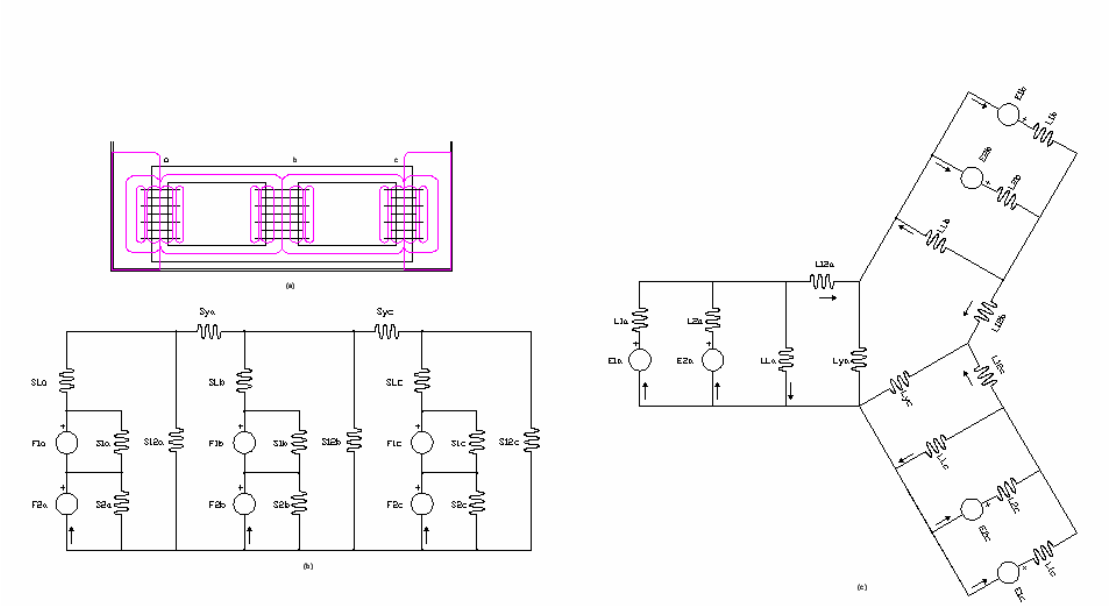

Figure 3.4
Equivalent circuit of three-phase core-type transformer.
(d) mean flux paths
(e) magnetic circuit
(f) equivalent electric circuit

As can be seen by the simplified magnetic circuit, we assume no linkage between windings of different phases. There are two main reasons for this assumption:

- The linkage between windings of different phases is very small in comparison to the linkage between windings of the same phase, especially in a core-type transformer where the core offers one extra leakage path.
- The introduction of leakage paths linking windings of different phases would make the simplified circuit non-planar, thus calling for negative circuit elements and making the whole model unclear.

The second step is the derivation of an electric circuit that is the equivalent of the lumped magnetic circuit and its linking coils, in a way that has been already described in the previous section. Each nonlinear magnetic element whose value is dependent on its magnetic flux is represented in the equivalent electric circuit by a nonlinear electric element whose value is dependent on the corresponding voltage. For the three-phase core-type transformer the equivalent electric circuit is shown in figure 3.4(c). In this figure we do not show the ideal transformers for reasons of clarity. All six voltages must, however, be considered as connected trough ideal transformers.

The nonlinear inductances corresponding to the three winding limbs are $L_{La}, L_{Lb,} L_{Lc}$, whereas those corresponding to the two core yokes are L_{ya}, L_{yc}. The inductances $L_{12a}, L_{12b}, L_{12c}$ represent the leakage paths through the transformer's tank, so they should also be taken as nonlinear, in order to describe effects due to the tank's residual magnetization [82]. The equivalent circuit of figure 3.4(c) is almost symmetrical, except for the absence of L_{yb}. It is this missing element of the circuit that introduces the asymmetry of the three-phase core-type transformer. During normal operation, the asymmetry can be neglected, but if there is a significant dc-component at the magnetizing field, then it can lead to severe voltage and current distortion.

3.4 Some other duality-based models

There exist various duality-based transformer models like the one presented in the previous paragraph. In this section we will briefly present some of the most interesting duality-based models for three-phase core-type transformers.

Perhaps the most known such model is the one introduced by Stuehm in [91]. The model was intended to be used in the Electro Magnetic Transient Program (EMTP) of the Bonneville Power Administration. EMTP is a simulation program of great importance not only for academics and researchers, but also for electrical apparatus designers.

Another duality-derived model for use with EMTP was developed at the same time with the previous by Chen [78] [79] [92]. However, this last model seems to be based more on the decoupled electric – magnetic approach than on the duality theory.

In [75] another topology-based magnetic model for the three-phase core-type transformer is introduced. It is based on – at that time – existing transformer models in EMTP, the major difference being the including of transformer data obtained by the zero-sequence short-circuit tests.

4. Decoupled Electric – Magnetic Circuits

4.1 Introduction

This approach is actually the most obvious way to solve Maxwell's Equations (2.1). The electric and magnetic behavior of the transformer is modeled separately and a set of restrictions are imposed to the solution of the equations. The present chapter will mainly focus on the derivation of a computer model for a three-phase core-type transformer based on the decoupled electric – magnetic approach.

As will be seen later, the major disadvantage of transformer models based on the decoupled electric – magnetic approach is that they are not as general as other models. In contrary to the duality-based models presented in the previous section, the decoupled electric – magnetic approach requires the winding connections to be known from before. In other words, for every different primary-secondary winding connection, another model should be used, which leads to loss of generality.

In order to build a model one has to first define the proper inputs and outputs. The source currents are the cause of the magnetizing process inside the transformer, so they could be defined as input to the system. However, it is actually the voltage that is imposed to a transformer, so that the magnetizing currents are rather the output than the input to the system. For this reason we define as input the source voltages.

The transformer's terminal connections must also be fed as input to the system. We can assume that the source voltages are applied at the transformer's terminals. Then the other input to the system must be the load-side $(v-i)$ characteristic, that is the load-side impedances.

4.2 The developed model

The model developed in this work is based on the circuit analysis of the transformer's magnetic core. It should be seen as an extension of some already existing models, like the "geometrical" model introduced in [74]. The main difference of the hereby proposed model lies in the representation of the core's nonlinearities.

The subject of the model is the two-winding three-phase core-type transformer. The model was developed in order to mainly simulate the steady-state operation under dc bias of the source currents, but it still can be used for studying some low-frequency transient phenomena. It does not take into account the capacitive coupling of the windings, which can appear at higher frequencies.

We assume, without loss of generality, that the source voltage is applied on the primary side. The system's behavior is then described by the State Equation (4.1), whereas the outputs are given by the Output Equation (4.2):

$$\dot{\underline{\phi}}_s = f\left(t, \underline{\phi}_s\right) = A\left(\underline{\phi}_s\right) \cdot \underline{\phi}_s + B \cdot \underline{u}_{pri}(t) \tag{4.1}$$

$$\underline{i}_s = C\left(\underline{\phi}_s\right) \cdot \underline{\phi}_s \tag{4.2}$$

As can be seen from equation (4.1), the system can be described by a set of nonlinear ordinary differential equations. The more suitable state variables for the system are the magnetic fluxes of the nonlinear iron core sections. The equivalent magnetic circuit of the transformer is shown in figure 4.1. The derivation of this lumped circuit is presented in the following paragraphs.

For reasons of better control over the system, only the windings' magnetic fluxes, $\underline{\phi}_s$, are used as state variables. The magnetic core's nonlinearities are described in equation (4.1) by the nonlinear state matrix $A\left(\underline{\phi}_s\right)$. The solution of the system (4.1), (4.2) is not an easy task and cannot be found with analytical tools. In contrary, advanced iterative arithmetic methods have to be applied. The mathematical expression of the proposed model can be found in Appendix A.

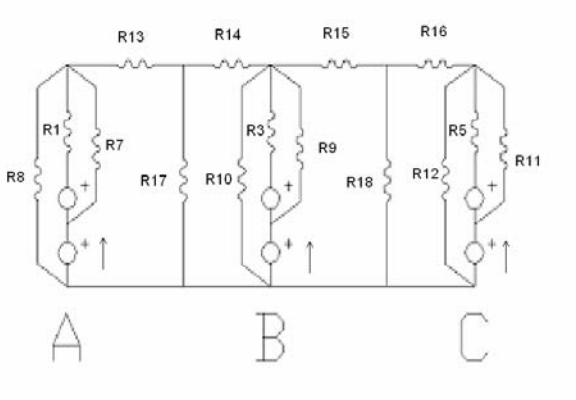

Figure 4.1
Magnetic equivalent circuit

The main assumption made for the development of the magnetic equivalent circuit (figure 4.1) is that there is no coupling between windings of different phases. The leakage air paths are represented by the constant magnetic reluctances $R_{7-11}, R_{17,18}$. It should be stated here that in the developed model the nonlinear behavior of the transformer's tank has not been included. This makes the model inappropriate for "full-tank" transformers which have small gaps between the magnetic core and the tank. However, an extension of the model in order to also describe the tank's behavior is possible with the decoupled electric – magnetic approach.

The transformer's magnetic core is represented in figure 4.1 by the nonlinear magnetic reluctances R_1, R_3, R_5, R_{13-16}, with the first three terms corresponding to the core's limbs and the latter four to the yokes.

The secondary connections of the transformer is given by matrix Z. In the general case this should be a (3×3) complex matrix, but for reasons of simplicity our model supports only open-circuited secondary windings or pure ohmic load. A generalization of the load representation would require either the usage of complex numbers arithmetic or the introduction of some more state variables, namely the currents and the voltages at the load's inductances and capacitances, respectively.

For the solution of the mathematical model found in Appendix A, a computer program has been developed. The program was written in C programming language and the source code is given in Appendix C. It mainly consists of an iterative loop, from heron named "Runge-Kutta loop", which in turn is based on the well-known Runge-Kutta algorithm, as the name states. The 4^{th} order Runge-Kutta algorithm is used in order to solve the state equation (4.1) directly in the time domain. In the Runge-Kutta loop, the state equation is, for the same time step, solved more times by updating the nonlinear magnetic reluctances of the core, until two successive solutions show the desired convergence. The flowchart of the developed computer program is shown in figure 4.2.

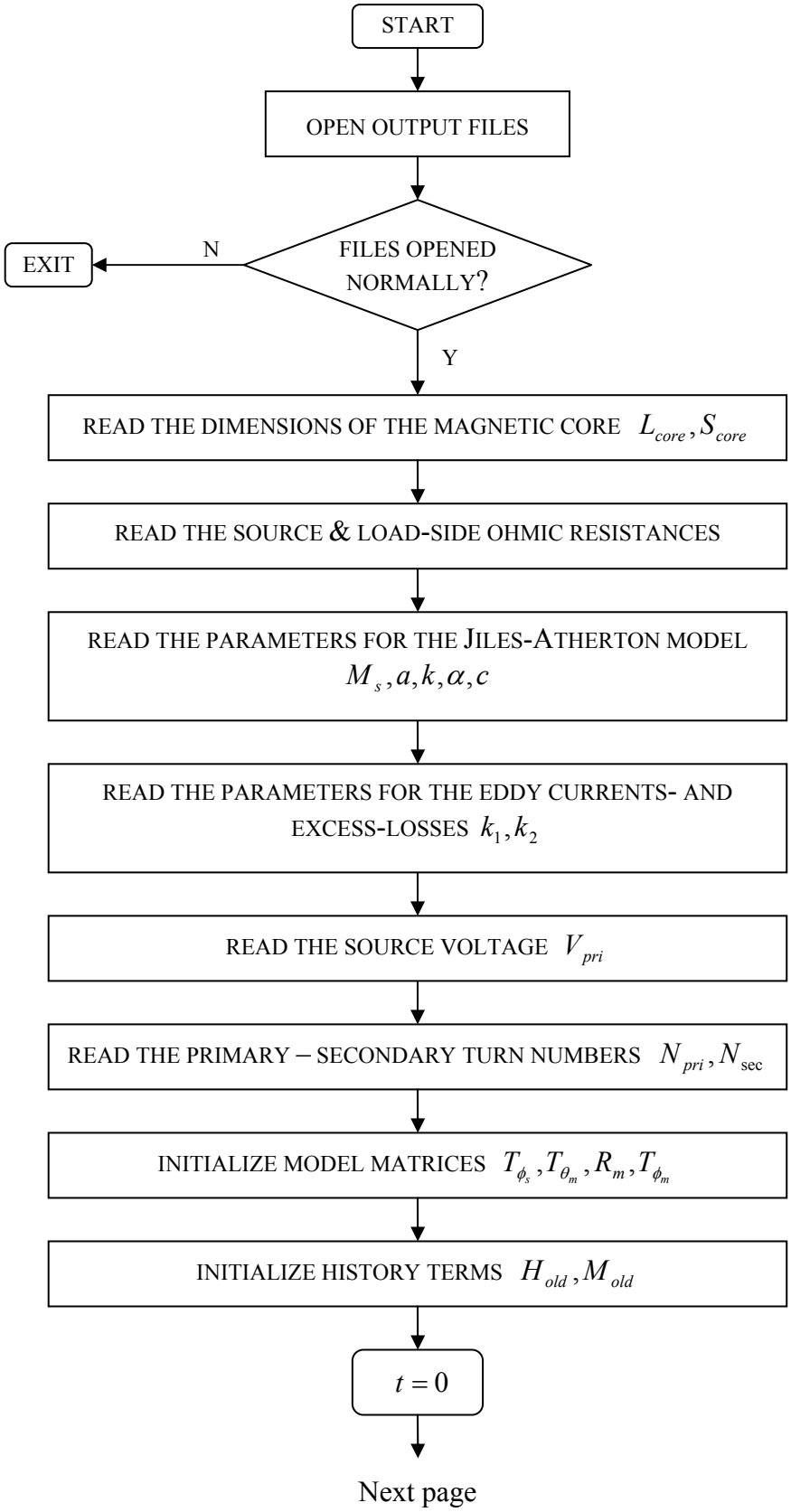

Figure 4.2
Flowchart (part 1) of program listed in Appendix C

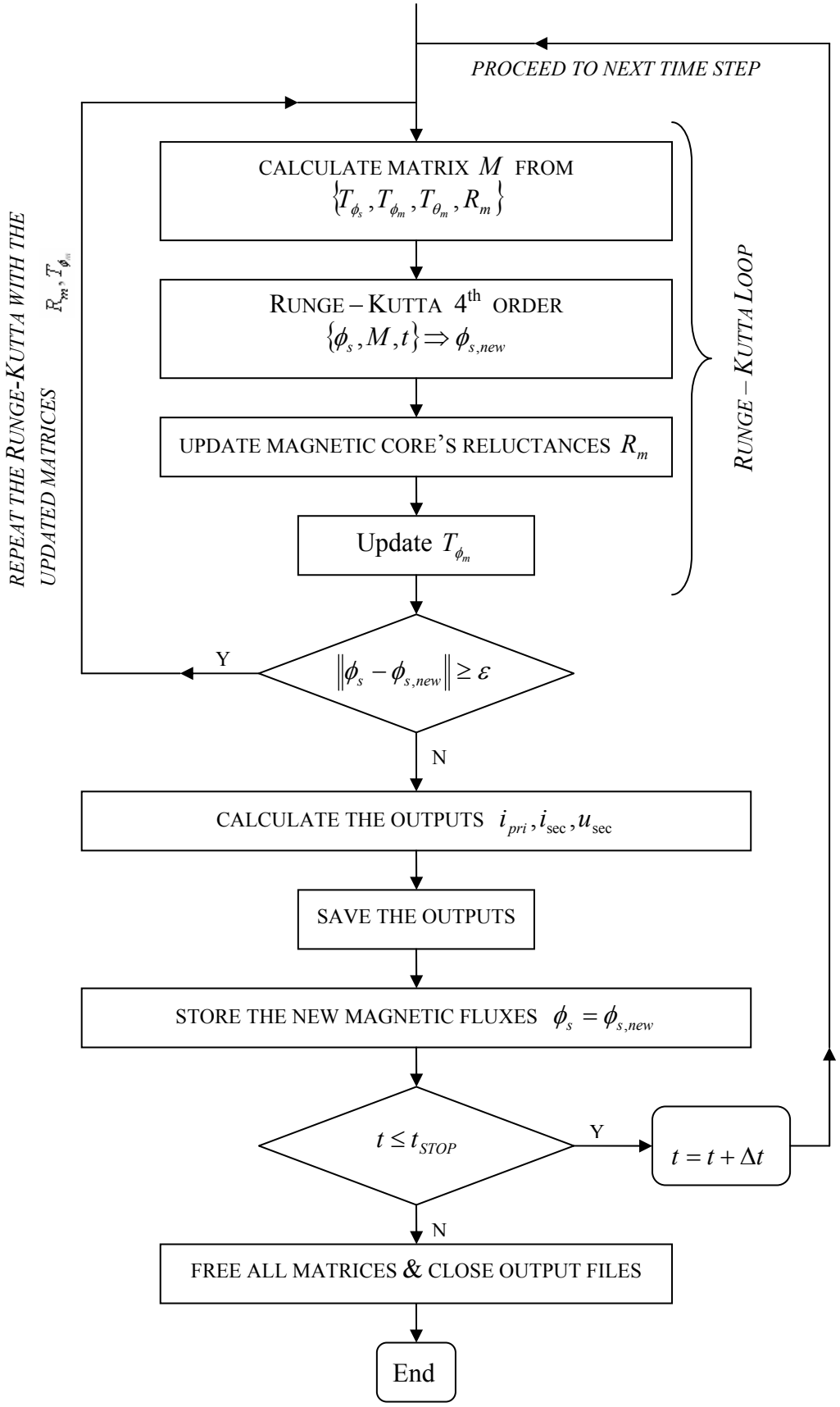

Figure 4.2
Flowchart (part 2) of program listed in Appendix C

4.3 Test case and simulation results

The model proposed in §4.2 was used for the simulation of the behavior of a three-phase core-type transformer. Unfortunately, there was no test transformer available at the laboratory of the Institute at the time this work was written. This introduced following difficulties:

- Lack of necessary data for the transformer model. As these data are not listed on transformer designers' brochures, the only possible solution was to search in already published papers about transformer modeling.
- It was not possible to compare the simulation results with actual measurements. This makes the results of the proposed model just a speculation of what could be the behavior of the modeled transformer.

The data for the Jiles- Atherton hysteresis model were obtained from [27] for a low-carbon steel $\{Fe, 0.6\% wt.C\}$ magnetic core. For the core dimensions and the rest of the necessary transformer data, the transformer used in [76] was used. Detailed information about the modeled transformer can be found in table 4.1.

J-A hysteresis model	M_s	a	k	α	c
	$1.6 \cdot 10^6$	972	672	$1.4 \cdot 10^{-3}$	0.14
Transformer data	Limb length	Limb cross-sectional area	Yoke length	Yoke cross-sectional area	$N_{pri}/N_{\sec}$
	$3.59m$	$0.4536m^2$	$2.656m$	$0.4536m^2$	$65/450$

Table 4.1
Model parameters of the test transformer

The behavior of the test transformer was simulated with the program of Appendix C for the following operating instances:

- Open-circuited secondary without dc bias on the source voltages
- Open-circuited secondary with 15% dc bias on the source voltages
- Open-circuited secondary with 30% dc bias on the source voltages

Unfortunately, the effect of the connection of the load to the behavior of the transformer was not examined, because of the short period of time granted by the Erasmus exchange program. However, it is possible to adjust the model's parameters in such a way that the model represents closely the measured waveforms of three-phase core-type transformers.

In the following pages, the simulations results are listed in form of diagrams.

4.3.1 Open-circuited secondary without dc bias on the source voltages

Figures 4.3 to 4.5 show the behavior of the three-phase core-type transformer with the features listed in the previous section under normal excitation.

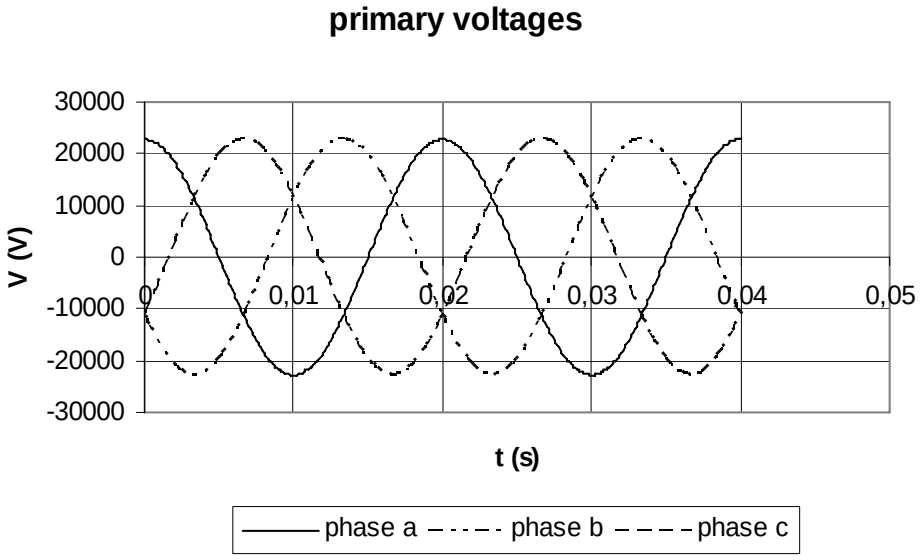

Figure 5.3
Primary voltages under normal excitation

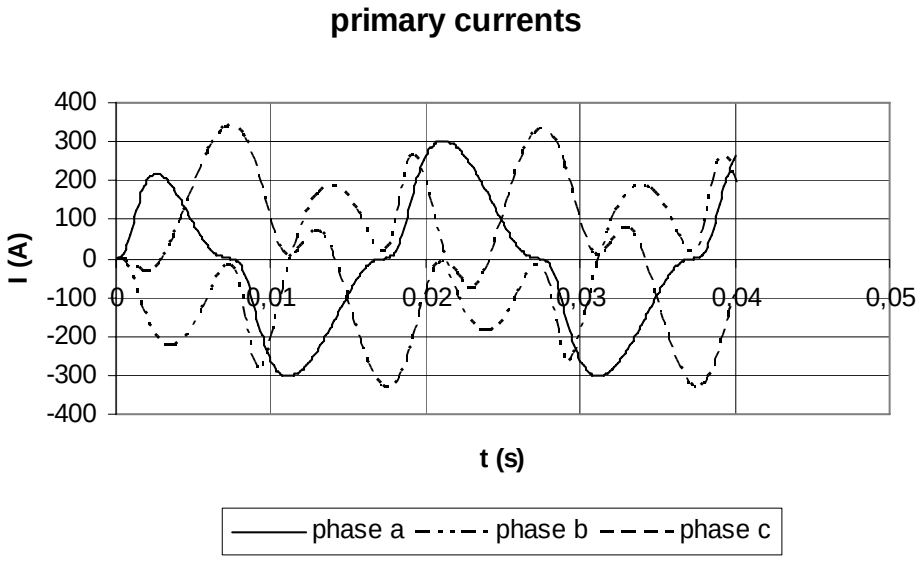

Figure 4.4
Primary currents under normal excitation

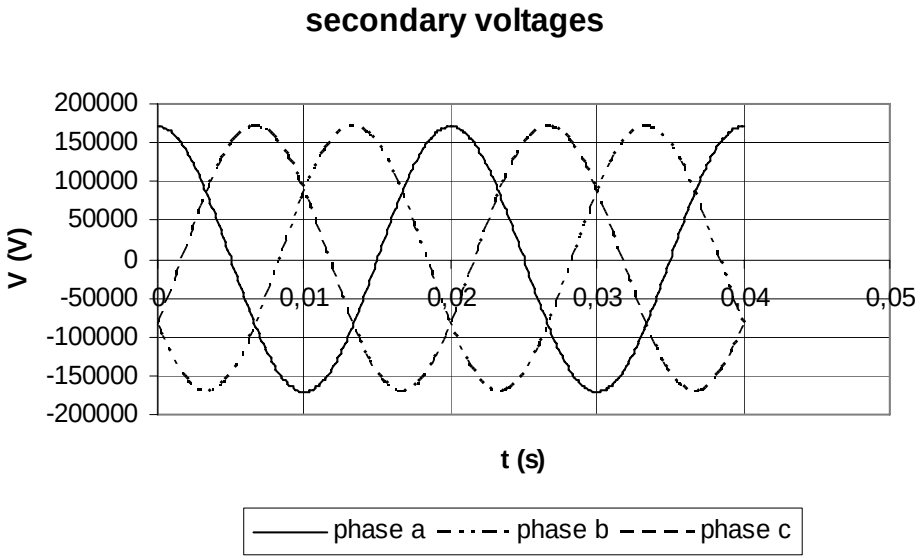

Figure 4.5
Secondary voltages under normal excitation

4.3.2 Open-circuited secondary with 15% dc bias on the source voltages

We applied 15% dc bias on one phase's voltage (phase a, b, c – one at each time). The results are illustrates in figures 4.6 to 4.14:

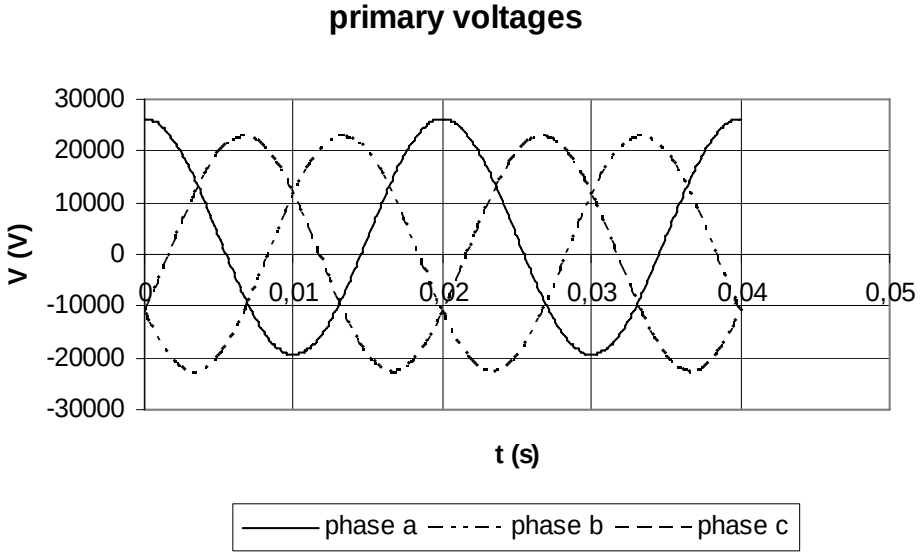

Figure 4.6
Primary voltages under 15% over excitation (phase a)

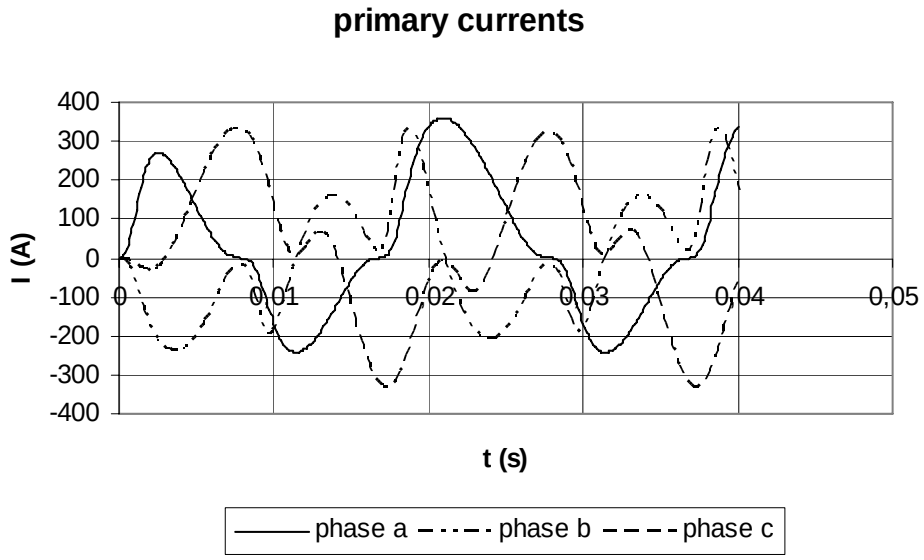

Figure 4.7
Primary currents under 15% over excitation (phase a)

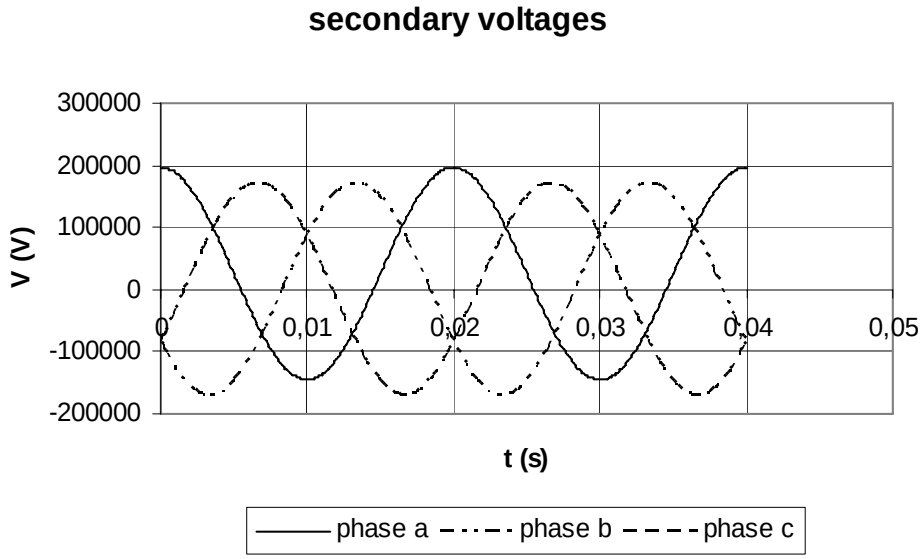

Figure 4.8
Secondary voltages under 15% over excitation (phase a)

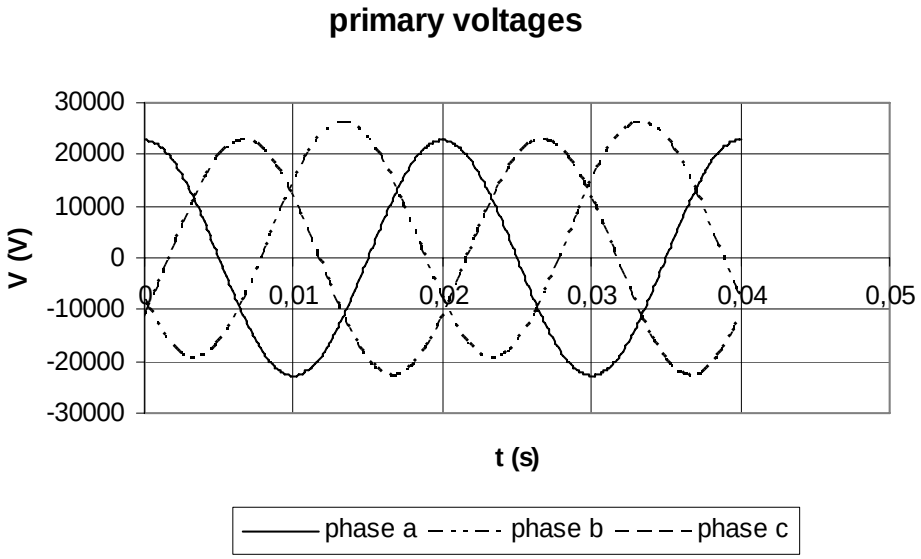

Figure 4.9
Primary voltages under 15% over excitation (phase b)

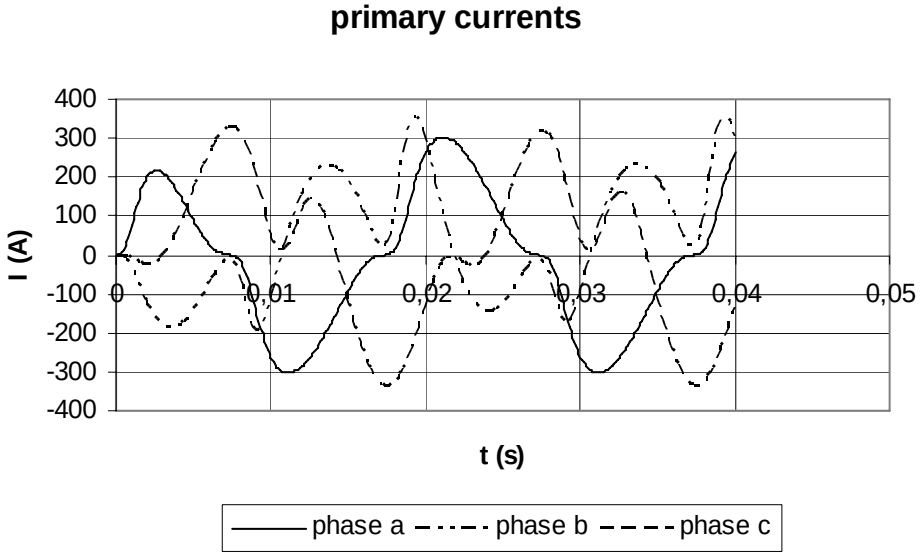

Figure 4.10
Primary currents under 15% over excitation (phase b)

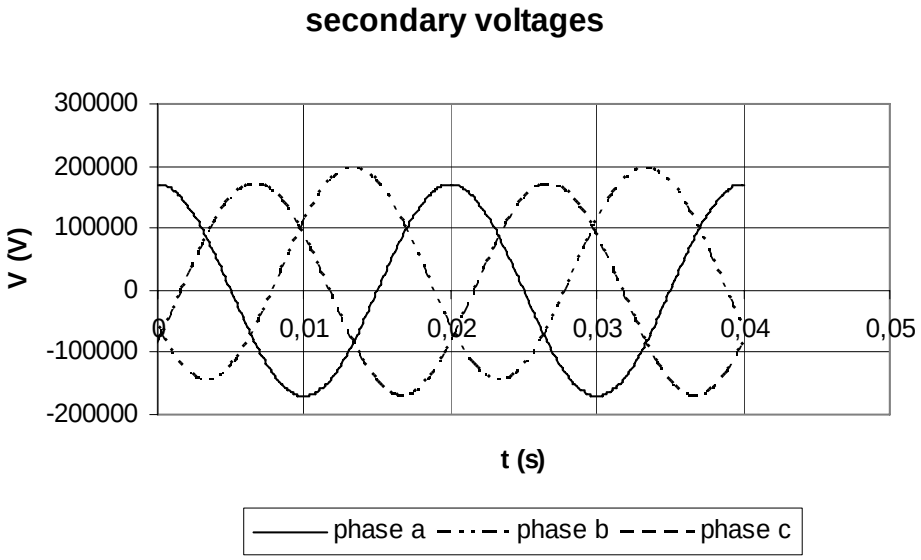

Figure 4.11
Secondary voltages under 15% over excitation (phase b)

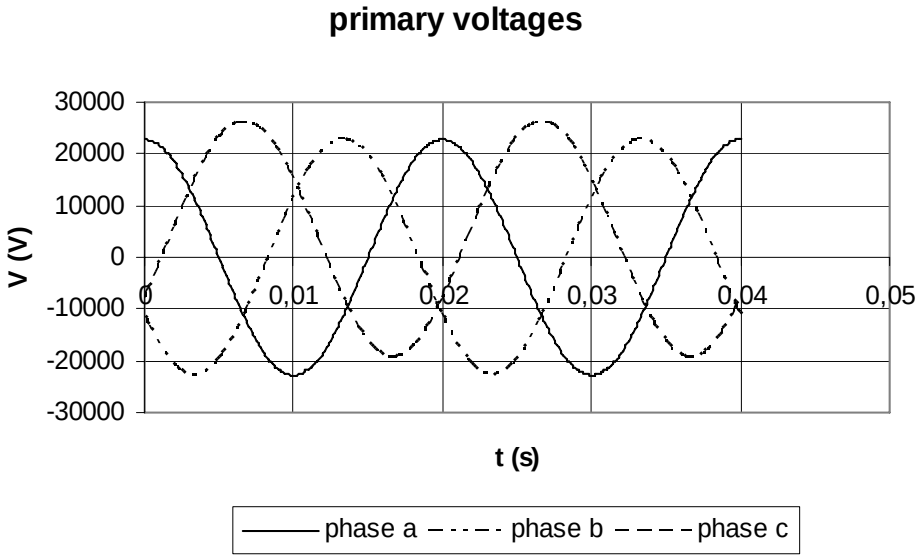

Figure 4.12
Primary voltages under 15% over excitation (phase c)

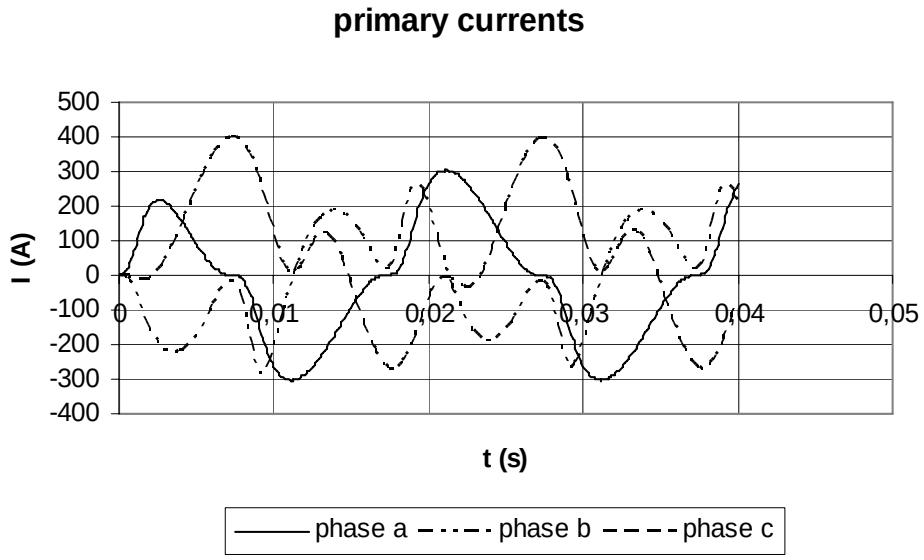

Figure 4.13
Primary currents under 15% over excitation (phase c)

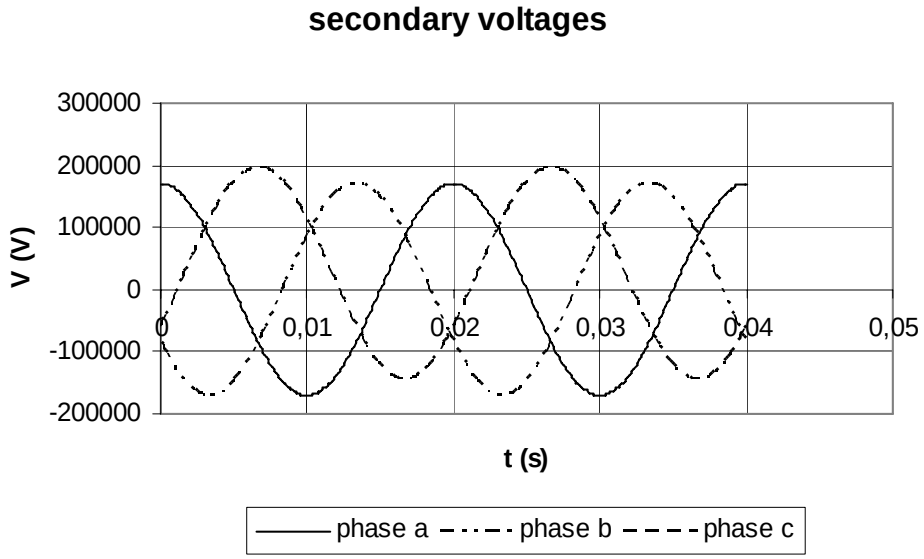

Figure 4.14
Secondary voltages under 15% over excitation (phase c)

4.3.3 Open-circuited secondary with 30% dc bias on the source voltages

We also applied 30% dc bias on one phase's voltage (phase b). The results are illustrates in figures 4.14 to 4.17:

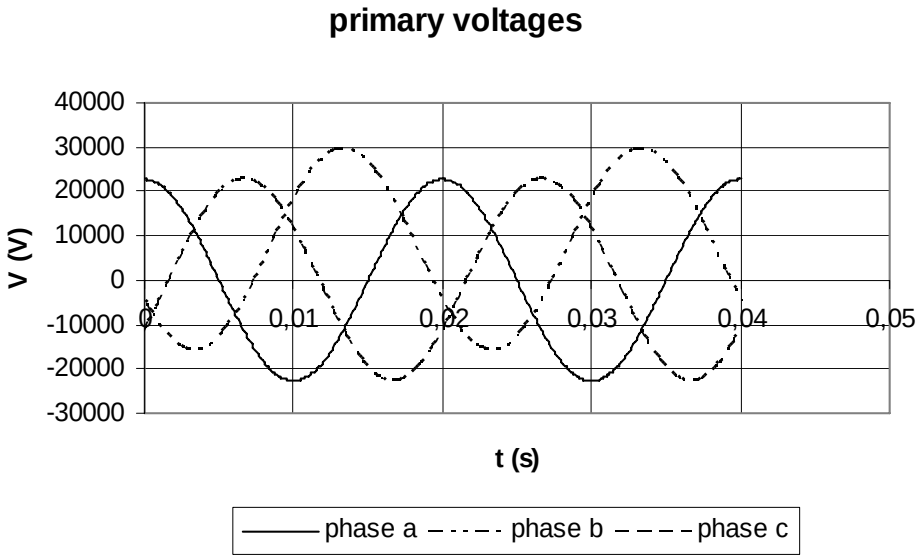

Figure 4.15
Primary voltages under 30% over excitation (phase b)

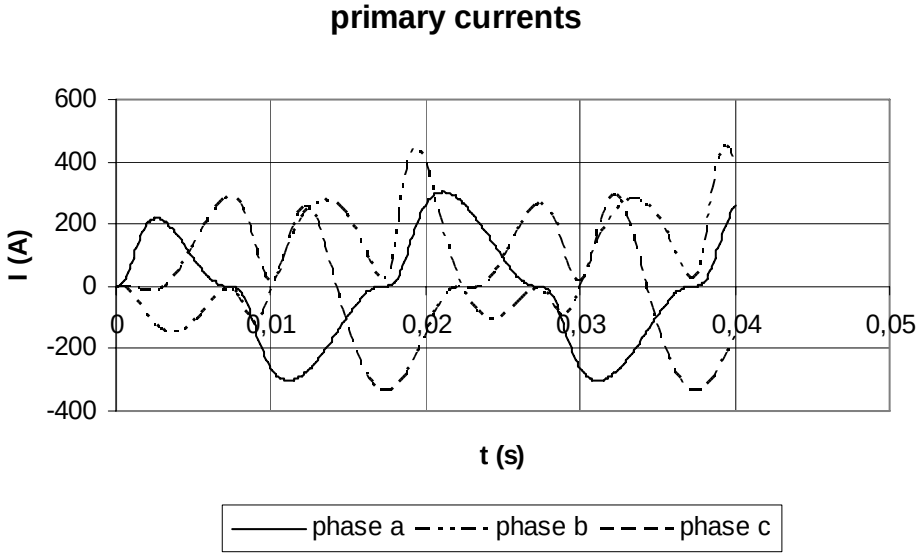

Figure 4.16
Primary currents under 30% over excitation (phase b)

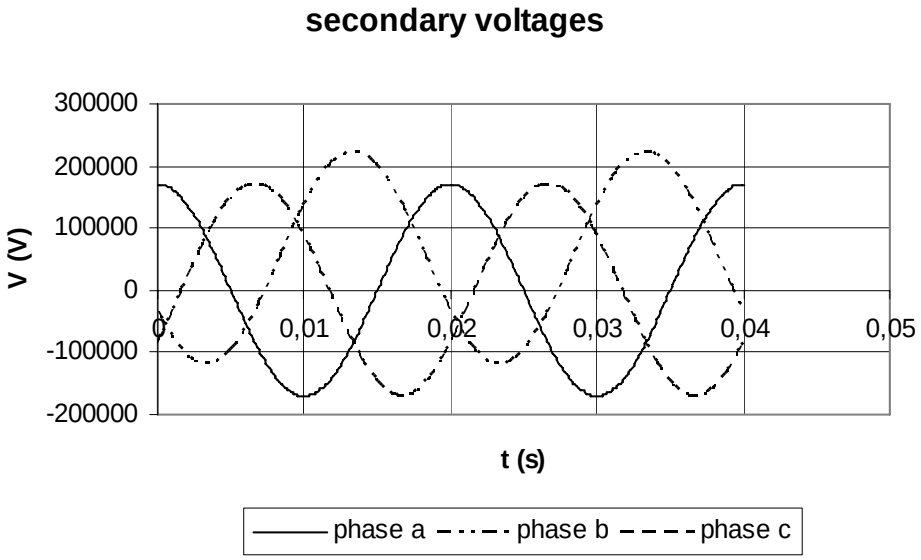

Figure 4.17
Secondary voltages under 30% over excitation (phase b)

4.3.4 Effect of the parameter k_1 representing the classical eddy-currents losses

Figures 4.18 to 4.21 show the primary currents simulated for different values of the parameter k_1, standing for the classical eddy currents losses. Normal excitation is supposed.

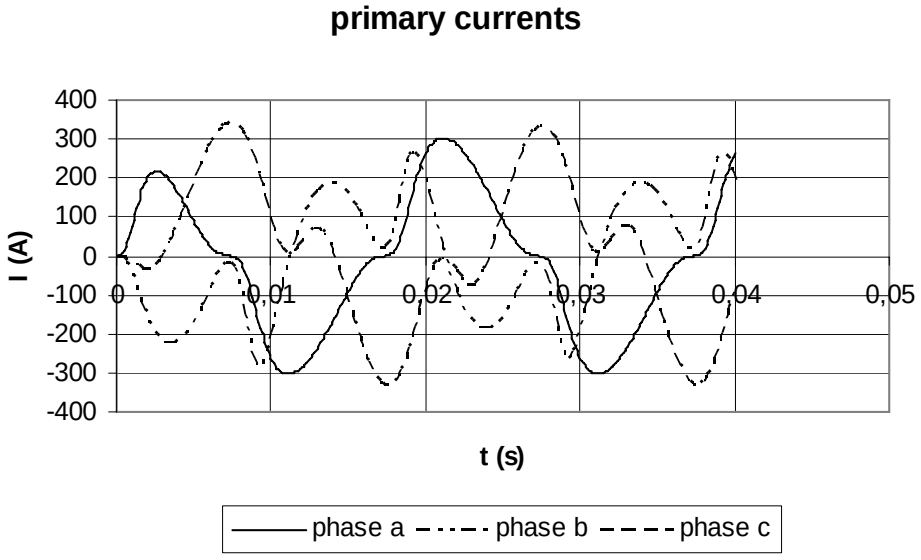

Figure 4.18
Primary currents under normal excitation $(k_1 = 10.0)$

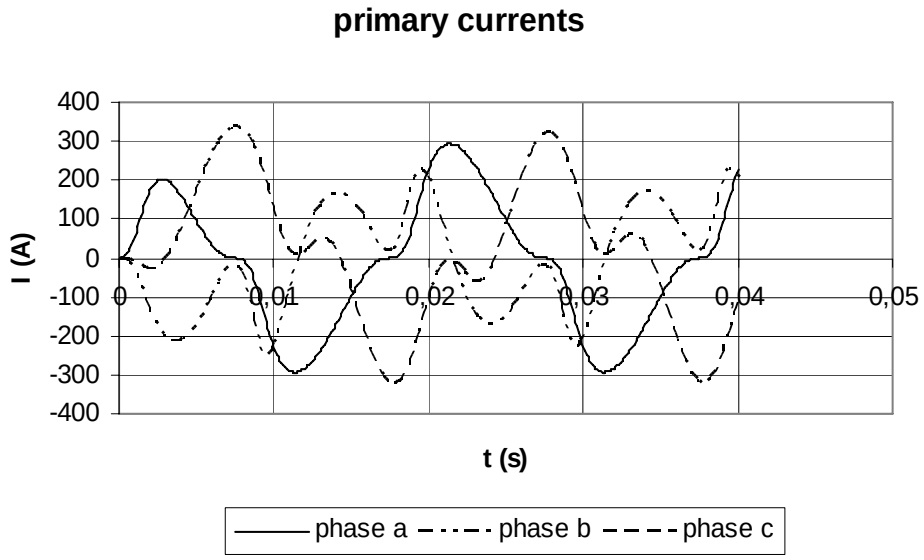

Figure 4.19
Primary currents under normal excitation $(k_1 = 1.0)$

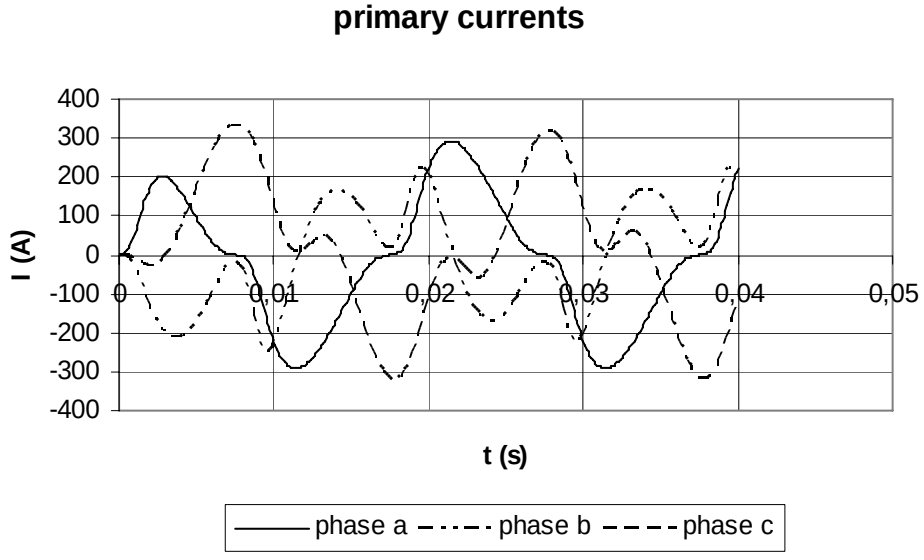

Figure 4.20
Primary currents under normal excitation $(k_1 = 0.1)$

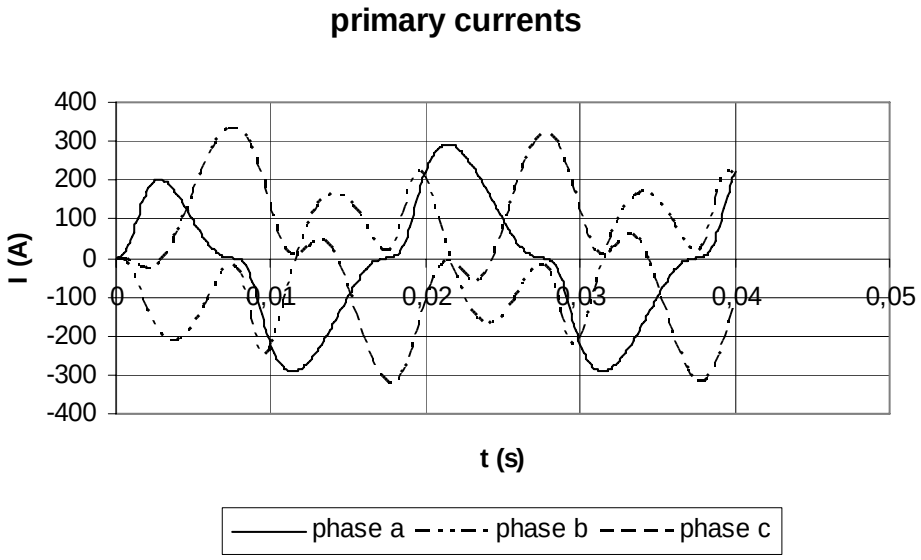

Figure 4.21
Primary currents under normal excitation $(k_1 = 0.01)$

5. Conclusions

The main nonlinearities of the three-phase core-type transformer are:

- Core saturation
- Ferromagnetic hysteresis
- Eddy currents
- Phase asymmetry

In section 2 we have briefly presented the most known representations of these phenomena. The models presented in that section vary from experimental (curve fitting) to theoretical (physical explanation).

However, a complete transformer model which takes into account all the nonlinearities cannot be found in literature. The available models are mostly designed for system studies, thus they do not describe accurately the behavior of the transformer as a separate unit.

In section 3 the principle of duality was introduced. Duality can be applied on electromagnetic devices such as transformers; however, there are two main difficulties in this application:

- High complexity of the lumped parameter magnetic circuit of the three-phase core-type transformer, and
- Duality can be applied only for a constant frequency, that is to say, for steady-state operation.

Section 4 dealt with the decoupled electric – magnetic approach to the transformer. A program in C programming language has been developed for computer simulations of low-frequency transient phenomena. Because of lack of time, the program has not been completely debugged, thus enabling only the simulation of open-circuit tests. Following development of the program is proposed for future work:

- Correct determination of the model's parameters
- Studies of load – connection effect
- Generalization of the connected resistances, in order to also include inductive loads
- Solving the reported problems of numerical instabilities

6. References

[1] E. Lowdon
"Practical Transformer Design Handbook"
Howard W. Sams & Co., 1980

[2] L.F. Blume, A. Boyajian, G. Camilli, T.C. Lennox, S. Minneci, V.M. Montsinger
"Transformer Engineering"
John Wiley & Sons, 1951

[3] W.M. Flanagan
"Handbook of Transformer Design and Applications"
McGraw-Hill, 1992

[4] R. Feinberg
"Modern Power Transformer Practice"
The Macmillan Press, 1979

[5] Hosemann-Boeck
"Grundlagen der elektrischen Energietechnik"
Springer Verlag, Berlin-Heidelberg, 1991

[6] J. Arrillaga, C.P. Arnold, B.J. Hasker
"Computer Modelling of Electrical Power Systems"
John Wiley & Sons, 1983

[7] J.B. Gibbs
"Transformer Principles and Practice"
McGraw-Hill, 1949

[8] H.E. Dijk
"On Transformer Modelling"
PhD thesis

[9] H.W. Dommel
"Electromagnetic Transient Program, Reference Manual (EMTP Theory Book)"
August 1986

[10] F.W. Bradley
"Materials for Magnetic Functions"
Hayden Book Company, 1971

[11] G.R. Slemon
"Magnetoelectric Devices – Transducers, Transformers and Machines"
John Wiley & Sons, 1966

[12] S. Chikazumi
"Physics of Magnetism"
John Wiley & Sons, 1964

[13] D.C. Jiles
"Introduction to Magnetism and Magnetic Materials"
Chapman & Hall, 1991

[14] A. Greenwood
"Electrical Transients in Power Systems"
John Wiley & Sons, 1991

[15] V. Ostovic
"Dynamics of Saturated Electrical Machines"
Springer Verlag, New York, 1989

[16] T. Kleineberg
"Modellierung nichtlinearer induktiver Bauelemente der Leistungselektronik"
VDI-Verlag Duesseldorf, 1995

[17] C. Pérez-Rojas
"Fitting Saturation and Hysteresis via Arctangent Functions"
IEEE Power Engineering Review, November 2000

[18] F. Preisach
"Ueber die magnetische Nachwirkung"
Zeitschrift der Physik, vol. B 94, 1935

[19] M. Krasnoselskii, A. Pokrovskii
"Systems with Hysteresis"
Nauka, Moscow, 1983

[20] I.D. Mayergoyz
"Mathematical Models of Hysteresis (Invited)"
IEEE Transactions on Magnetics, vol. MAG-22, no.5, September 1986

[21] I.D. Mayergoyz, G. Friedman
"Generalized Preisach Model of Hysteresis (Invited)"
IEEE Transactions on Magnetics, vol.24, no.1, January 1988

[22] I.D. Mayergoyz
"The Classical Preisach Model of Hysteresis and Reversibility"
Journal Applied Physics, vol. 69, no.8, 1991

[23] J.M. Prousalidis, N.D. Hatziargyriou, B.C. Papadias
"Representation of Hysteresis in Three-Phase Transformer Models for Electromagnetic Transients"
IEE Proceedings on Electrical Power Applications, vol. 143, no. 4, July 1996

[24] D.C. Jiles
"Theory of Ferromagnetic Hysteresis"
J. Appl. Phys., vol. 55, no.6, 1984

[25] D.C. Jiles, D.L. Atherton
"Theory of Ferromagnetic Hysteresis"
JMMM, vol. 61, 1986

[26] D.C. Jiles, D.L. Atherton
"Ferromagnetic Hysteresis"
IEEE Transactions on Magnetics, vol. MAG-19

[27] D.C. Jiles, J.B. Thoelke, M.K. Devine
"Numerical Determination of Hysteresis Parameters for the Modeling of Magnetic properties Using the Theory of Ferromagnetic Hysteresis"
IEEE Transactions on Magnetics, vol. 28, no. 1, January 1992

[28] R.P. Jayasinghe, P.G. McLaren
"Transformer Core Models Based on the Jiles-Atherton Algorithm"
1997 Conference on Communications, Power and Computing

[29] K.H. Carpenter
"A Differential Equation Approach to Minor Loops in the Jiles-Atherton Hysteresis Model"
IEEE Transactions on Magnetics, vol. 27, no.6, November 1991

[30] E.C. Stoner, E.P. Wolhfarth
"A Mechanism of Magnetic Hysteresis in Heterogeneous Alloys"
Phil. Trans. Roy. Soc., vol. 240A, May 4, 1948

[31] D.L. Atherton, J.R. Beattie
"A Mean Field Stoner-Wolhfarth Hysteresis Model"
IEEE Transactions on Magnetics, vol. 26, November 1990

[32] A. Globus
"Universal Hysteresis Loop for Soft Ferrimagnetic Material"
Proceedings European Physical Society, Conference on Soft Magnetic Material 2, 1975

[33] A. Globus, P. Dublex, M. Guyot
"Determination of Initial Magnetization Curve from Crystallites Size and Effective Anisotropy Field"
IEEE Transactions on Magnetics, vol. MAG-7, May 1971

[34] M. Le Floc'h
"Analytical Expression of the Initial Magnetization Curve in Soft Magnetic Polycrystalline Materials"
Journal Applied Physics, vol. 67, no.1, 1990

[35] M. Guyot, A. Globus
"Determination of the Domain Wall Energy and the Exchange Constant from Hysteresis in Ferrimagnetic Polycrystals"
Phys. Stat. Sol. (b), vol.59, 1973

[36] M. Popov, L. van der Sluis, G.C. Paap, P.H. Schavemaker
"On a Hysteresis Model for Transient Analysis"
IEEE Power Engineering Review, May 2000

[37] B.D. Coleman, M.L. Hodgdon
"A Constitutive Relation for rate-Independent Hysteresis in Ferromagnetic Soft Materials"
Int. J. Engin. Sci., 24, no.6, 1986

[38] B.D. Coleman, M.L. Hodgdon
"On a Class of Constitutive Relations for Ferromagnetic Hysteresis"
Arch. Rational Mech. Anal.

[39] M.L. Hodgdon
"Applications of a Theory of Ferromagnetic Hysteresis"
IEEE Transactions on Magnetics, vol. 24, no.1, January 1988

[40] F. Ossart, G. Meunier
"Comparison between Various Hysteresis Models and Experimental Data"
IEEE Transactions on Magnetics, vol. 26, no. 5, September 1990

[41] F. Liorzou, B. Phelps, D.L. Atherton
"Macroscopic Models of Magnetization"
IEEE Transactions on Magnetics, vol. 36, no. 2, March 2000

[42] B.F. Phelps, F. Liorzou, D.L. Atherton
"Inclusive Model of Ferromagnetic Hysteresis"
IEEE Transactions on Magnetics, vol. 38, no. 2, March 2002

[43] Z. Tao, L. Jianfei, L. Wanshum, L. Guicun
"Simulation of Transformer Hysteresis Loop Using Fractal Theory"
Proceedings of the 2002 IEEE Canadian Conference on Electrical & Computer Engineering

[44] F. de Leon, A. Semlyen
"A Simple Representation of Dynamic Hysteresis Losses in Power Transformers"
IEEE Transactions on Power Delivery, vol. 10, no. 1, January 1995

[45] C.E. Lin, J.-B. Wei, C.-L. Huang, C.-J. Huang
"A New Model for Transformer Saturation Characteristics by Including Hysteresis Loops"
IEEE Transactions on Magnetics, vol. 25, no.3, May 1989

[46] C.E. Lin, J.-B. Wei, C.-L. Huang, C.-J. Huang
"A New Method for Representation of Hysteresis Loops"
IEEE Transactions on Power Delivery, vol. 4, no.1, January 1989

[47] J.G. Frame, N. Mohan, T. Liu
"Hysteresis Modeling in an Electro-Magnetic Transients Program"
IEEE Transactions on Power Apparatus and Systems, vol. PAS-101, no.9, September 1982

[48] R.I. Potter, R.J. Schmulian
"Self-Consistently Computed Magnetization Patterns in Thin Magnetic Recording Media"
IEEE Transactions on Magnetics, vol. MAG-7, no.4 December 1971

[49] L.O. Chua, S.C. Bass
"A Generalized Hysteresis Model"
IEEE Transactions on Circuit Theory, vol. CT-19, no. 1, January 1972

[50] E.J. Tarasiewicz, A.S. Morched, A. Narang, E.P. Dick
"Frequency Dependent Eddy Current Models for Nonlinear Iron Cores"
IEEE Transactions on Power Systems, vol. 8, no. 2, May 1993

[51] J. Avila-Rosales, F.L. Alvarado
"Nonlinear Frequency Dependent Transformer Model for Electromagnetic Transient Studies in Power Systems"
IEEE Transactions on Power Apparatus and Systems, vol. PAS-101, no.11, November 1982

[52] J. Avila-Rosales, A. Semlyen
"Iron Core Modeling for Electrical Transients"
IEEE Transactions on Power Apparatus and Systems, vol. PAS-104, no.11, November 1985

[53] E.P. Dick, W. Watson
"Transformer Models for Transient Studies Based on Field Measurements"
IEEE Transactions on Power Apparatus and Systems, vol. PAS-100, no.1, January 1981

[54] J. Juillard, B. de Barmon, G. Berthiau
"Simple Analytical Three-Dimensional Eddy-Current Model"
IEEE Transactions on Magnetics, vol. 36, no.1, January 2000

[55] A.G. Kladas, J.A. Tegopoulos
"3D Eddy Currents Modelling by means of a Particular Reduced Scalar Potential Technique"
IEEE Transactions on Magnetics, vol. 33, no.2, March 1997

[56] A.G. Kladas, J.A. Tegopoulos
"Eddy Currents Modeling in Solid Iron by Using Analytical Elements"
IEEE Transactions on Magnetics, vol. 30, no.5, September 1994

[57] W. Chandrasena, P.G. McLaren, U.D. Annakkage, R.P. Jayasinghe, E. Dirks
"Simulation of Eddy Current Effects in Transformers"
Proceedings of the 2002 IEEE Canadian Conference on Electrical & Computer Engineering

[58] U.D. Annakkage, P.G. McLaren, E. Dirks, R.P. Jayasinghe, A.D. Parker
"A Current Transformer Model Based on the Jiles-Atherton Theory of Ferromagnetic Hysteresis"
IEEE Transactions on Power Delivery, vol. 15, no.1, January 2000

[59] D.C. Jiles
"Modeling the Effects of Eddy Currents Losses on Frequency Dependent Hysteresis in Electrically Conducting Media"
IEEE Transactions on Magnetics, vol. 30, no.6, 1994

[60] F. Fiorillo, A. Nikonov
"An Improved Approach to Power Losses in Magnetic Laminations under Nonsinusoidal Induction Waveform"
IEEE Transactions on Magnetics, vol. 26, no.5, September 1990

[61] F. de Leon, A. Semlyen
"Efficient Calculation of Elementary Parameters of Transformers"
IEEE Transactions on Power Delivery, vol. 7, no.1, January 1992

[62] C.G.A. Koreman
"Determination of the Magnetizing Characteristic of Three-Phase Transformers in Field Tests"
IEEE Transactions on Power Delivery, vol. 4, no.3, July 1989

[63] T. Stensland, E.F. Fuchs, W.M. Grady, M.T. Doyle
"Modeling of Magnetizing and Core-Loss Currents in Single-Phase Transformers with Voltage Harmonics for Use in Power Flow"
IEEE Transactions on Power Delivery, vol. 12, no.2, April 1997

[64] D. Lin, E.F. Fuchs, M. Doyle
"Computer-Aided Testing of Electrical Apparatus Supplying Nonlinear Loads"
IEEE Transactions on Power Systems, vol. 12, no.1, February 1997

[65] E.F. Fuchs, D. Yildirim, W. Mack Grady
"Measurements of Eddy-Current Loss Coefficient P_{EC-R}, Derating of Single-Phase Transformers, and Comparison with K-Factor Approach"
IEEE Transactions on Power Delivery, vol. 15, no.1, January 2000

[66] E.F. Fuchs, Y. You
"Measurement of $\lambda - i$ Characteristics of Asymmetric Three-Phase Transformers and Their Applications"

[67] J.A. Martinez, B.A. Mork
"Transformer Modeling for Low- and Mid-Frequency Transients – A Review"
IEEE Transactions on Power Delivery, vol. 20, no.2, April 2005

[68] E.C. Cherry
"The Duality Between Interlinked Electric and Magnetic Circuits and the Formation of Transformer Equivalent Circuits"
Proceedings of the Physical Society, vol. 62, 1949

[69] G.R. Slemon
"Equivalent Circuits for Transformers and Machines Including Non-Linear Effects"
Proceedings IEE IV, vol. 100, 1953

[70] V. Brandwajn, H.W. Dommel, I.I. Dommel
"Matrix Representation of Three-Phase N-Winding Transformers for Steasy-State and Transient Studies"
IEEE Transactions on Power Apparatus and Systems, vol. PAS-101, no.6, June 1982

[71] D.N. Ewart
"Digital Computer Simulation Model of a Steel-Core Transformer"
IEEE Transactions on Power Delivery, vol. 1, no.3, July 1986

[72] A. Medina, J. Arrillaga
"Simulation of Multilimb Power Transformers in the Harmonic Domain"
IEE Proceedings-C, vol. 139, no. 3, May I992

[73] D. Dolinar, J. Pihler, B. GrEar
"Dynamic Model of a Three-Phase Power Transformer"
IEEE Transactions on Power Delivery, vol. 8, no. 4, October 1993

[74] N.D. Hatziargyriou, J.M. Prousalidis, B.C. Papadias
"Generalized Transformer Model Based on the Analysis of its Magnetic Core Circuit"
IEE Proceedings –C, vol. 140, no.4, July 1993

[75] A. Narang, R.H. Brierley
"Topology Based Model for Steady-State and Transient Studies for Three-Phase Core Type Transformers"
IEEE Transactions on Power Systems, vol. 9, no.3, August 1994

[76] J.Arrillaga, W. Enright, N. R . Watson, A.R. Wood
"Improved Simulation of HVDC Converter Transformers in Electromagnetic Transients Programs"
IEE Proceedings- Generation Transmission Distribution, vol. 144, no. 2, March 1997

[77] L.C.O. de Oliveira, J.C. Rossi, F.A. de Camargo Pires
"Asymmetrical Magnetization in Three-Phase Core Type Transformers"
Proceedings of the 38th Midwest Symposium on Circuits and Systems, vol. 2, August 1995

[78] X. Chen
"A Three-Phase Multi-Legged Transformer Model in ATP Using the Directly-Formed Inverse Inductance Matrix"
IEEE Transactions on Power Delivery, vol. 11, no.3, July 1996

[79] X. Chen, S.S. Venkata
"A Three-Phase Three-Winding Core-Type Transformer Model for Low-Frequency Transient Studies"
IEEE Transactions on Power Delivery, vol. 12, no.2, April 1997

[80] M. Vakilian, R.C. Degeneff
"A Method for Modeling Nonlinear Core Characteristics of Transformers During Transients"
IEEE Transactions on Power Delivery, vol. 9, no.4, October 1994

[81] E.F. Fuchs, Y. You, D. Lin
"Development and Validation of GIC Transformer Models"
Research Project 19Z-SK205V, Final Report prepared for Martin Marietta Energy Systems

[82] E.F. Fuchs, Y. You, D.J. Roesler
"Modeling and Simulation, and Their Validation of Three-Phase Transformers with Three Legs Under DC Bias"
IEEE Transactions on Power Delivery, vol. 14, no.2, April 1999

[83] F. de Leon, A. Semlyen
"Complete Transformer Model for Electromagnetic Transients"
IEEE Transactions on Power Delivery, vol. 9, no.1, January 1994

[84] F. de Leon, A. Semlyen
"Reduced Order Model for Transformer Transients"
IEEE Transactions on Power Delivery, vol. 7, no.1, January 1992

[85] J. Pedra, L. Sainz, R. Lopez, S. Bogarra
"Transformer Saturation Model for the Harmonic Analysis on Power Systems"
8th International Conference on Harmonics and Quality of Power, 1998

[86] L. Guash, F. Corcoles, J. Pedra
"Effects of Voltage Sags on Three-Phase Three-Legged Transformers"
10th International Conference on Harmonics and Quality of Power, 2002

[87] F. Corcoles, L. Sainz, J. Pedra, L. Guash, S. Herraiz
"Study of Voltage Sag Effects on Three-Phase Transformers"
11th International Conference on Harmonics and Quality of Power, 2004

[88] J. Pedra, L. Sainz, F. Córcoles, R. Lopez, M. Salichs
"PSPICE computer model of a nonlinear three-phase three-legged transformer"
IEEE Transactions on Power Delivery, vol. 19, no. 1, January 2004

[89] J. Pedra, F. Corcoles, L. Sainz, R. Lopez
"Harmonic Nonlinear Transformer Modeling"
IEEE Transactions on Power Delivery, vol. 19, no.2, April 2004

[90] L. Guash, F. Corcoles, J. Pedra, L. Sainz
"Effects of Symmetrical Voltage Sags on Three-Phase Three-Legged Transformers"
IEEE Transactions on Power Delivery, vol. 19, no.2, April 2004

[91] D.L. Stuehm
"Three-Phase Transformer Core Modeling"
Final Report to the Bonneville Power Administration Award no. DE-BI79-92BP26700, February 1993

[92] X.S. Chen, P. Neudorfer, L. Zhuang
"The Development of a Three-Phase Multi-Legged Transformer Model for Use with EMTP"
Final Report and Amendment to the Bonneville Power Administration on DOE contract no. DE-AC79-92BP26702, 1993

[93] S. Carneiro, J.A. Martins
"Measurement and Model Validation on Three-Phase Core-Type Distribution Transformers"

[94] S. Chimklai, J.R. Marti
"Simplified Three-Phase Transformer Model for Electromagnetic Transient Studies"
IEEE Transactions on Power Delivery, vol. 10, no.3, July 1995

APPENDIX A

MATHEMATICAL EXPRESSION OF THE PROPOSED MODEL

The proposed model is described by the two fundamental equations (4.1) and (4.2), namely the State- and the Output-Equation. The subject of this chapter is the derivation of these equations.

From the modified Maxwell's Equations for slow-varying fields, equations (2.1), we have:

$$u(t) = -N \cdot \dot{\phi}(t) \tag{A.1}$$

and

$$\theta(t) = N \cdot i(t) \tag{A.2}$$

Equations (A.1) and (A.2) represent Faraday's and Ampere's law, respectively. $u(t)$ is the voltage induced at the winding's terminals, $i(t)$ is the current flowing through it, N is the number of the winding's turns, ϕ is the magnetic flux inside the winding and $\theta(t)$ is the Magneto Motive Force applied on the magnetic material inside the winding. For the solution of Maxwell's Equations, we assume a uniform magnetic flux inside the core. This last restriction cannot be seen here, it is, however, introduced at the calculation of the core's magnetic reluctances. We can rewrite equation (A.1) in a vector form for all six transformer windings:

$$\underline{u}_s(t) = -\underline{N} \cdot \dot{\underline{\phi}}_s^{\mathrm{T}}(t) \tag{A.3}$$

It should be noted here that the suffix $(_s)$ stands for the values associated with the transformers windings.

From the magnetic equivalent circuit, figure 4.1, we get following equations:

$$\underline{\theta}_s = T_{\theta_m} \cdot \underline{\theta}_m \tag{A.4}$$

$$\underline{\theta}_m = -R_m \cdot \underline{\phi}_m \tag{A.5}$$

$$T_{\phi_s} \cdot \underline{\phi}_s - T_{\phi_m} \cdot \underline{\phi}_m = 0 \tag{A.6}$$

Suffix $(_m)$ stands for the values associated with the rest of the magnetic equivalent circuit.

We can also write equation (A.2) in a vector form for the modeled transformer:

$$\underline{\theta}_s(t) = \underline{N} \cdot \underline{i}_s^{\mathrm{T}}(t) - \underline{R}_s \cdot \underline{\phi}_s^{\mathrm{T}}(t) \tag{A.7}$$

As far, the load is not described in the model. The representation of the load is done by equation (A.8):

$$\underline{u}_{\mathrm{sec}}(t) = \underline{Z}_{\mathrm{sec}} \cdot \underline{i}_{\mathrm{sec}}^{\mathrm{T}}(t) \tag{A.8}$$

The primary side ohmic resistance of the windings is described by equation (A.9):

$$\underline{u}_{pri}(t) = \underline{U}_{source} - \underline{Z}_{pri} \cdot \underline{i}_{pri}^{\mathrm{T}}(t) \tag{A.8}$$

where $\underline{U}_{source}$ are the source voltages applied on the primary side.

Equations (A.3) – (A.9) fully define the proposed model.

From the previous study of the electric and magnetic circuits we are now ready to derive the State- and Output-Equations:

$$\begin{cases} \begin{pmatrix} \dot{\underline{\phi}}_{pri}(t) \\ \dot{\underline{\phi}}_{\mathrm{sec}}(t) \end{pmatrix} = \begin{pmatrix} \underline{N}_{pri}^{-1} \cdot \left(\underline{U}_{source}(t) - \underline{Z}_{pri}^{\mathrm{T}} \cdot \left(\underline{N}_{pri}^{-1} \right)^{\mathrm{T}} \cdot \left(\underline{\theta}_{pri}(t) + \underline{R}_{pri} \cdot \underline{\phi}_{pri}^{\mathrm{T}} \right)^{\mathrm{T}} \right)^{\mathrm{T}} \\ \underline{N}_{\mathrm{sec}}^{-1} \cdot \underline{Z}_{\mathrm{sec}}^{\mathrm{T}} \cdot \left(\underline{N}_{\mathrm{sec}}^{-1} \right)^{\mathrm{T}} \cdot \underline{\theta}_{\mathrm{sec}}^{\mathrm{T}}(t) \end{pmatrix} \\ \theta_s(t) = M \cdot \underline{\phi}_s^{\mathrm{T}}(t) = -T_{\theta_m} \cdot R_m \cdot T_{\phi_m}^{-1} \cdot T_{\phi_s} \cdot \underline{\phi}_s^{\mathrm{T}}(t) \end{cases} \tag{A.10}$$

$$\begin{cases} \begin{pmatrix} i_{pri}(t) \\ i_{\mathrm{sec}}(t) \end{pmatrix} = \begin{pmatrix} \underline{N}_{pri}^{-1} \cdot \left(\theta_{pri}(t) + \underline{R}_{pri} \cdot \underline{\phi}_{pri}^{\mathrm{T}}(t) \right)^{\mathrm{T}} \\ \underline{N}_{\mathrm{sec}}^{-1} \cdot \underline{\theta}_{\mathrm{sec}}^{\mathrm{T}}(t) \end{pmatrix} \\ \underline{u}_{\mathrm{sec}}(t) = \underline{Z}_{\mathrm{sec}} \cdot \underline{i}_{\mathrm{sec}}^{\mathrm{T}}(t) \\ \theta_s(t) = M \cdot \underline{\phi}_s^{\mathrm{T}}(t) = -T_{\theta_m} \cdot R_m \cdot T_{\phi_m}^{-1} \cdot T_{\phi_s} \cdot \underline{\phi}_s^{\mathrm{T}}(t) \end{cases} \tag{A.11}$$

The parameters of the proposed model are then the matrices $T_{\phi_m}, T_{\phi_s}, R_m, T_{\theta_m}$ and the vectors $\underline{N}, \underline{Z}_{\mathrm{sec}}, \underline{Z}_{pri}$. The analytical form of these parameters is as follows:

$$T_{\phi_s} = \begin{pmatrix} 1 & 0 & 0 & 0 & 0 & 0 \\ 1 & -1 & 0 & 0 & 0 & 0 \\ 0 & 0 & 1 & 0 & 0 & 0 \\ 0 & 0 & 1 & -1 & 0 & 0 \\ 0 & 0 & 0 & 0 & 1 & 0 \\ 0 & 0 & 0 & 0 & 1 & -1 \\ 0 & 0 & 0 & 0 & 0 & 0 \\ 0 & 0 & 0 & 0 & 0 & 0 \\ 0 & 0 & 0 & 0 & 0 & 0 \\ 0 & 0 & 0 & 0 & 0 & 0 \\ 0 & 0 & 0 & 0 & 0 & 0 \\ 0 & 0 & 0 & 0 & 0 & 0 \end{pmatrix}$$

$$T_{\theta_m} = \begin{pmatrix} -1 & 0 & 0 & 0 & 0 & 0 & 0 & 0 & 0 & 0 & 0 & 0 \\ 1 & -1 & 0 & 0 & 0 & 0 & 0 & 0 & 0 & 0 & 0 & 0 \\ 0 & 0 & -1 & 0 & 0 & 0 & 0 & 0 & 0 & 0 & 0 & 0 \\ 0 & 0 & 1 & -1 & 0 & 0 & 0 & 0 & 0 & 0 & 0 & 0 \\ 0 & 0 & 0 & 0 & -1 & 0 & 0 & 0 & 0 & 0 & 0 & 0 \\ 0 & 0 & 0 & 0 & 1 & -1 & 0 & 0 & 0 & 0 & 0 & 0 \end{pmatrix}$$

$$T_{\phi_m} = \begin{pmatrix} 1 & 1 & 0 & 0 & 0 & 0 & 1 & 0 & 0 & 0 & 0 & 0 \\ 1 & 0 & 0 & 0 & 0 & 0 & 0 & 0 & 0 & 0 & 0 & 0 \\ 0 & 0 & 1 & 1 & 0 & 0 & 0 & 1 & 1 & 0 & 0 & 0 \\ 0 & 0 & 1 & 0 & 0 & 0 & 0 & 0 & 0 & 0 & 0 & 0 \\ 0 & 0 & 0 & 0 & 1 & 1 & 0 & 0 & 0 & 1 & 0 & 0 \\ 0 & 0 & 0 & 0 & 1 & 0 & 0 & 0 & 0 & 0 & 0 & 0 \\ 0 & 0 & 0 & 0 & 0 & 0 & -1 & -1 & 0 & 0 & 1 & 0 \\ 0 & 0 & 0 & 0 & 0 & 0 & 0 & 0 & -1 & -1 & 0 & 1 \\ 0 & R_0 & 0 & 0 & 0 & 0 & -R_{13} & 0 & 0 & 0 & -R_0 & 0 \\ 0 & 0 & 0 & R_0 & 0 & 0 & 0 & -R_{14} & 0 & 0 & -R_0 & 0 \\ 0 & 0 & 0 & R_0 & 0 & 0 & 0 & 0 & 0 & -R_{15} & 0 & -R_0 \\ 0 & 0 & 0 & 0 & 0 & R_0 & 0 & 0 & 0 & -R_{16} & 0 & -R_0 \end{pmatrix}$$

$$R_m = \begin{pmatrix} R_0 & 0 & 0 & 0 & 0 & 0 & 0 & 0 & 0 & 0 & 0 & 0 \\ 0 & R_0 & 0 & 0 & 0 & 0 & 0 & 0 & 0 & 0 & 0 & 0 \\ 0 & 0 & R_0 & 0 & 0 & 0 & 0 & 0 & 0 & 0 & 0 & 0 \\ 0 & 0 & 0 & R_0 & 0 & 0 & 0 & 0 & 0 & 0 & 0 & 0 \\ 0 & 0 & 0 & 0 & R_0 & 0 & 0 & 0 & 0 & 0 & 0 & 0 \\ 0 & 0 & 0 & 0 & 0 & R_0 & 0 & 0 & 0 & 0 & 0 & 0 \\ 0 & 0 & 0 & 0 & 0 & 0 & R_{13} & 0 & 0 & 0 & 0 & 0 \\ 0 & 0 & 0 & 0 & 0 & 0 & 0 & R_{14} & 0 & 0 & 0 & 0 \\ 0 & 0 & 0 & 0 & 0 & 0 & 0 & 0 & R_{15} & 0 & 0 & 0 \\ 0 & 0 & 0 & 0 & 0 & 0 & 0 & 0 & 0 & R_{16} & 0 & 0 \\ 0 & 0 & 0 & 0 & 0 & 0 & 0 & 0 & 0 & 0 & R_0 & 0 \\ 0 & 0 & 0 & 0 & 0 & 0 & 0 & 0 & 0 & 0 & 0 & R_0 \end{pmatrix}$$

$$\underline{N} = \begin{pmatrix} N_{pri} \\ N_{\sec} \\ N_{pri} \\ N_{\sec} \\ N_{pri} \\ N_{\sec} \end{pmatrix}, \underline{Z}_{\sec} = \begin{pmatrix} Z_{A,\sec} \\ Z_{B,\sec} \\ Z_{C,\sec} \end{pmatrix}, \underline{Z}_{pri} = \begin{pmatrix} Z_{A,pri} \\ Z_{B,pri} \\ Z_{C,pri} \end{pmatrix}$$

APPENDIX B

PROGRAM FOR MODELING THE THREE-PHASE CORE-TYPE TRANSFORMER – DOCUMENTATION

Functions overview

1. **double **my_model (double ** T_{θ_m} , double ** R_m , double ** T_{ϕ_m} , double ** T_{ϕ_s})**

   this function builds the transformer matrix, from which one can calculate:

   $$\underline{\theta}_s = M \cdot \underline{\phi}_s \tag{B.1}$$

   for the determination of M we use equation (B.2):

   $$M = T_{\theta_m} \cdot R_m \cdot T_{\phi_m}^{-1} \cdot T_{\phi_s} \tag{B.2}$$

   where the matrices T_{θ_m}, T_{ϕ_s} are constant, whereas the matrices R_m, T_{ϕ_m} depend on the yokes' nonlinear magnetic reluctances. For this reason, matrix M needs to be recalculated whenever the matrices R_m, T_{ϕ_m} are updated.

2. **double **update_fm (double ** T_{ϕ_m} , double ** T_{ϕ_s} , double * $\underline{\phi}_s$)**

   this function returns the magnetic fluxes of the equivalent magnetic circuit, given the windings' magnetic fluxes $\underline{\phi}_s$. For the calculation of $\underline{\phi}_m$ equation (B.3) is used:

   $$\underline{\phi}_m = T_{\phi_m}^{-1} \cdot T_{\phi_s} \cdot \underline{\phi}_s \tag{B.3}$$

   Vector $\underline{\phi}_m$ is updated in order to then update the yokes' magnetic reluctances by calling the function **update_Rm**.

3. **void update_Rm (double ** R_m , double * $\underline{\phi}_m$, double * $\underline{\phi}_{m,new}$)**

   this function updates in situ the yokes' magnetic reluctances. For the calculation of the latter, the modified Jiles-Atherton model is used (incorporated in the function **JA_mod**).

4. **double **update_Rs (double * $\underline{R}_s$, double * $\underline{\phi}_s$, double * $\underline{\phi}_{s,new}$)**

   this function is the same with the previous function, only it is used to update the core limbs' magnetic reluctances. In contrary to **update_Rm**, function **update_Rs** is called only once at each time step, in order to afterwards solve the Output-Equation.

5. **void update_TFM (double ** T_{ϕ_m} , double ** R_m)**

   this function updates matrix T_{ϕ_m} with the new (yokes') magnetic reluctances of matrix R_m , therefore it is called whenever the latter is updated with a call to **update_Rm**.

6. **double **JA_mod (double ϕ, double ϕ_{new}, double S, double* H_{old}, double* M_{old})**

   this function calculates the magnetic permeability reluctance of a core's section by using the modified Jiles-Atherton model. It accepts as input the differential magnetic flux $\Delta\phi = \phi_{new} - \phi$, as well as the history terms for the magnetic field H_{old}, M_{old}. The output of the function is the differential magnetic permeability μ_{dif}. When called, it also updates the history terms for the next call.

7. **void derivs (double t, double * $\underline{Z}_{load}$, double ** M, double * $\underline{\phi}_s$, double * $\Delta\underline{\phi}_s$)**

   this function solves the State-Equation for $\Delta\underline{\phi}_s$:

$$\Delta\underline{\phi}_s = f\left(t, \underline{\phi}_s\right) = A \cdot \underline{\phi}_s + B \cdot \underline{u}_{pri}(t) \tag{B.4}$$

   It is called by the 4th order Runge-Kutta algorithm.

8. **void output (double t, double * $\underline{Z}_{load}$, double ** M, double * $\underline{R}_s$, double * $\underline{\phi}_s$, double * $\underline{\phi}_{s,new}$, double * $\underline{I}$, double * $\underline{V}$)**

   this function solves the Output-Equation. It first calls **update_Rs** to update the limbs' magnetic reluctances and then uses the new vector $\underline{\phi}_{s,new}$, given as a result from the Runge-Kutta algorithm, to calculate the currents $\underline{I}$ and voltages $\underline{V}$ at the time step t.

9. **int convergence (double * $\underline{\phi}_s$, double * $\underline{\phi}_{s,new}$)**

   this function is used to check the convergence of the Runge-Kutta loop. It compares the square norm of the magnetic fluxes' difference $\left(\underline{\phi}_s - \underline{\phi}_{s,new}\right)$ with the predefined tolerance TOL.

10. **double v1 (double t), double v3 (double t), double v5 (double t)**

    these functions are the primary-side source voltages applied to the transformer windings. They are considered to be a symmetric source, however, it is easy to apply any time-controlled voltage.

11. **double *vector (int n)**

    this functions defines a vector $[1..n]$.

12. **double **matrix (int n_{row}, int n_{col})**

    this is the definition of a two-dimensional matrix $[1..n_{row}][1..n_{col}]$. It is more general than the static definition of arrays in C $(A[i][j])$, and it is preferred here, because some of the supportive routines use such matrices.

13. **void free_vector (double * $\underline{v}$)**

    this routine is used to free the memory space allocated by the function **vector**.

14. void free_matrix (double ** A, int n_{row})

this routine is used to free the memory space allocated by the function **matrix**.

15. double **mult_matrix (double ** A, int $n_{row,A}$, int $n_{col,A}$, double ** B, int $n_{row,B}$, int $n_{col,B}$)

this function returns the product of a left-multiplication of two matrices.

16. float *mult_matrix_vector (double ** A, int $n_{row,A}$, int $n_{col,A}$, double * $\underline{b}$, int $n_{row,\underline{b}}$)

this function returns the product of a left-multiplication of a matrix and a vector.

17. void ludcmp (double ** A, int n, int * $\underline{index}$, double * d)

Given a matrix a[1..n][1..n], this routine replaces it by the LU decomposition of a row-wise permutation of itself. A and n are input. A is output, index[1..n] is an output vector that records the row permutation effected by the partial pivoting; d is output as ±1 depending on whether the number of row interchanges was even or odd, respectively. This routine is used in combination with **lubksb** to solve linear equations or invert a matrix.

18. void lubksb (double ** A, int n, int * $\underline{index}$, double b[])

Solves the set of n linear equations A·X = B. Here A[1..n][1..n] is input, not as the matrix A but rather as its LU decomposition, determined by the routine **ludcmp**. index[1..n] is input as the permutation vector returned by **ludcmp**. b[1..n] is input as the right-hand side vector B, and returns with the solution vector X. a, n, and index are not modified by this routine and can be left in place for successive calls with different right-hand sides b. This routine takes into account the possibility that b will begin with many zero elements, so it is efficient for use in matrix inversion.

19. double **inverse_matrix (double ** A, int n)

Using the above LU decomposition and back substitution routines, this function finds find the inverse of a matrix column by column. The matrix B will now contain the inverse of the original matrix A[1..n][1..n].

APPENDIX C

PROGRAM FOR MODELING THE THREE-PHASE CORE-TYPE TRANSFORMER – SOURCE CODE

```
#include <stdio.h>
#include <stdlib.h>
#include <math.h>
#include <stddef.h>

#define NR_END 1
#define FREE_ARG char*
#define SWAP(a,b) {temp=(a);(a)=(b);(b)=temp;}

#define DT              1.0E-4                  // time step size
#define TSTOP           1.0                     // stop time
#define TOL             1.0E-3                  // convergence tolerance
#define m0              1.2566370614E-6         // vacuum's magnetic permebility

double Ms, a, k, alpha, c, k1, k2;              // parameters for hysteresis model
double Vpri, Npri, Nsec;                        // transformer data
double R0;                                      // air-path magnetic reluctance

// basic model functions
void my_model   (double **TTHM, double **RM, double **TFM, double **TFS, double **M);
void update_fm  (double **TFM, double **TFS, double *fs, double *fm);
void update_RM  (double **RM, double *fm, double *fm_new, double *S, double *L, double *H_old,
                 double *M_old);
void update_RS  (double *RS, double *fs, double *fs_new, double *S, double *L, double *H_old,
                 double *M_old);
void update_TFM (double **TFM, double **RM);
void derives (double t, double *Z_pri, double *Z_sec, double *RS, double **M, double *fs,
                 double *dfs);
void output (double t, double *Z_sec, double **M, double *RS, double *fs, double *fs_new,
        double *S,double *L, double *H_old, double *M_old, double *I, double *V);
double JA_mod   (double f, double f_new, double S, double* H_old, double* M_old);
int convergence (double *fs, double *fs_new);

// source voltage functions
double v1(double t);
double v3(double t);
double v5(double t);

// mathematical functions
void nrerror(char error_text[]);
int *ivector(long nl, long nh);
double *vector(long nl, long nh);
double **matrix(long nrl, long nrh, long ncl, long nch);
void free_ivector(int *v, long nl, long nh);
void free_vector(double *v, long nl, long nh);
void free_matrix(double **m, long nrl, long nrh, long ncl, long nch);
void mult_matrix (double **A, long nrowA, long ncolA, double **B, long nrowB, long ncolB,
                 double **C, long nrowC, long ncolC);
void mult_matrix_vector (double **A, long nrowA, long ncolA, double *b, long nb, double *c,
                  long nc);
void gaussj(double **a, int n, double **b, int m);
void invert_matrix(double **a, long n, double **b);
```

```
int main()
{
	double *I=vector(1,6);				// Terminal currents
	double *V=vector(1,6);				// Terminal voltages

	// Vectors for Runge-Kutta algorithm
	double *dym=vector(1,6);
	double *dyt=vector(1,6);
	double *yt=vector(1,6);
	double *dydx=vector(1,6);

	double *fs=vector(1,6);				// Windings' magnetic fluxes
	double *fs_new=vector(1,6);			// Windings' magnetic fluxes (updated)
	double *fm=vector(1,12);			// non-windings' magnetic fluxes
	double *fm_new=vector(1,12);			// non-windings' magnetic fluxes (updated)

	// Model's matrices
	double **TFS=matrix(1,12,1,6);
	double **TTHM=matrix(1,6,1,12);
	double **RM=matrix(1,12,1,12);
	double **TFM=matrix(1,12,1,12);
	double **M=matrix(1,6,1,6);

	double *H_old=vector(1,7);			// Magnetic field intensity history term
	double *M_old=vector(1,7);			// Magnetization history term
	double *RS=vector(1,3);				// Core limbs' magnetic reluctances
	double *Z_pri=vector(1,3);			// Primary windings' ohmic resistances
	double *Z_sec=vector(1,3);			// Load side ohmic resistances
	double *L=vector(1,7);				// Mangetic core's dimensions (lengths)
	double *S=vector(1,7);		// Magnetic core's dimensions (cross-sectional areas)

	int i,j;

	char *out1, *out2, *out3, *out4, *out5, *out6;
	FILE *fp1, *fp2, *fp3, *fp4, *fp5, *fp6;

	// Open files for writing output
	out1="C:\\Trafo\\a_pri.txt";
	out2="C:\\Trafo\\a_sec.txt";
	out3="C:\\Trafo\\b_pri.txt";
	out4="C:\\Trafo\\b_sec.txt";
	out5="C:\\Trafo\\c_pri.txt";
	out6="C:\\Trafo\\c_sec.txt";

	if (!(fp1=fopen(out1, "w")))
	{
		printf ("Can not open output file: %s\n", out1);
		exit(1);
	}
	if (!(fp2=fopen(out2, "w")))
	{
		printf ("Can not open output file: %s\n", out2);
		exit(1);
	}
	if (!(fp3=fopen(out3, "w")))
	{
		printf ("Can not open output file: %s\n", out3);
		exit(1);
	}
```

```
if (!(fp4=fopen(out4, "w")))
        {
                printf ("Can not open output file: %s\n", out4);
                exit(1);
        }
        if (!(fp5=fopen(out5, "w")))
        {
                printf ("Can not open output file: %s\n", out5);
                exit(1);
        }
        if (!(fp6=fopen(out6, "w")))
        {
                printf ("Can not open output file: %s\n", out6);
                exit(1);
        }

        // Transformer data

        // Read the dimensions of the magnetic core
        printf("Please insert the dimensions of core's limb (length, cross-section) :\n");
        scanf ("%f %f", &L[1], &S[1]);

        L[2]=L[1]; S[2]=S[1];
        L[3]=L[1]; S[3]=S[1];

        printf("Please insert the dimensions of core's yoke (length, cross-section) :\n");
        scanf ("%f %f", &L[4], &S[4]); L[4]/=2.0;
        L[5]=L[4]; S[5]=S[4];
        L[6]=L[4]; S[6]=S[4];
        L[7]=L[4]; S[7]=S[4];

        // Read the load-side resistances
        printf("Please insert the load-side resistances (phase A, phase B, phase C) \n");
        printf("(for open-circuit insert -1) :\n");
        scanf ("%f %f %f", &Z_sec[1], &Z_sec[2], &Z_sec[3]);

        // Read the source-side resistances
        printf("Please insert the source-side resistances (phase A, phase B, phase C) \n");
        scanf ("%f %f %f", &Z_pri[1], &Z_pri[2], &Z_pri[3]);

        // Read the parameters of the Jiles-Atherton model
        printf("Please insert the parameters of the Jiles-Atherton model (Ms, a, k, alpha, c) :\n");
        scanf ("%f %f %f %f %f", &Ms, &a, &k, &alpha, &c);

        // Read the parameters for the eddy currents and excess losses
        printf("Please insert the parameters for the eddy currents and excess losses (k1, k2): \n");
        scanf ("%f %f", &k1, &k2);

        // Read the source voltage
        printf("Please insert the source voltage rms value :\n");
        scanf ("%f", &Vpri);

        // Read the primary-secondary turn numbers
        printf("Please insert the number of turns (primary, secondary) :\n");
        scanf ("%f %f", &Npri, &Nsec);

        // Define the air-path magnetic reluctance
        R0=m0*L[1]/(4.0*S[1]);
```

```
// Initialization

// Matrix TFS - constant
for (i=1; i<=12; i++)
        for (j=1; j<=6; j++) TFS[i][j]=0.0;

TFS[1][1]=1.0;   TFS[2][1]=1.0;   TFS[2][2]=-1.0;  TFS[3][3]=1.0;   TFS[4][3]=1.0;
TFS[4][4]=-1.0;  TFS[5][5]=1.0;   TFS[6][5]=1.0;   TFS[6][6]=-1.0;

// Matrix TTHM - constant
for (i=1; i<=6; i++)
        for (j=1; j<=12; j++) TTHM[i][j]=0.0;

TTHM[1][1]=-1.0; TTHM[2][1]=1.0; TTHM[2][2]=-1.0; TTHM[3][3]=-1.0;
TTHM[4][3]=1.0;  TTHM[4][4]=-1.0;TTHM[5][5]=-1.0;TTHM[6][5]=1.0;
TTHM[6][6]=-1.0;

// Matrix RM - nonconstant
for (i=1; i<=12; i++)
        for (j=1; j<=12; j++)
        {
                if (i==j) RM[i][j]=-R0;
                else RM[i][j]=0.0;
        }

// Matrix TFM - nonconstant
for (i=1; i<=12; i++)
        for (j=1; j<=12; j++) TFM[i][j]=0.0;

TFM[1][1]=1.0;  TFM[1][2]=1.0;  TFM[1][7]=1.0;  TFM[2][1]=1.0;  TFM[3][3]=1.0;
TFM[3][4]=1.0;  TFM[3][8]=1.0;  TFM[3][9]=1.0;  TFM[4][3]=1.0;  TFM[5][5]=1.0;
TFM[5][6]=1.0;  TFM[5][10]=1.0; TFM[6][5]=1.0;  TFM[7][7]=-1.0; TFM[7][8]=-1.0;
TFM[7][11]=1.0; TFM[8][9]=-1.0; TFM[8][10]=-1.0;TFM[8][12]=1.0; TFM[9][2]=R0;
TFM[9][11]=-R0;TFM[10][4]=R0; TFM[10][11]=-R0;TFM[11][4]=R0;
TFM[11][12]=-R0;TFM[12][6]=R0;TFM[12][12]=-R0;

// vector H_old - magnetic field history
for (i=1; i<=7; i++) H_old[i]=0.0;

// vector M_old - magnetization history
for (i=1; i<=7; i++) M_old[i]=0.0;

for (i=1; i<=6; i++) fs[i]=0.0;
for (i=1; i<=6; i++) fs_new[i]=0.0;
for (i=1; i<=12; i++) fm[i]=0.0;
for (i=1; i<=6; i++) fm_new[i]=0.0;

// Implicit initialization of the magnetic core's permeability

RM[7][7]=-0.0001*R0;
RM[8][8]=-0.0001*R0;
RM[9][9]=-0.0001*R0;
RM[10][10]=-0.0001*R0;
RS[1]=-0.0001*R0;
RS[2]=-0.0001*R0;
RS[3]=-0.0001*R0;

update_TFM(TFM, RM);
```

```
double t;

for (t=0.0; t<=TSTOP; t+=DT)
{
        int j=0;
        do
                        // Runge-Kutta loop
        {
                j++;

                // Runge-Kutta 4th order

                my_model(TTHM, RM, TFM, TFS, M);

                derivs (t, Z_pri, Z_sec, RS, M, fs, dydx);
                for (i=1; i<=6; i++) yt[i]=fs[i]+DT*0.5*dydx[i];
                derivs (t+DT*0.5, Z_pri, Z_sec, RS, M, yt, dyt);
                for (i=1; i<=6; i++) yt[i]=fs[i]+DT*0.5*dyt[i];
                derivs (t+DT*0.5, Z_pri, Z_sec, RS, M, yt, dym);
                for (i=1; i<=6; i++)
                {
                        yt[i]=fs[i]+DT*dym[i];
                        dym[i] +=dyt[i];
                }
                derivs (t+DT, Z_pri, Z_sec, RS, M, yt, dyt);
                for (i=1; i<=6; i++)
                        fs_new[i]=fs[i]+DT/6.0*(dydx[i]+dyt[i]+2.0*dym[i]);

                // update the magnetic reluctances
                update_fm (TFM, TFS, fs_new, fm_new);
                update_RM (RM, fm, fm_new, S, L, H_old, M_old);
                update_TFM (TFM, RM);

        } while ((convergence(fs, fs_new)==0) && (j<=7));   // check for convergence

        // calculate the outputs
        my_model(TTHM, RM, TFM, TFS, M);
        output (t, Z_sec, M, RS, fs, fs_new, S, L, H_old, M_old, I, V);

        // save the outputs
        fprintf (fp1, "%f \t %f \t %f \n", t, V[1], I[1]);
        fprintf (fp2, "%f \t %f \t %f \n", t, V[2], I[2]);
        fprintf (fp3, "%f \t %f \t %f \n", t, V[3], I[3]);
        fprintf (fp4, "%f \t %f \t %f \n", t, V[4], I[4]);
        fprintf (fp5, "%f \t %f \t %f \n", t, V[5], I[5]);
        fprintf (fp6, "%f \t %f \t %f \n", t, V[6], I[6]);

        // store the new values for the magnetic fluxes
        for (i=1; i<=6; i++) fs[i]=fs_new[i];
        for (i=1; i<=12; i++) fm[i]=fm_new[i];

        // proceed to next time step
}
```

```
        // free all matrices and vectors
        free_matrix(TTHM,1,6,1,12);
        free_matrix(RM,1,12,1,12);
        free_matrix(TFM,1,12,1,12);
        free_matrix(TFS,1,12,1,6);
        free_matrix(M,1,6,1,6);
        free_vector(I,1,6);
        free_vector(V,1,6);
        free_vector(yt,1,6);
        free_vector(dydx,1,6);
        free_vector(dyt,1,6);
        free_vector(dym,1,6);
        free_vector(fs,1,6);
        free_vector(fs_new,1,6);
        free_vector(fm,1,12);
        free_vector(fm_new,1,12);
        free_vector(H_old,1,7);
        free_vector(M_old,1,7);
        free_vector(L,1,7);
        free_vector(S,1,7);
        free_vector(RS,1,3);
        free_vector(Z_pri,1,3);
        free_vector(Z_sec,1,3);

        // close output files
        fclose(fp1);
        fclose(fp2);
        fclose(fp3);
        fclose(fp4);
        fclose(fp5);
        fclose(fp6);

        printf("\n Simulation results stored in the files: \n \n %s \n %s \n %s \n %s \n %s \n %s \n",
        out1, out2, out3, out4, out5, out6);
        exit(0);
}

void my_model (double **TTHM, double **RM, double **TFM, double **TFS, double **M)
// this function calculates the matrix M
{
        double **TFM_INV=matrix(1,12,1,12);
        double **ST1=matrix(1,6,1,12);
        double **ST2=matrix(1,6,1,12);

        invert_matrix(TFM,12,TFM_INV);
        mult_matrix(TTHM,6,12,RM,12,12,ST1,6,12);
        mult_matrix(ST1,6,12,TFM_INV,12,12,ST2,6,12);
        mult_matrix(ST2,6,12,TFS,12,6,M,6,6);

        free_matrix(TFM_INV,1,12,1,12);
        free_matrix(ST1,1,6,1,12);
        free_matrix(ST2,1,6,1,12);
}
```

```
void update_fm (double **TFM, double **TFS, double *fs, double *fm)
// this function returns the non-winding magnetic fluxes
{
        double **TFM_INV=matrix(1,12,1,12);
        double **ST1=matrix(1,12,1,6);
        invert_matrix(TFM,12,TFM_INV);
        mult_matrix(TFM_INV,12,12,TFS,12,6,ST1,12,6);
        mult_matrix_vector(ST1,12,6,fs,6,fm,12);

        free_matrix(TFM_INV,1,12,1,12);
        free_matrix(ST1,1,12,1,6);
}

void update_TFM (double **TFM, double **RM)
// this function updates the matrix TFM
{
        TFM[9][7]  = RM[7][7];
        TFM[10][8] = RM[8][8];
        TFM[11][9] = RM[9][9];
        TFM[12][10]= RM[10][10];
}

double JA_mod (double f, double f_new, double S, double* H_old, double* M_old)
// this fuction returns the differential permeability using the modified Jiles-Atherton model
// parameters for classical JA-model
//                      alpha, a, c, k, Ms
// parameters for modified model
//                      k1 (classical eddy-currents losses), k2 (excess losses), Q
{
        double Q=0.5;                                           // parameter for curve fitting
        double Df=f_new-f;
        double DH=Q*Df/(S*m0);
        double DM=(1-Q)*Df/(S*m0);
        double H=*H_old + DH + k1*Df/(S*DT);                    // k2*sqrt(Df/(S*DT)) ommited
                                                                // due to arithmetic problems
        double M=*M_old + DM;
        int d=(Df>0.0)? 1: -1;
        double He=H + alpha*M;
        double Man=Ms*(cosh(He/a)/sinh(He/a)-a/He);
        double dMan_dHe=-Ms/(a*sinh(He/a)*sinh(He/a))+a*Ms/(He*He);

//for anisotropic materials use other function for efficient field intensity He
//float Man=Ms*(a1*He+He*He)/(a3+a2*He+He*He);
//float dMan_dHe=Ms*(a1*a3+2.0*a3*He+(a2-a1)*He*He) \
/((a3+a2*He+He*He)*(a3+a2*He+He*He));

        double dM_dH=((Man-M)*d>0.0)? dM_dH=(c*dMan_dHe+(Man-M)/(d*k/m0-alpha*(Man-\
                M)/(1.0-c)))/(1.0-alpha*c*dMan_dHe): c*dMan_dHe/(1.0-alpha*c*dMan_dHe);
        double mdif=m0*(1.0+dM_dH);

        // update history terms
        *H_old=H;
        *M_old=M;

        return(mdif);
}
```

```
void update_RM (double **RM, double *fm, double *fm_new, double *S, double *L, double *H_old,
            double *M_old)
// this function updates the magnetic reluctances of the core's yokes
{
            double mdif;
            mdif=JA_mod(fm[7], fm_new[7], S[4], &H_old[4], &M_old[4]);
            RM[7][7]=-L[4]/(mdif*S[4]);
            mdif=JA_mod(fm[8], fm_new[8], S[5], &H_old[5], &M_old[5]);
            RM[8][8]=-L[5]/(mdif*S[5]);
            mdif=JA_mod(fm[9], fm_new[9], S[6], &H_old[6], &M_old[6]);
            RM[9][9]=-L[6]/(mdif*S[6]);
            mdif=JA_mod(fm[10], fm_new[10], S[7], &H_old[7], &M_old[7]);
            RM[10][10]=-L[7]/(mdif*S[7]);
}

void update_RS (double *RS, double *fs, double *fs_new, double *S, double *L, double *H_old,
            double *M_old)
// this function updates the magnetic reluctances of the core's limbs
{
            double mdif;
            mdif=JA_mod(fs[1], fs_new[1], S[1], &H_old[1], &M_old[1]);
            RS[1]=L[1]/(mdif*S[1]);
            mdif=JA_mod(fs[2], fs_new[2], S[2], &H_old[2], &M_old[2]);
            RS[2]=L[2]/(mdif*S[2]);
            mdif=JA_mod(fs[3], fs_new[3], S[3], &H_old[3], &M_old[3]);
            RS[3]=L[3]/(mdif*S[3]);
}

double v1(double t)
// primary voltage phase A
{
            double v=Vpri*cos(100*PI*t);
            return(v);
}

double v3(double t)
// primary voltage phase B
{
            double v=Vpri*cos(100*PI*t+PI*2.0/3.0);
            return(v);
}

double v5(double t)
// primary voltage phase C
{
            double v=Vpri*cos(100*PI*t+PI*4.0/3.0);
            return(v);
}
```

```
void derivs (double t, double *Z_pri, double *Z_sec, double *RS, double **M, double *fs,
        double *dfs)
// this function solves the equation dfs=f(t,fs)
{
        double *ths=vector(1,6);
        mult_matrix_vector(M,6,6,fs,6,ths,6);

        dfs[1]=1/Npri*(v1(t)-Z_pri[1]*1/Npri*(ths[1]+RS[1]*fs[1]));
        dfs[2]=(Z_sec[1]>=0) ? 1/Nsec*(Z_sec[1]*ths[2]/Nsec) : dfs[1];
        dfs[3]=1/Npri*(v3(t)-Z_pri[2]*1/Npri*(ths[3]+RS[2]*fs[3]));
        dfs[4]=(Z_sec[2]>=0) ? 1/Nsec*(Z_sec[2]*ths[4]/Nsec) : dfs[3];
        dfs[5]=1/Npri*(v5(t)-Z_pri[3]*1/Npri*(ths[5]+RS[3]*fs[5]));
        dfs[6]=(Z_sec[3]>=0) ? 1/Nsec*(Z_sec[3]*ths[6]/Nsec) : dfs[5];

        free_vector(ths,1,6);
}

void output (double t, double *Z_sec, double **M, double *RS, double *fs, double *fs_new,
         double *S,double *L, double *H_old, double *M_old, double *I, double *V)
// this function saves the output
{
        // update the windings' reluctances
        update_RS (RS, fs, fs_new, S, L, H_old, M_old);

        double *ths=vector(1,6);

        mult_matrix_vector(M,6,6,fs,6,ths,6);

        I[1]=1/Npri*(ths[1]+RS[1]*fs[1]);
        I[2]=(Z_sec[1]>=0) ? 1/Nsec*ths[2] : 0.0;
        I[3]=1/Npri*(ths[3]+RS[2]*fs[3]);
        I[4]=(Z_sec[2]>=0) ? 1/Nsec*ths[4] : 0.0;
        I[5]=1/Npri*(ths[5]+RS[3]*fs[5]);
        I[6]=(Z_sec[3]>=0) ? 1/Nsec*ths[6] : 0.0;
        V[1]=v1(t);
        V[2]=(Z_sec[1]>=0) ? Z_sec[1]*I[1] : Nsec/Npri*v1(t);
        V[3]=v3(t);
        V[4]=(Z_sec[2]>=0) ? Z_sec[2]*I[3] : Nsec/Npri*v3(t);
        V[5]=v5(t);
        V[6]=(Z_sec[3]>=0) ? Z_sec[3]*I[6] : Nsec/Npri*v5(t);

        free_vector(ths,1,6);
}

int convergence (double *fs, double *fs_new)
// check for convergence of the solution
{
        int i;
        double norm=0.0;
        double sum=0.0;
        for (i=1; i<=6; i++)
        {
                norm += (fs[i]-fs_new[i])*(fs[i]-fs_new[i]);
                sum += fs[i]*fs[i];
        }
        if (norm/sum>TOL) return(0);
        else return(1);
}
```

```
/* Programs Copyright (C) 1988-1992 by Numerical Recipes Software */

void nrerror(char error_text[])
/* Numerical Recipes standard error handler */
{
	fprintf(stderr,"Numerical Recipes run-time error...\n");
	fprintf(stderr,"%s\n",error_text);
	fprintf(stderr,"...now exiting to system...\n");
	exit(1);
}

int *ivector(long nl, long nh)
/* allocate an int vector with subscript range v[nl..nh] */
{
	int *v;
	v=(int *)malloc((size_t) ((nh-nl+1+NR_END)*sizeof(int)));
	if (!v) nrerror("allocation failure in ivector()");
	return v-nl+NR_END;
}

double *vector(long nl, long nh)
/* allocate a double vector with subscript range v[nl..nh] */
{
	double *v;
	v=(double *)malloc((size_t) ((nh-nl+1+NR_END)*sizeof(double)));
	if (!v) nrerror("allocation failure in dvector()");
	return v-nl+NR_END;
}

double **matrix(long nrl, long nrh, long ncl, long nch)
/* allocate a double matrix with subscript range m[nrl..nrh][ncl..nch] */
{
	long i, nrow=nrh-nrl+1,ncol=nch-ncl+1;
	double **m;
	/* allocate pointers to rows */
	m=(double **) malloc((size_t)((nrow+NR_END)*sizeof(double*)));
	if (!m) nrerror("allocation failure 1 in matrix()");
	m += NR_END;
	m -= nrl;
	/* allocate rows and set pointers to them */
	m[nrl]=(double *) malloc((size_t)((nrow*ncol+NR_END)*sizeof(double)));
	if (!m[nrl]) nrerror("allocation failure 2 in matrix()");
	m[nrl] += NR_END;
	m[nrl] -= ncl;
	for(i=nrl+1;i<=nrh;i++) m[i]=m[i-1]+ncol;
	/* return pointer to array of pointers to rows */
	return m;
}

void free_ivector(int *v, long nl, long nh)
/* free an int vector allocated with ivector() */
{
	free((FREE_ARG) (v+nl-NR_END));
}

void free_vector(double *v, long nl, long nh)
/* free a double vector allocated with dvector() */
{
	free((FREE_ARG) (v+nl-NR_END));
}
```

```
void free_matrix(double **m, long nrl, long nrh, long ncl, long nch)
/* free a double matrix allocated by dmatrix() */
{
	free((FREE_ARG) (m[nrl]+ncl-NR_END));
	free((FREE_ARG) (m+nrl-NR_END));
}

void mult_matrix (double **A, long nrowA, long ncolA, double **B, long nrowB, long ncolB,
	double **C, long nrowC, long ncolC)
// this function performs a left matrix multiplication of matrices A and B and stores their product in C
{
	long i,j,k;
	// check dimensions of matrices
	if ( (ncolA!=nrowB) || (nrowA!=nrowC) || (ncolB!=ncolC) )
		nrerror ("dimensions error in multiplication of matrices \n");

	for (i=1; i<=nrowA; i++)
	for (j=1; j<=ncolB; j++)
		{
			C[i][j]=0;
			for (k=1; k<=ncolA; k++)
				C[i][j]+=A[i][k]*B[k][j];
		}
}

void mult_matrix_vector (double **A, long nrowA, long ncolA, double *b, long nb, double *c,
	long nc)
// this function performs a matrix-vector left multiplication
{
	long i,j;
	// check dimensions of matrices
	if (ncolA!=nb)
		nrerror ("dimensions error in multiplication of matrices \n");

	for (i=1; i<=nrowA; i++)
   {
		c[i]=0;
		for (j=1; j<=nb; j++)
			c[i]+=A[i][j]*b[j];
	}
}

void invert_matrix (double **A, long n, double **B)
// This function uses the Gauss-Jordan elimination to find the inverse of a given matrix [1..n][1..n]
{
	int i,j;

	for (i=1; i<=n; i++)
		for (j=1; j<=n; j++) B[i][j]=A[i][j];		// Copy the original matrix

	double **C=matrix(1,n,1,1);
	for (i=1; i<=n; i++) C[i][1]=0.0;

	gaussj (B,n,C,1);					// Gauss-Jordan elimination

	free_matrix(C,1,n,1,1);
}

void gaussj(double **a, int n, double **b, int m)
```

```
// Linear equation solution by Gauss-Jordan elimination, equation (2.1.1) above. a[1..n][1..n]
// is the input matrix. b[1..n][1..m] is input containing the m right-hand side vectors. On
// output, a is replaced by its matrix inverse, and b is replaced by the corresponding set of solution
// vectors.
{
	int *indxc,*indxr,*ipiv;
	int i,icol,irow,j,k,l,ll;
	double big,dum,pivinv,temp;
	indxc=ivector(1,n);			// The integer arrays ipiv, indxr, and indxc are
	indxr=ivector(1,n);			// used for bookkeeping on the pivoting.
	ipiv=ivector(1,n);
	for (j=1;j<=n;j++) ipiv[j]=0;
	for (i=1;i<=n;i++)
	{					// This is the main loop over the columns to be
		big=0.0;			// reduced.
		for (j=1;j<=n;j++)		// This is the outer loop of the search for a pivot
		if (ipiv[j] != 1)		// element.
		for (k=1;k<=n;k++)
		{
			if (ipiv[k] == 0)
			{
				if (fabs(a[j][k]) >= big)
				{
					big=fabs(a[j][k]);
					irow=j;
					icol=k;
				}
			}
		}
		++(ipiv[icol]);	// We now have the pivot element, so we interchange rows, if
				// needed, to put the pivot element on the diagonal. The columns
				// are not physically interchanged, only relabeled: indxc[i], the
				// column of the ith pivot element, is the ith column that is reduced,
				// while indxr[i] is the row in which that pivot element was
				// originally located. If indxr[i] .= indxc[i] there is an implied
				// column interchange. With this form of bookkeeping, the
				// solution b's will end up in the correct order, and the inverse
				// matrix will be scrambled by columns.
		if (irow != icol)
		{
			for (l=1;l<=n;l++) SWAP(a[irow][l],a[icol][l])
			for (l=1;l<=m;l++) SWAP(b[irow][l],b[icol][l])
		}
		indxr[i]=irow;		// We are now ready to divide the pivot row by the
		indxc[i]=icol;		// pivot element, located at irow and icol.
		if (a[icol][icol] == 0.0) nrerror("gaussj: Singular Matrix");
		pivinv=1.0/a[icol][icol];
		a[icol][icol]=1.0;
		for (l=1;l<=n;l++) a[icol][l] *= pivinv;
		for (l=1;l<=m;l++) b[icol][l] *= pivinv;
		for (ll=1;ll<=n;ll++)		// Next, we reduce the rows...
		if (ll != icol)
		{				// ...except for the pivot one, of course.
			dum=a[ll][icol];
			a[ll][icol]=0.0;
			for (l=1;l<=n;l++) a[ll][l] -= a[icol][l]*dum;
			for (l=1;l<=m;l++) b[ll][l] -= b[icol][l]*dum;
		}
	}
```

```
        // This is the end of the main loop over columns of the reduction. It only remains to
        // unscramble
        // the solution in view of the column interchanges. We do this by interchanging pairs of
        // columns in the reverse order that the permutation was built up.
        for (l=n;l>=1;l--)
        {
                if (indxr[l] != indxc[l])
                for (k=1;k<=n;k++)
                SWAP(a[k][indxr[l]],a[k][indxc[l]]);
        }                                       // And we are done.
        free_ivector(ipiv,1,n);
        free_ivector(indxr,1,n);
        free_ivector(indxc,1,n);
}
```